Gravity and magnetic interpretation and modelling of the Dinantian carbonates in the Dutch subsurface

Report by SCAN

May 2020

Ministerie van Economische Zaken en Klimaat

ebn

TNO

Interreg North-West Europe DGE-ROLLOUT

Gravity and magnetic interpretation and modelling of the Dinantian carbonates in the Dutch subsurface

Report written by Pieter van Heiningen
Provenance Exploration Consultancy BV

31st of May 2020

Dit rapport is een product van het SCAN-programma en wordt mogelijk gemaakt door het Ministerie van Economische Zaken en Klimaat

Table of Contents

1. SAMENVATTING/SUMMARY, CONCLUSIONS & RECOMMENDATIONS

1.1. Samenvatting

Zwaartekracht- en aardmagnetische metingen worden veel gebruikt in een vroeg stadium van de exploratie naar koolwaterstoffen, mineralen en aardwarmte. Het bestuderen van de ondergrond kan in veel gevallen ondersteund worden door de kaart representatie van deze gegevens visueel te correleren met interpretaties van seismische data. Grote delen van Nederland zijn redelijk tot goed bedekt met 3D- en 2D-seismische gegevens. Echter, in gebieden waar de exploratie naar koolwaterstoffen niet of beperkt heeft plaatsgevonden, zijn die gegevens schaars (of afwezig) en meestal niet geschikt voor het weergeven van diepere lagen zoals de Dinantien kalkstenen uit het Onder-Carboon. Gegevens uit zwaartekracht- en aardmagnetische metingen in Nederland zijn openbaar en hebben een goede landelijke dekking. Deze kunnen daarom worden gebruikt om seismische interpretaties en structureel-geologische analyses te valideren zodra de relatie tussen deze geofysische eigenschappen (gemeten aan het aardoppervlak) en de geologie van de ondergrond kan worden vastgesteld.

Het doel van de hier gerapporteerde studie was om de bestaande zwaartekracht- en magnetische datasets in Nederland te gebruiken om de binnen het SCAN Dinantien programma uitgevoerde analyses van de verdeling, diepte- en diktevariaties en van de structurele geschiedenis van de Dinantian kalkstenen in de Nederlandse ondergrond te ondersteunen. De studie is in december 2018 gestart en in mei 2019 afgerond.

Hierbij zijn zgn. “Differential Reduced To Pole” magnetische anomalie data en “Terrain Corrected Bouguer” zwaartekracht anomalie data (en gefilterde versies van die datasets) gebruikt, om structureel-geologische elementen, waaronder bekkens en (basement) hogen, en vulkanische intrusies in kaart te brengen. Om grenseffecten aan de randen van de Nederlandse datasets te vermijden en de Nederlandse data in een grotere context te begrijpen, zijn ook Duitse en Belgische datasets gebruikt.

De structuren die geïnterpreteerd zijn in de aardmagnetische en zwaartekrachtsdata kunnen als richtlijnen dienen bij het karteren van het Dinantien in gebieden met weinig tot geen seismische data. Uit de magnetische data zijn magnetische diepteoplossingen voor intrusies (“dykes”) verkregen, met een dieptebereik tussen 8 en 1 km, deze oplossingen lijnen op met de flanken van structurele hogen. Ook lijkt het erop dat deze magnetische dijkoplossingen op sommige locaties overeenkomen met de randen van vulkanische stollingscomplexen. Uit de magnetische data zijn ook magnetische diepteoplossingen voor diepgelegen “basement” lagen verkregen. Deze zijn vergeleken met de dieptekaarten van boven- en onderkant van de Dinantien en Devoon gesteenten, verkregen uit seismische interpretatie en diepte-conversie. De vergelijking van de magnetische diepteoplossingen met de seismische kaarten op verschillende niveaus kan indicatief zijn voor hoeveel Dinantien en Devoon gesteente er aanwezig kan zijn. De hierboven genoemde magnetische diepteoplossingen voor intrusies lijken overwegend de magnetische “basement” dieptes te ondersteunen.

Lokaal bevindt de bovenkant van het magnetische “basement” zich op het diepteniveau van de clastische gesteenten uit het Devoon. Dit leidde tot de interpretatie dat de magnetische diepteoplossingen daar het resultaat zijn van zeer magnetisch clastisch gesteente, bekend van ontsluitingen van Devoon clastica in het VK. Elders bevindt het magnetische “basement” zich op het (uit seismische interpretatie verwachte) diepte niveau van het Dinantien of zelfs daarboven. In het algemeen is er een grote gelijkenis tussen de vorm van het magnetische basement en de uit seismiek verkregen beeld van de structuratie van de Dinantien kalkstenen. Lokaal kunnen de exacte dieptes echter behoorlijk verschillen. Daarom zal een dichtere en uniform gecombineerde aardmagnetische en zwaartekrachts dataset de onzekerheid in positionering van het aardmagnetische “basement” verkleinen, waardoor het begrip van de evolutie van de diepere ondergrond verder vergroot kan worden. Het rapport bevat een aantal aanbevelingen voor mogelijke additionele activiteiten.

De belangrijkste producten van dit onderzoek zijn dit rapport en een aantal kaarten. De onderliggende gegevens zijn opgeslagen in een ArcGIS database en een Oasis Montaj-Geosoft project.

1.2. Executive Summary

The use of gravity and magnetic anomaly data is common pratice in early stages of hydrocarbon, mineral and geothermal exploration. The data, usually presented as grids, often permit confident visual correlation with interpretations based on seismic lines.

The Netherlands has a dense coverage of 3D and 2D seismic data but in areas where exploration never matures, the data is sparse or not suitable for imaging deeper strata such as the Lower Carboniferous (Dinantian) Limestones. Magnetic and gravity data sets are public and have a full nationwide coverage and potentially can be used to validate seismic interpretation and structural analysis once the relationship between these geophysical properties and geology can be established.

The purpose of this study was to investigate the applicability of the exisiting gravity and magnetic data sets that cover the Netherlands to support the understanding of the distribution, thickness variations and structural history of the Dinantian carbonates in the Netherlands sub-surface. In order to avoid boundary effects and to understand the Dutch data in a regional context, also German and Belgian data sets were used. The project started in December 2018 and was completed in May 2019.

The followed methodology focused on the use of Differentially Reduced To Pole magnetic anomaly data and Terrain Corrected Bouguer gravity anomaly data grids and their filtered derivatives, to map structural elements, basins and basement highs and also igneous intrusions.
Magnetic depth solutions for dikes and for magnetic basement surfaces have been obtained from the magnetic grids. Dike solutions show alignment along the flanks of structural highs and it appears that occasionally and locally these magnetic dike solutions correspond to edges of igneous complexes. The depth range of the dike solutions is between 8 and 1 km. Igneous intrusive complexes appear to predominantly support the Magnetic Basement highs.

The seismic interpretation yielded depth grids of the Top and Base Dinantian carbonates and locally of Devonian clastics and limestones. The surface resulting from gridding of the magnetic surface depth solutions, the "Magnetic Basement" surface, was checked against these seismic interpretation depth grids with the objective to identify the available volume of Dinantian and Devonian rocks.
Locally, the top of the Magnetic Basement is situated within the Devonian clastic section. This lead to the interpretation that the magnetic depth solutions are the result of highly magnetic clastics, known from Devonian clastic outcrops in the UK. Elsewhere, the top Magnetic Basement is situated within the Dinantian section or even above the top Dinantian seismic depth grid. In general though, there is great resemblance between the top Magnetic Basement and the base Dinantian carbonates as far as structuration and morphology are concerned. Locally however, the exact depths of both grids differ considerably. Therefore, a denser and more uniform combined magnetic and gravity data set will increase the certainty of the Magnetic Basement depth surface grid, thereby improving the understanding of the geological evolution of the Dutch sub-surface.

Main deliverables of this study are this report and a number of maps. The underlying data is stored in an ArcGIS Geodata-base and a Oasis Montaj-Geosoft Project.

1.3. Conclusions

- Analyses and interpretation of the gravity and magnetic data supports deep subsurface strcuturation of the Netherlands as derived from seismic interpretation.
- There is a strong spatial relationship between Magnetic Basement morphology and sedimentary basin and basement highs configuration.
- The dominant gravity & magnetic structural elements 1) curve W-E to WSW-ENE to SW-NE to SSW-NNE, 2) in many cases cut and offset structures of other orientations and 3) appear to dictate the lateral steps of the LBM front, RVG, WNB, FP, TAH and LST for instance. As such, these structures provide guidelines for the mapping of the Dinantian in areas with poor or no seismic data.
- Magnetic Basement highs are often supported by large igneous intrusions and flanked by dikes.
- If and where the top Devonian locally comprises magnetized clastics , it represents the top Magnetic Basement. It would thus be a good proxy the base of the Lower Carboniferous limestones.
- Comparison of the Base Dinantian (Top Devonian) depth grid with the Top Magnetic Basement depth grid learns that locally there are differences of more than 1 km that need to be further investigated. And uncertainties should be taken into account as well.
- North of the RVG the Magnetic Basement highs support many of the Dinantian carbonate build-ups.
- Volcanic dikes and -sills predominantly occur associated with sedimentary cover fault zones along flanks of Magnetic Basement highs.

1.4. Recommendations

- Acquire high-resolution airborne gravity and magnetic data across NL that is focussed on the 3-15 km depth interval.
- Re-iterate (on a smaller scale) gravity and magnetic modeling and interpretation when new gravity and magnetic data and new and/or re-processed seismic data become available.
- Perform levelling on the German and Belgium to the Dutch Bouguer Gravity and (Differentially) Reduced To Pole Magnetic anomaly grids, to be able to include these data combined with German and Belgian well data in future in similar studies.
- Undertake 2D gravity & magnetic modelling, iteratively with seismic interpretation and structural balancing & restoration, along profiles with the objective to iteratively test the seismic interpretation of the Top Dinantian and Base Dinantian-Top Devonian. Requirement for the gravity and magnetic modelling is to make use of fully corrected (thus reliable) density and velocity logs from surface to TD of as many key wells as possible along those lines in order to be able to arrive at reliable 2D gravity & magnetic depth models for all formations and the top Magnetic Basement.
- Undertake a thourough study into the density structure of Dutch subsurface down to and beyond the base of the Lower Carboniferous. Only realistic density information allows for geologically realisitc gravity modelling that can potentially identify the 3D structure of deep rooted density anomalies and their relationship with (sediment build-up and thickness in) carbonate platform areas in the Netherlands sub-surface. One way of doing this is according the 3D data assimilation approach suggested by Van Wees et al. (2017) and as benchmarked by e.g. Sejan (2018). This

high resolution gravity forward modelling uses densities data assimilation and is capable of identifying residual density anomalies in the basement. Preliminary work by Van Wees et al. (2017) indicates that strong residual anomalies are present that in part correlate with the occurrence of anticipated Lower Carboniferous (Dinantian) carbonate platforms. Positive residual densities from the data assimilation may be indicative for a reduced Paleozoic sediment thickness (compared to existing structural interpretation), whereas negative residual densities can be indicative for a reduced sediment thickness.

- The amount of available density data can be significantly increased by making use of the velocity structure of the Dutch subsurface and known realtionships between density and velocity. For the Netherlands, this velocity is available in nationwide models (e.g. Velmod 3.1, see www.nlog.nl)

2. LIST OF FIGURES AND TABLES

3. INTRODUCTION

3.1. Scope

Geothermal energy systems have been considered as a potential alternative for the fossil fuel heating. Currently, there are geothermal projects already functioning in the Netherlands. However, the application of geothermal energy in existing projects is not adequate for the provision of high-temperature heat for, as an example the food process industry. It is anticipated that Ultra Deep Geothermal (UDG) energy could potentially make a substantial contribution to the transition towards a sustainable heat supply. To reach sufficiently high temperatures in the Netherlands, geothermal reservoirs at depths over 4 km are required. The Dutch subsurface at these depths has not been explored extensively until now and is therefore relatively unknown. Based on the limited amount of subsurface data, the Lower Carboniferous Dinantian Carbonates were identified by Boxem *et al.* (2016) as the most promising target matching the initial requirements for UDG.

The Gravity & Magnetic work reported in this document has been done as part of SCAN, a government funded program to scope out the potential of geothermal energy, including from the Dinantian Carbonates. This program includes a range of subsurface studies of the Dinantian Carbonates. The results of the SCAN studies will be released and become available via www.nlog.nl. The purpose of this study was to exploit existing gravity and magnetic data sets to support the assessment of the distribution and thickness variations of Dinantian carbonates in the Netherlands. This project started in December 2018 and was concluded in May 2019.

The Dinantian carbonates, igneous intrusions, structures and basement are the targets of interest in this project. Getting insight in the depth to basement not only improves the understanding of the geothermal gradient, as sediments have a blanketing effect on the heat producing basement, but also of the structure of the basement. The basement has experienced all the magmatic and tectonic deformation phases as opposed to the younger / overlying sediments. The orientations of many Paleozoic-Cenozoic basin margin faults are often dictated by basement stuctures that became (re-) activated during multiple tectonic phases. The basement in the Dutch subsurface is out of reach in most current seismic data sets.

The coverage of gravity and magnetic data is nation-wide whereas seismic campaigns have covered only certain parts fully with 3D, most parts sparsely with 2D and significant areas are virtually empty of seismic data. Moreover, the imaging focus of the seismic surveys for hydrocarbon exploration was on the depth range till 4km, thus not for the UDG depth range The objective of the Gravity & Magnetic Analysis was to bring added information to the seismic interpretation and facies analysis and finally also to the structural restoration process. More specific, structural elements, igneous intrusions and the Top Magnetic Basement grid obtained from gravity and magnetic data can complement and support the seismic interpretation.

3.2. Gravity and Magnetic Methods in Brief

Gravity is measured by a gravimeter that measures the gravitational acceleration at a location enforced by the total mass present below that location plus the acceleration related to the rotational movement of the gravimeter due to the rotation of the Earth. The unit of gravity is mGal, or 0,00001 m/s^2 (SI). The gravity field is a monopole field (Figure 1). If a body of relative high or low density is present below the subsurface, a gravity anomaly will be observed. The distribution of rock densities in the subsurface determine the shape of the gravity anomaly.

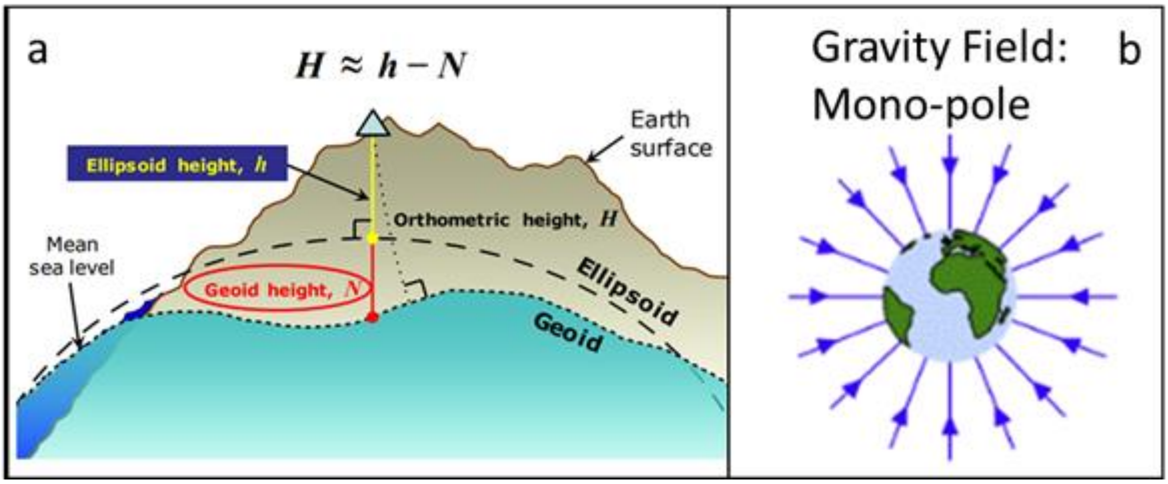

Figure 1. Explanation of the gravity field. Source: a) Geodesy.noaa.gov; b) IOP Spark Institute of physics.

Magnetic data is measured by a magnetometer. It records the magetic field strength, the Total Magnetic Intensity at location. The unit in which it is recorded is nano Tesla (10^{-9} T in SI). The Earth' magnetic field is a dipole field with a magnetic north and south pole (Figure 2). The magnetic field changes through time in strength and vector Inclination and – Declination (in degrees). As a consequence only there where the field vector is vertical (I=90°; D=0°), the measured anomaly is positioned truly vertically above the causative magnetic body at depth. Anywhere else a correction for inclination and declination via reduction to pole, or at low latitudes via reduction to equator, has to be performed prior to interpretation and modelling of magnetic anomalies can start.

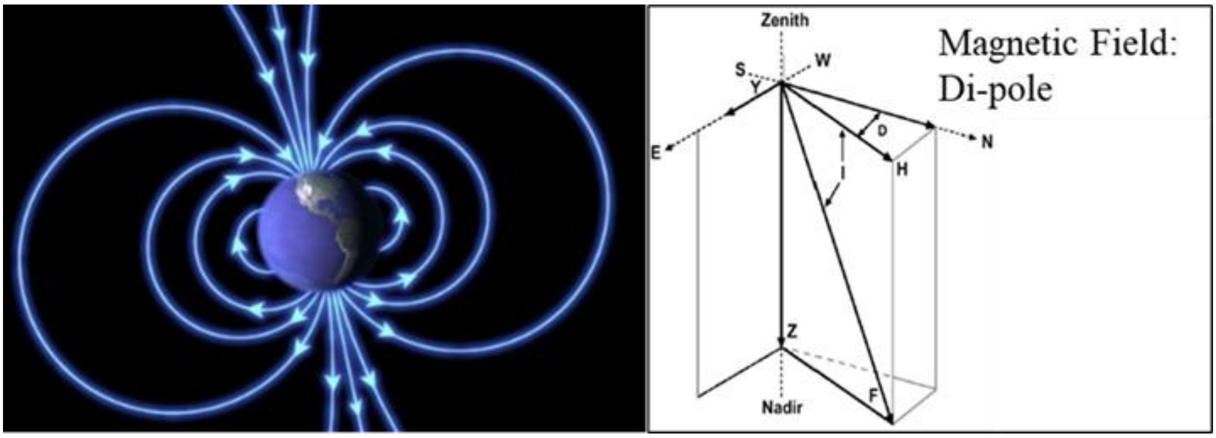

Figure 2. Explanation of the magnetic field. Source: UCAR Centre for education.

When volcanic deposits cool down, the magnetic minerals align their orienation to the imposed magnetic field line at that location. Same holds true for magnetic minerals in unconsolidated sediment prior to consolidation. When a rock is buried and is heated to temperatures above 500 °C, the so-called Curie temperature, the "frozen" orientation and signal strength of the magnetized minerals in the rock is made undone and removed, in other words de-magnetized Reeves (2005).

More details about the gravity and magnetic method and the definition of the terms used can be found in various textbooks, e.g. Gibson and Millegan (1998), Prieto (1998), Edwin S. Robinson, Cahit Coruh (1988) and Reeves (2005) and on AGSO and Geosoft websites Interpretation Concept. For in depth explanation to survey and processing and interpretation of magnetic data, please refer to Reeves (2005).

Rocks of higher density result in a higher gravity anomaly than rocks of a lower density. The same is true for magnetic susceptibility per rock type. Structural juxtaposition of rocks of different densities and/or susceptibilities results in juxtaposed highs and lows of gravity, respectively, magnetic anomalies. Figure 3a&b gives examples of various geological settings with their gravity and magnetic anomaly responses. If the basement is the only magnetic mineral bearing rock in the sub-surface, the magnetic curve will follow the basement morphology.

3.3. Gravity & Magnetic Applications Overview

In geothermal exploration, two different geological settings make different geophysical technique(s) favorable for application because of the distinghuished geophysical properties of the rocks under exploration (Reeves, 2005; Gibson and Millegan, 1998; Prieto, 1998 and AGSO website). Exploration in a volcanic setting requires application of non-seismic data including gravity, magnetic and magneto-telluric data whereas exploration in a sedimentary basin setting makes use of seismic data in addition to non-seismic data. In volcanic (high temperature) setting the seismic signal fades but resistivity measurements for instance bring important additional information of the subsurface as cap rocks and reservoir rock have different resisitivies (Van Heiningen *et al.*, 2018).

Typical applications of potential field data interpretation and modelling are:

- mapping of basement and structures and adequate correlation of structures from 2D seismic line to seismic line in absence of 3D seismic data
- depth to magnetic source detection for dikes, sills and larger intrusions; mapping of salt and shale intrusions
- detection of high density limestone and dolomite build ups, which are often flanked and draped by clastics of significant lower density. The draping often results in juxtaposition of rocks of different densities and produces lateral and vertical density contrasts.

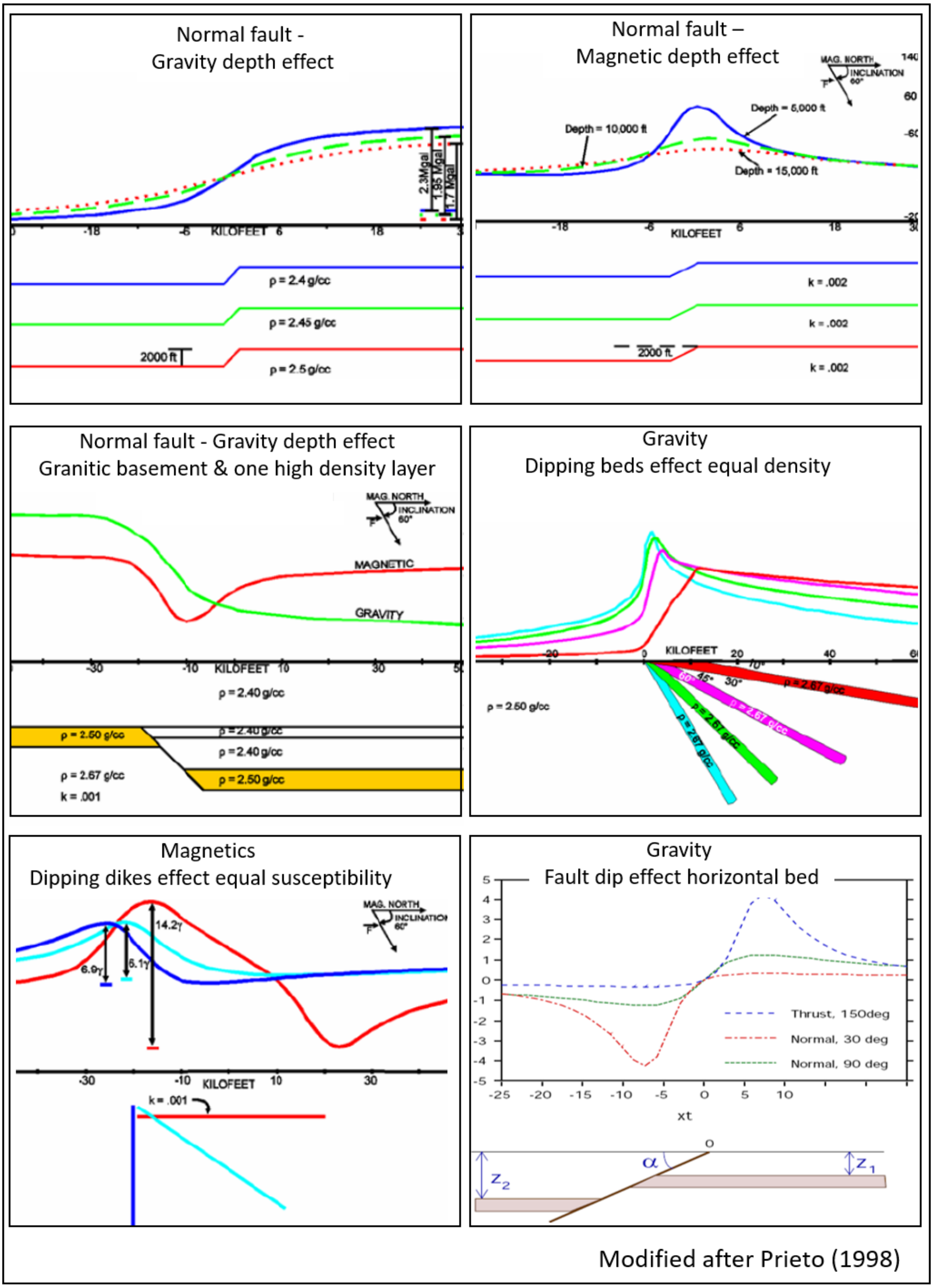

Figure 3.03a. Gravity and magnetic responses to various geological situations (Prieto, 1998).

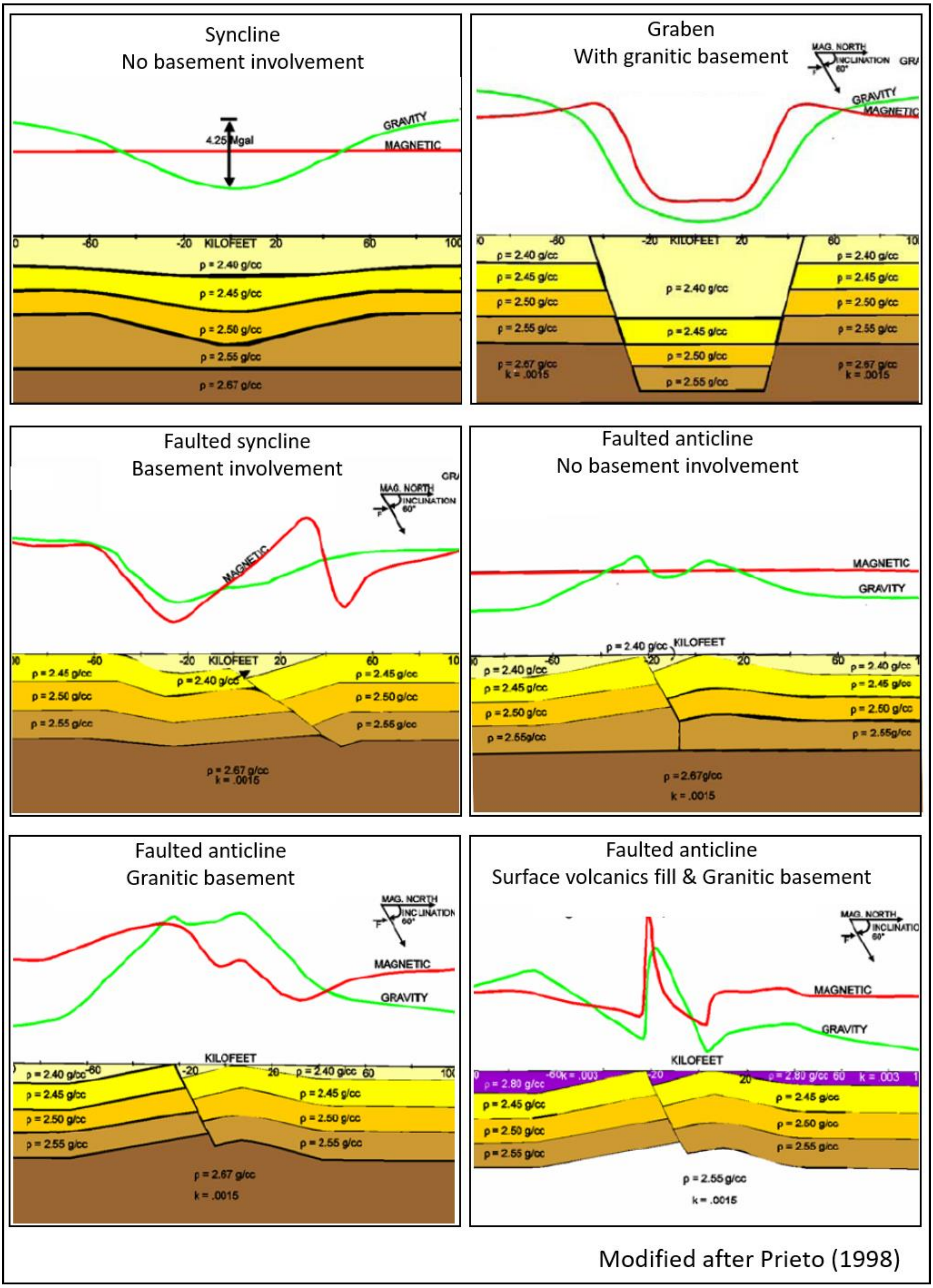

Figure 3.03b. Gravity and magnetic responses to various geological situations (Prieto, 1998).

3.4. List Of Abbreviations

FAG = Free Air Gravity anomaly
BG = (terrain corrected) Bouguer Gravity anomaly
TMI = Total Magnetic Intensity
(D)RTP = (Differentially) Reduced To Pole magnetic anomaly
TDR = Tilt Derivative
HG(c) = Horizontal Gradient
LP = Low Pass
HP = High Pass
BP = Band Pass
_bwBP = butterworth Band Pass
DTMS = Depth To Magnetic Source
GM = Gravity & Magnetics
UMHP = Uithuizermeeden Platform
LSB = Lower Saxony Basin
LST = Lauwers Zee Trough
ZDW = Zuidwal
TIJH = Texel IJselmeer High
TAH = Twente-Achterhoek High
OH = Osnabruck High
CNB = Central Netherlands Basin
MB = Munsterland Basin
ZH = Zantvoort High
ZP = Zeeland Platform
MBH = MaasBommel High
WNB = West Netherlands Basin
RVG = Roer Valley Grabe
LBM = London Brabant Massif
NL = Netherlands
D = German
B = Belgium

4 DATA

TNO delivered all inhouse gravity and magnetic data sets of the Dutch on- and offshore. In addition, German and Belgium data sets were obtained and used. The main data sources are: Rijkswaterstaat (RWS), Leibniz Instut für Angewandte Geophysik (LIAG) and Geological Survey of Belgium (GSB). In line with the project objectives, this project focused on the Netherlands onshore only. Therefore, the Dutch offshore and the German and Belgian gravity and magnetic data sets were only used for regional understanding and correlation, not for interpretation and modelling.

4.1. Gravity Data

Figure 4 and Table 1 present the coverage of the gravity data sets available in the study area.

	Gravity		
Country	**Anomaly**	**format**	**source**
NL	FAG & BG	point	RWS
D	BG	contour	LIAG
B	FAG & BG	geotif	GSB

Table 1. Overview of gravity data sets with format and source for the onshore Netherlands, Germany and Belgium.

For the Dutch Bouguer Gravity Anomaly computation onshore a surface density correction of 2,05 g/cm^3 from the Free Air Gravity Anomaly was considered valid and representative for the water-saturated soils with an average porosity of 36% that cover most of the onshore (source: TNO internal communication of 5th Dec 2018). The equation is:

$$BG\_2{,}05 = FAG - 0{,}0859 \cdot H$$

H is the station elevation with respect to NAP in meter. Anomaly values are listed in mGal.
The latest version of the TNO Bouguer Gravity Anomaly data is a compilation by TNO of various surveys executed by RWS, Topografische Dienst, Shell Netherlands, Utrecht University and Technical University Delft. The precision is estimated at 0.2 mGal. In this project we made use of the RWS data due to the regularly spaced and onshore nationwide coverage.

4.2. Magnetic Data

Figure 5 and Table 2 present the coverage of the magnetic data sets available in the study area.

	Magnetic		
Country	**Anomaly**	**format**	**source**
NL	TMI	point	RWS
D	TMI	contour	LIAG
B	RTP	point	GSB

Table 2. Overview of magnetic data sets with format and source for onshore Netherlands, Germany and Belgium. The magnetic data over Belgium was acquired by airborne surveying.

TNO made the most recent magnetic survey, that of 1985, available to the project. That survey was carried out Netherlands onshore nation-wide with the objective to replace previous data sets acquired which were severly effected by magnetic field conducting infrastructure such as pipelines and railroads. The onshore RWS 1985 magnetic field campaign used Witteveen as base station with anomaly value 0 nT (zero). The average precision of all field components is ~8nT (Rietman, 1988). However, for the interpretation and modelling of the magnetic anomaly data and calibration to the magnetic data in the surrounding areas, the Field Strength that existed at Witteveen at the time of acquisition of the 1985 survey, had to be added to the anomaly values of all the stations. In this way the Total Magnetic Intensity anomaly grid map was obtained for the Netherlands onshore. The Oasis Montaj-Geosoft International Geomagnetic Reference Field (IGRF) module provides such historic information. The IGRF Field Strength at Witteveen in 1985 was 48273.5995 nT.

5 METHODOLOGY

5.1. Qualitative & Quantitative Analyses

The Qualitative and Quantitative Analyses of the data is done in Oasis Montaj-Geosoft and consist of data import, database channel inspection, checking coordinate systems, projection and verification of unit details.

A general observation is that, onshore Netherlands, the gravity data is regularly spaced whereas the magnetic data is less dense and irregularly spaced (Figures 4 and 5).

The histograms of the used data sets are displayed in the Figures 6 and 7 and the cell size information of the grids is presented in Tables 1 and 2.

Regarding the visual inspection for artefacts in the gravity and magnetic grids, in the magnetic data linear artefacts can be produced by rail roads, pipelines or any other conductive infrastructure. Both the magnetic and gravity data appears to "clean", i.e. linear features have not been observed in them (Figures 8 and 9).

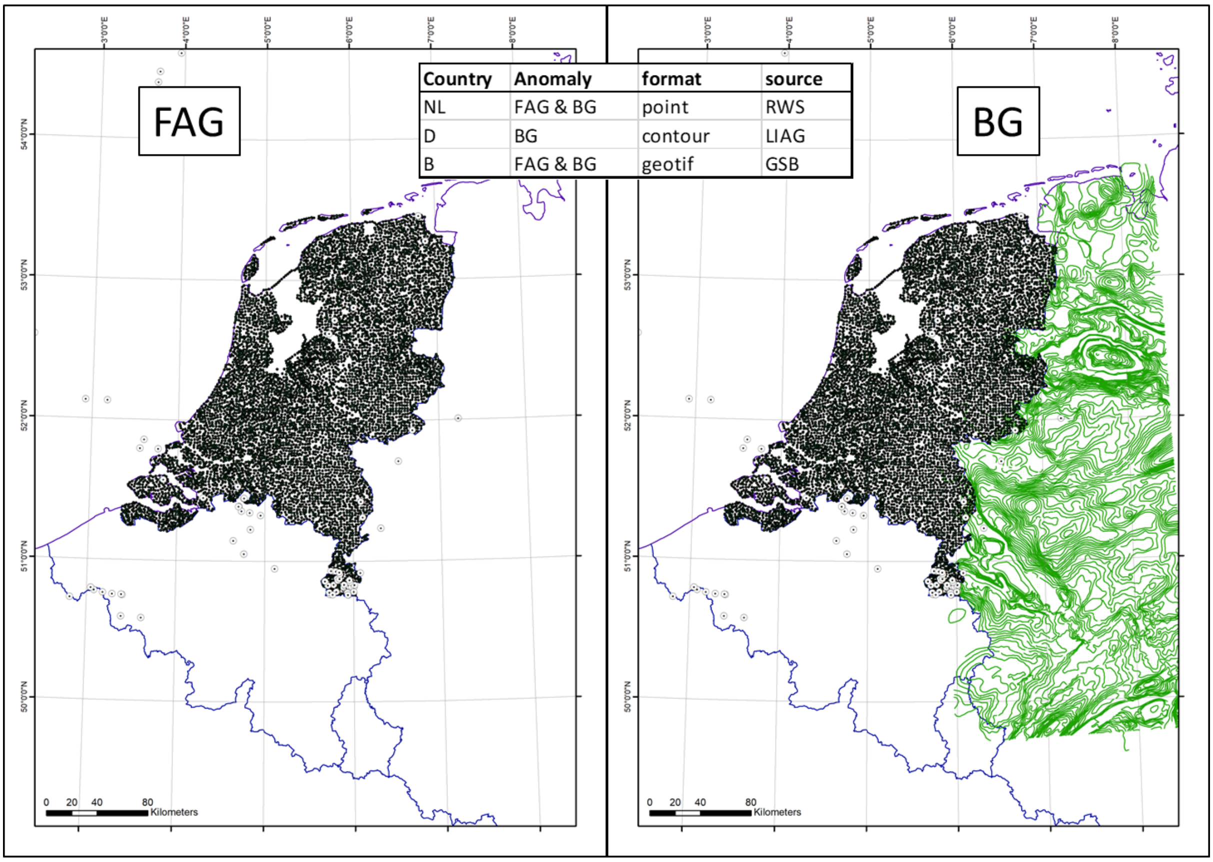

Figure 4. Coverage and type of gravity data (see also Table 1).

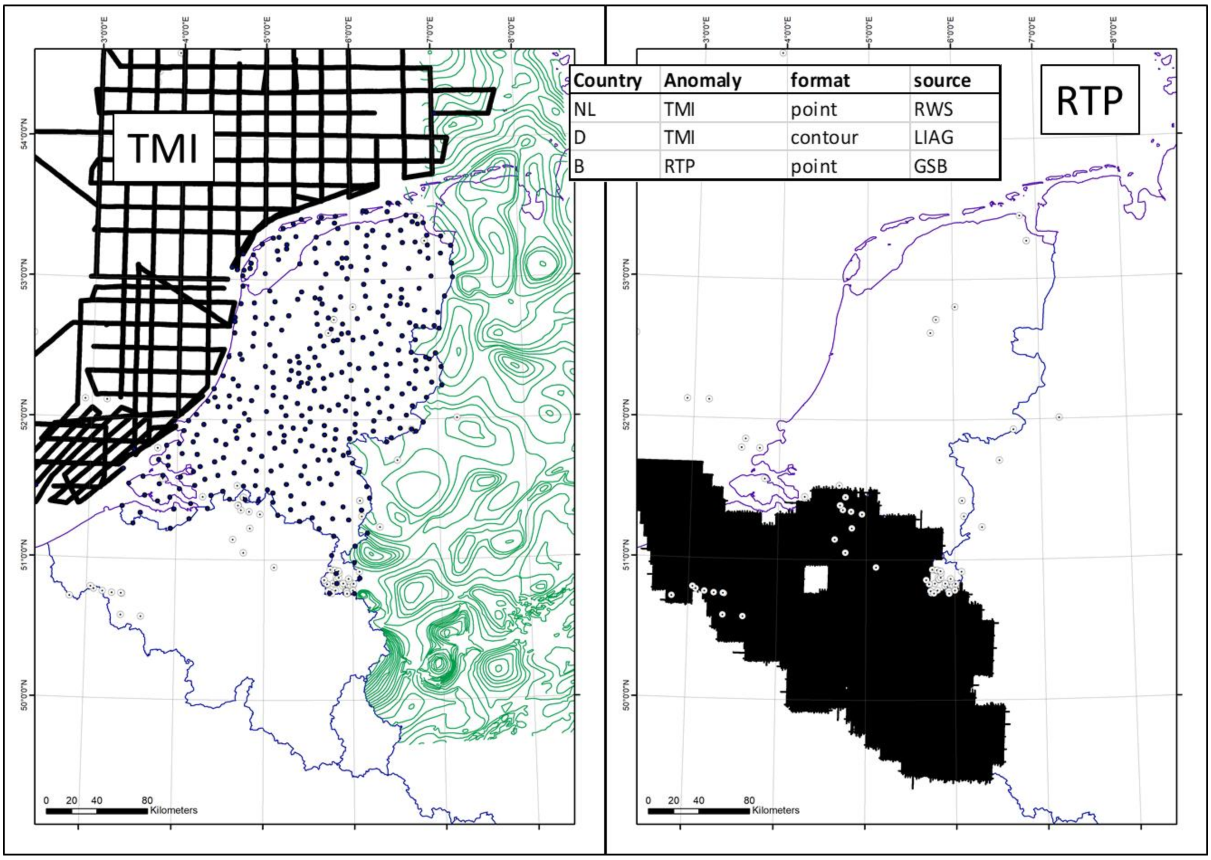

Figure 5. Coverage and type of magnetic data (see also Table 2).

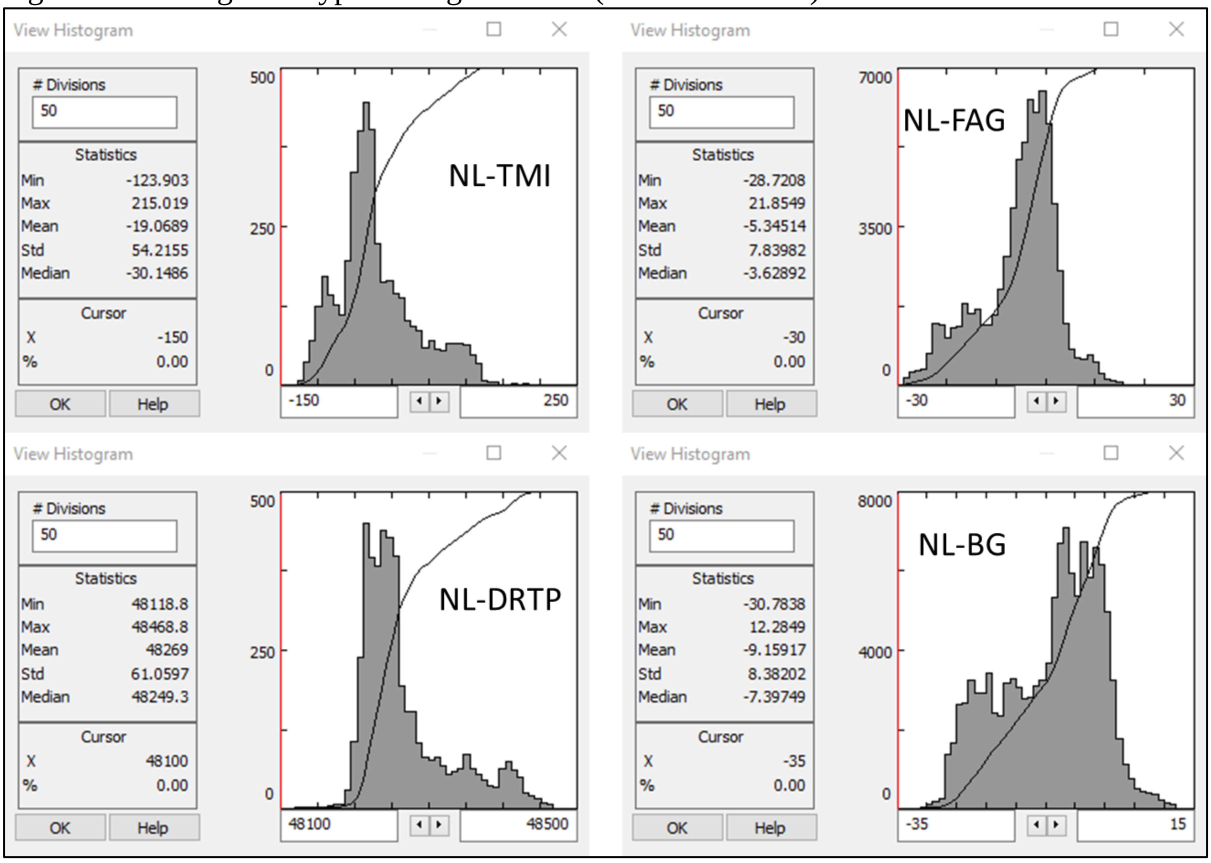

Figure 6. Spectral histograms of the Dutch TMI, DRTP magnetic and FAG and BG gravity grids.

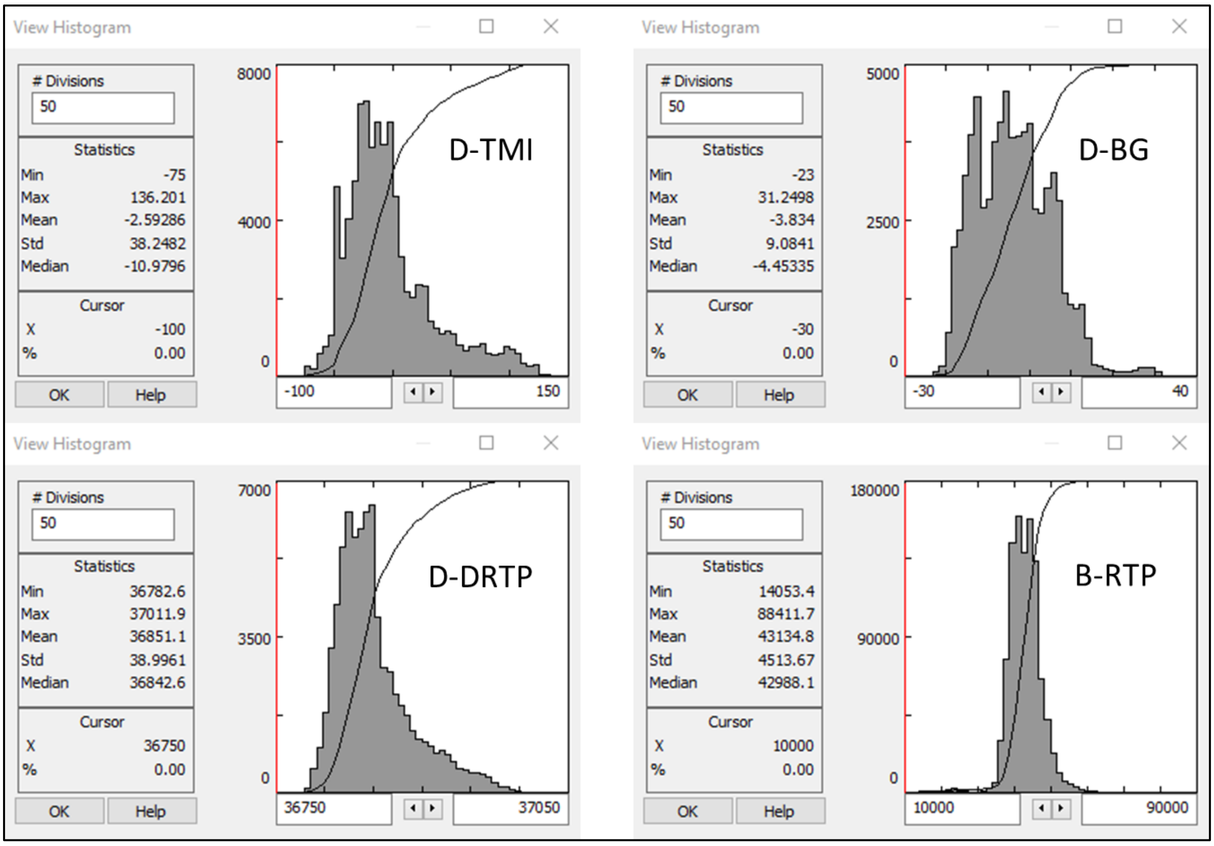

Figure 7. Spectral histograms of the German TMI, DRTP magnetic and BG gravity grids and of the Belgium RTP magnetic grid.

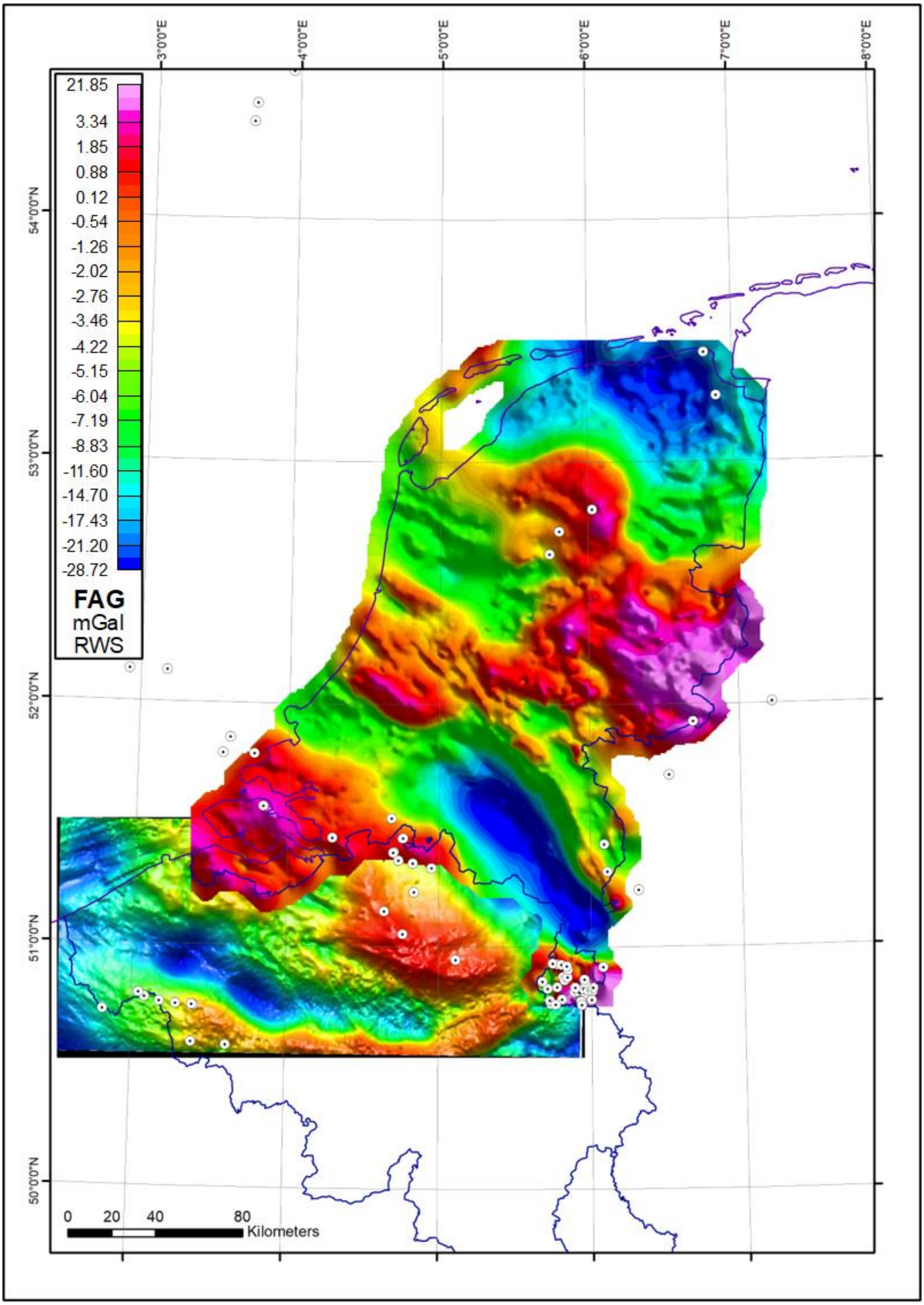

Figure 8. FAG grid of The Netherlands and FAG geotiff of Belgium.

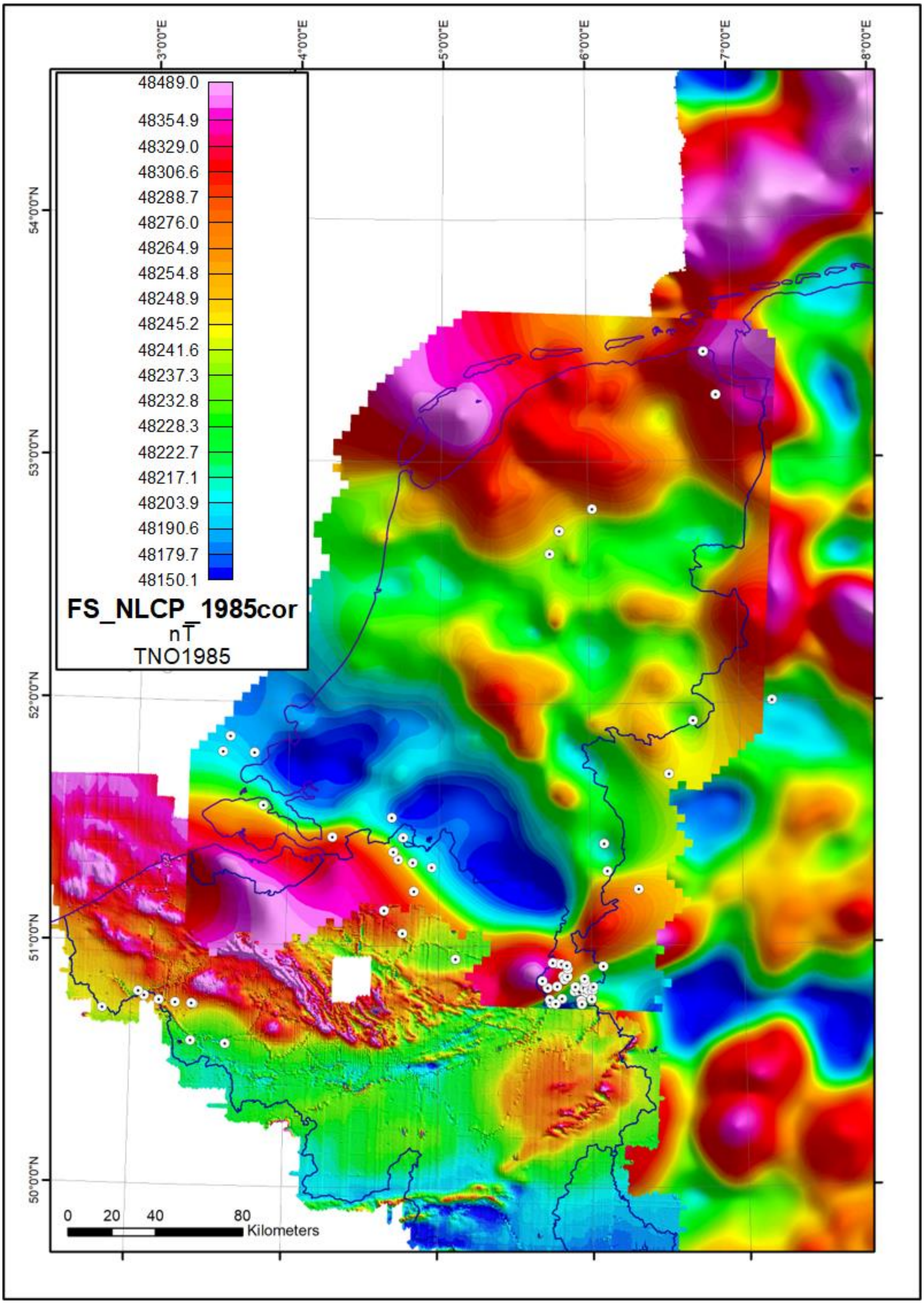

Figure 9. TMI grids of The Netherlands, Germany and Belgium. Obvious mismatch of the anomalies.

5.2. Pre-Filtering Corrections

Standard Industry Practice is to correct the Free Air Gravity (FAG) for terrain topography and surface geology (density) effects to obtain the Terrain Corrected Bouguer Gravity Anomaly grid (BG), suitable for geological interpretation, which is free of topographic and waterbody effects (e.g. Gibson and Milligam, 1998).
The BG computation was already performed by RWS for the Dutch FAG and by LIAG for the German FAG. The Belgium gravity data is only available as a geotiff raster of the FAG and BG (Figure 4). As mentioned before, the density correction applied to the FAG is 2.05 kg/cm^3, which is an average surface density correction value to account for the vast water masses and thick cover of low-density (loose) soil that make up the surface of the Netherlands. In a highly variable surface geology – rock density situation, it is strongly recommended to obtain the surface density via the Nettleton test procedure.

Compute Single Point GRF Values

	Netherlands	Germany	Belgium
* IGRF/DGRF:	IGRF	IGRF	IGRF
* Date required (yyyy/mm/dd):	1985/07/01	1980/07/01	1994/01/12
* IGRF Model Year (ignored for DGRF):	auto	1980	auto
* Longitude (-180 to 180):	5.1	50.5	4.65
* Latitude (-90 to 90):	52.2	10	50.7
* Elevation (metres):	0	1000	80
Field Strength (nT):	48273.5995	36853.4852	48046.1768
Inclination (degrees):	67.12557977	4.12042793	65.92522386
Declination (degrees):	-3.16218188	-0.13794955	-2.10254876

Table 3. Overview of the parameters of survey date, magnetic field strength, inclination and declination on the centre points of the grids.

The conversion from Total Magnetic Intensity (TMI) to Differentially Reduced To Pole (DRTP) Magnetic Anomaly passes via addition of the field strength at the period and location of the acquisition (e.g. Reeves, 2005). The TMI to DRTP correction was performed with the parameters listed in Table 3.

Information regarding the survey date, magnetic field strength, inclination and declination on the center points of the Dutch, German and Belgium grids was obtained from the sources: RWS, LIAG and BGS respectively. The cell size differs significantly between the surveys. Clearly, the Belgium aeromagnetic survey has the densest sample spacing, hence highest resolution. Mismatches between NL, G and B grids anomalies of BG (Figure 10) and (D)RTP (Figure 11) are visible. These mismatches are considered to be due to differences data resolution and spacing as well as national base station reference values. However, these aspects do not explain all border mismatches. For a proper calibration, recommended is to undertake data levelling prior to regridding the three data sets into one single grid.

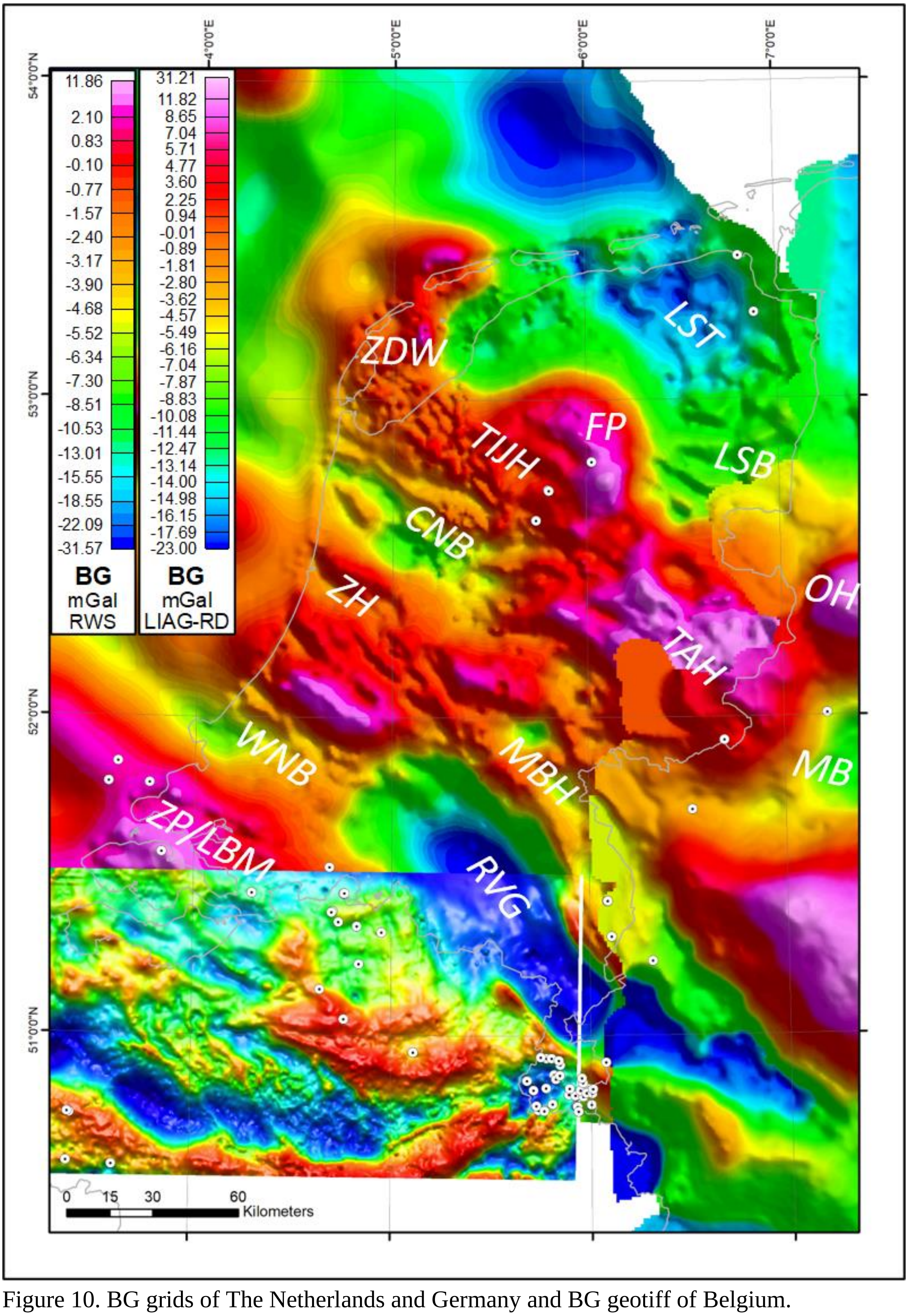

Figure 10. BG grids of The Netherlands and Germany and BG geotiff of Belgium.

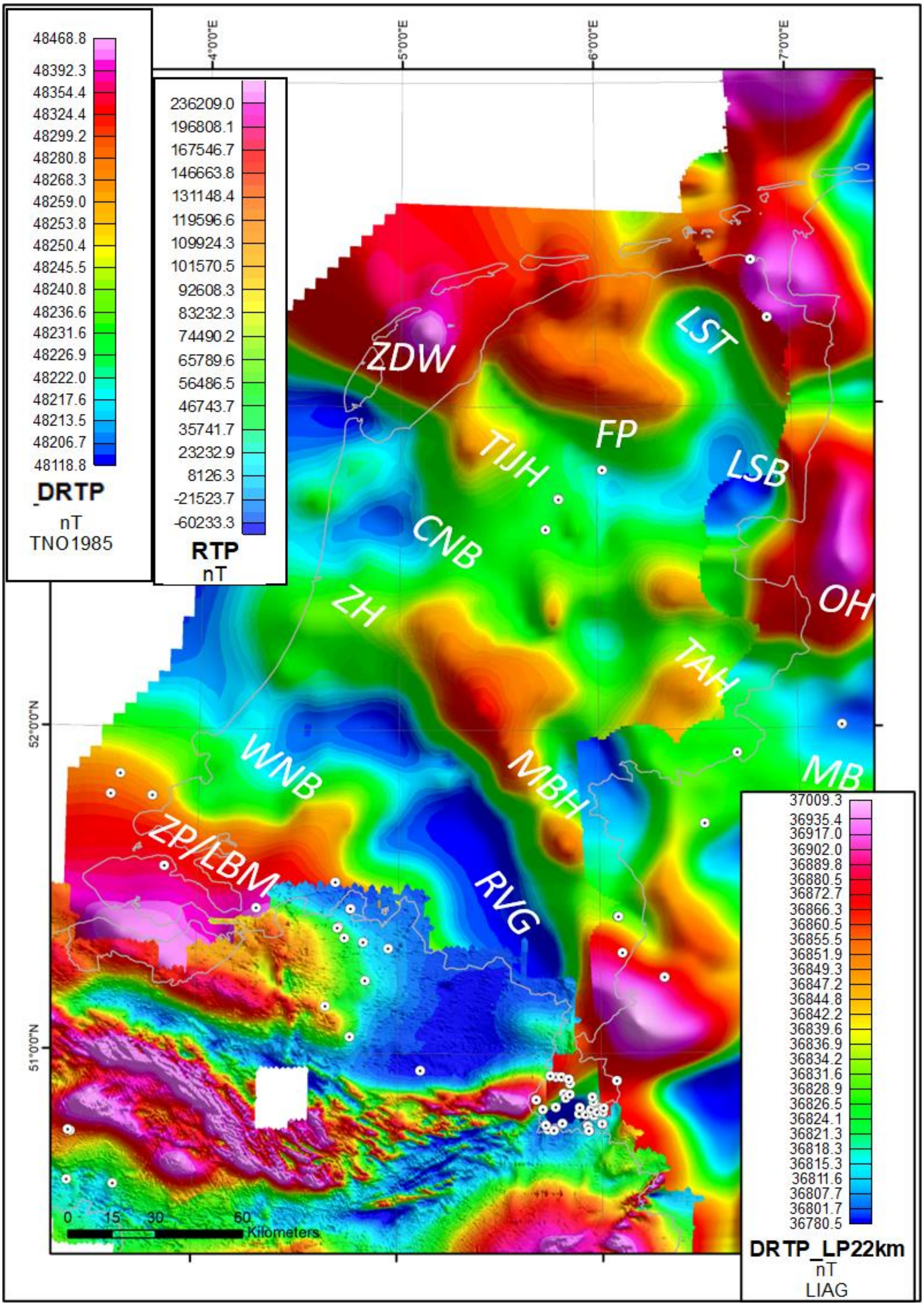

Figure 11. (D)RTP grids of The Netherlands, Germany and Belgium. Clearly a better match of anomalies than for the TMI.

5.3. Radial Average Power Spectrum Analysis

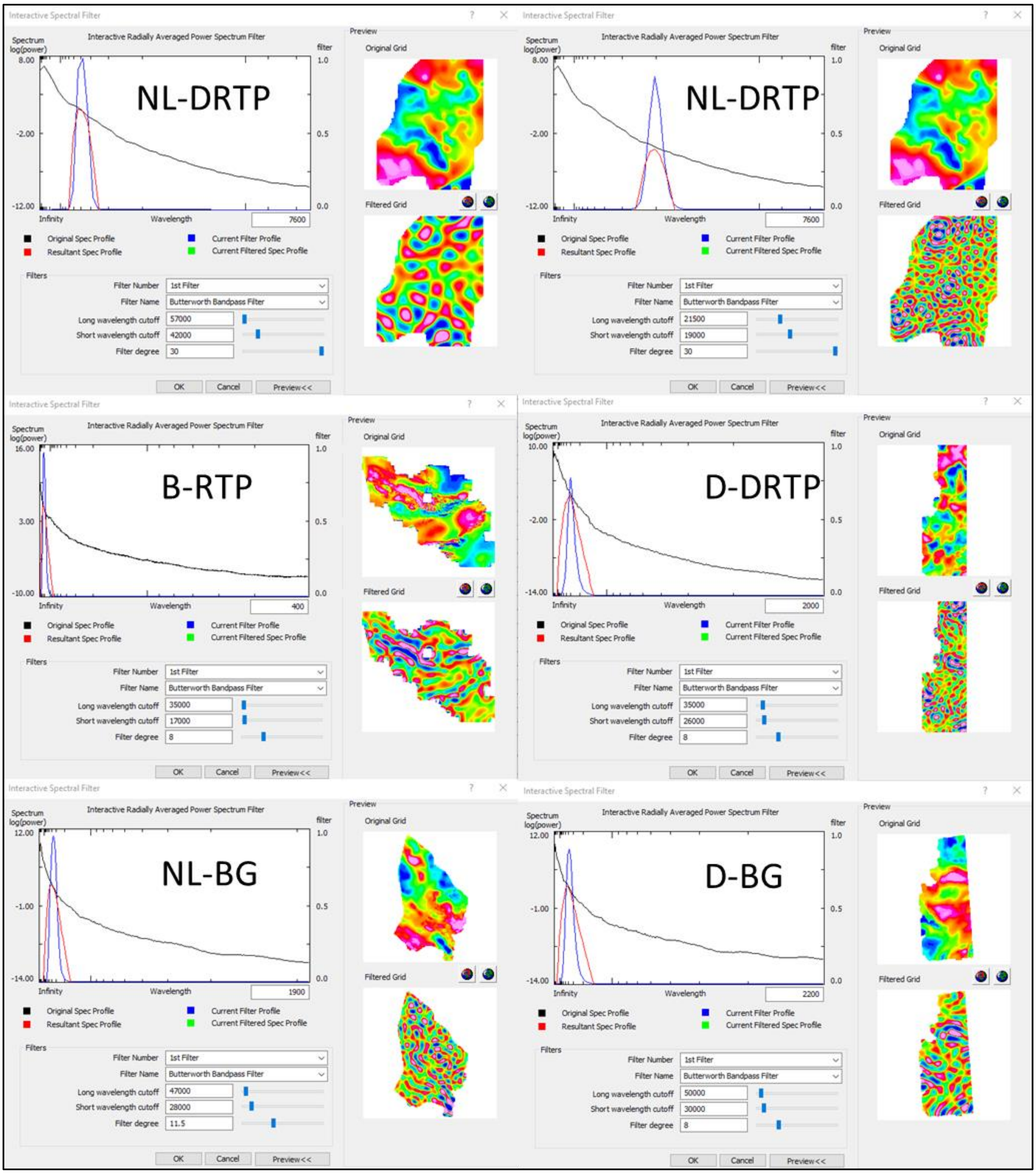

Figure 12. Radial Average Power Spectrum Analysis Band Pass filtering results examples. In each example the upper right map is the parent grid and the lower right map the result. Wavelengths in meters (NL = Netherlands, D = German and B = Belgium).

In order to identify geologically meaningful wavelength cut-off values for filtering, enhancing and interpretation, Radial Average Power Spectrum Analysis was performed on the DRTP and BG grids. Examples of the Radial Average Power Spectrum Analysis with Band Pass cut-off values are presented in Figure 12. Generally, the longer the wavelength, the deeper the origin of the anomaly. The shortest wavelengths (Nyquist range) in the Power Spectrum represent the noise in the data and are therefore excluded from the interpretation.

The wavelength (meters) cut-off values are then to be used for subsequent high pass (HP), low pass (LP) and (butterworth – BW) band pass (BP) filtering to respectively remove longer wavelengths, shorter wavelengths or isolate particular wavelengths from the full spectrum.

The reason for filtering is to not only remove noise of the frequency domain but mainly to identify geological meaningful anomalies at different depths. Figures 13 and 14 present examples of the results of BP filtering and subsequent HG and TDR computation on DRTP. Figures 15 and 16 present the anomaly wavelengths present in the LP8.5km and LP47km filters of the BG as examples. All filter maps and enhancements thereof with their contours and color bars are part of the ArcGIS geodatabase.

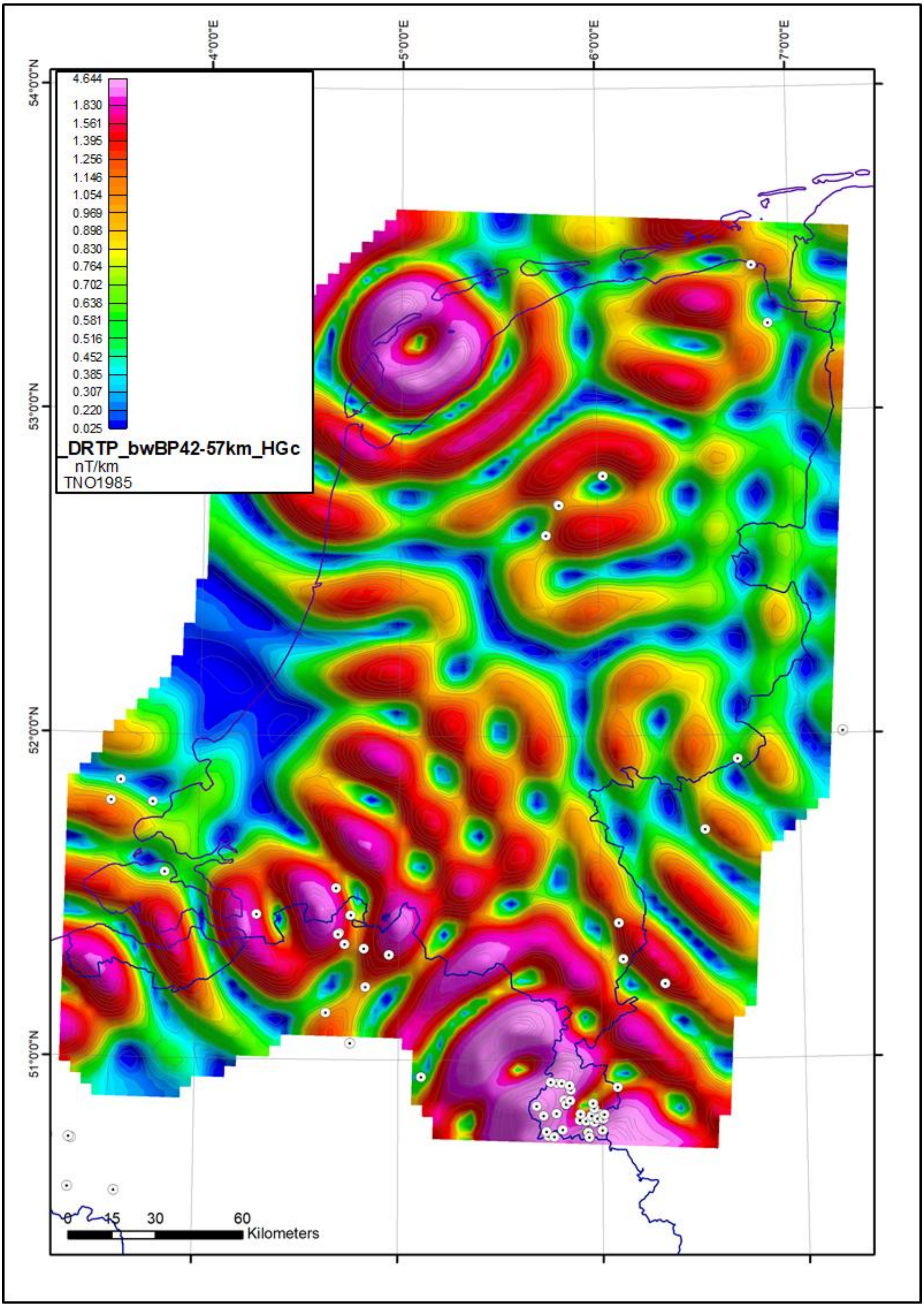

Figure 13. DRTP_BP42-57km_HG map. Ring shape anomalies stand out: Zuidwal and Bergen op Zoom intrusive complexes.

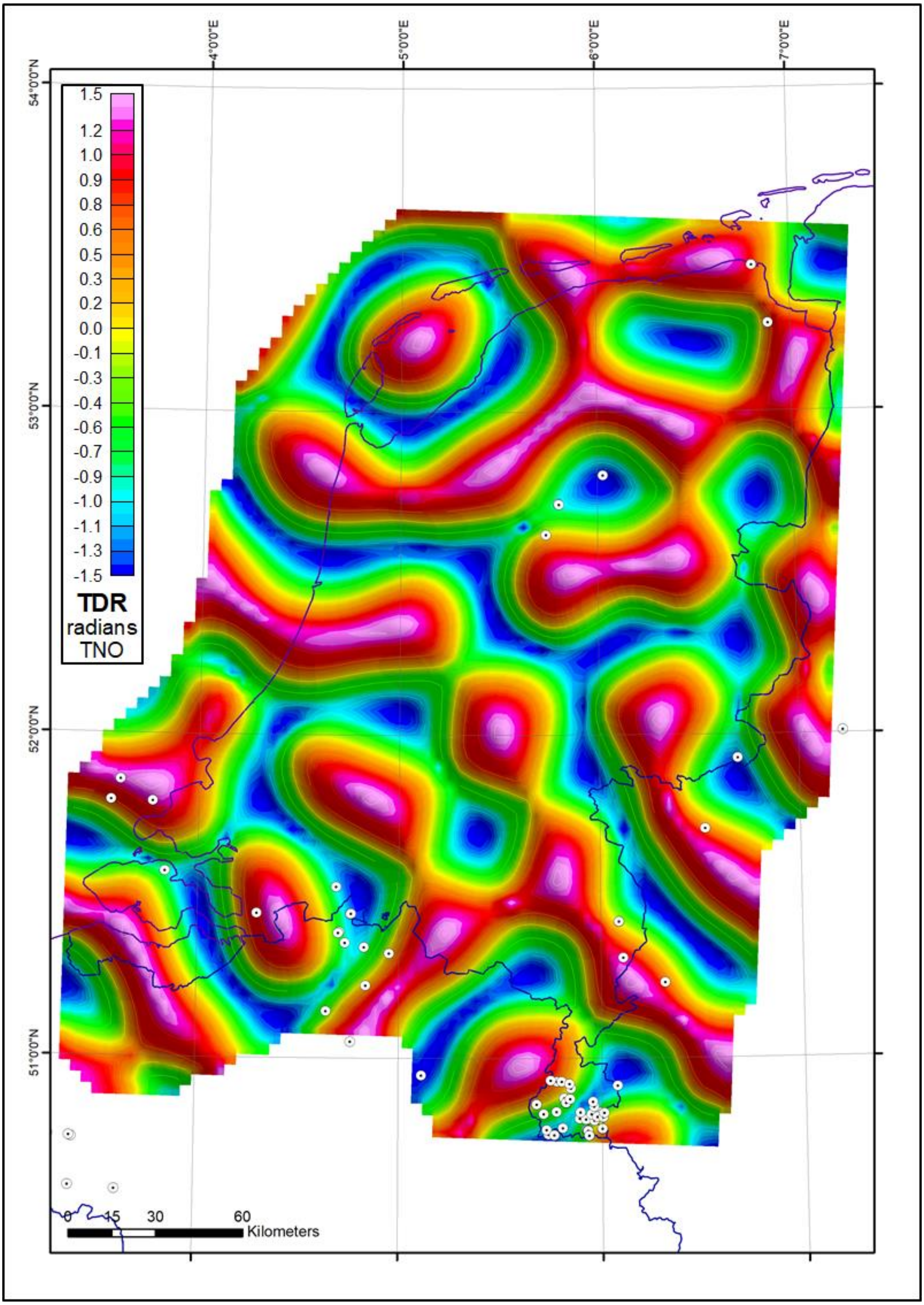

Figure 14. DRTP_BP42-57km_TDR map. Dome shape anomalies stand out: Zuidwal and Bergen op Zoom intrusive complexes.

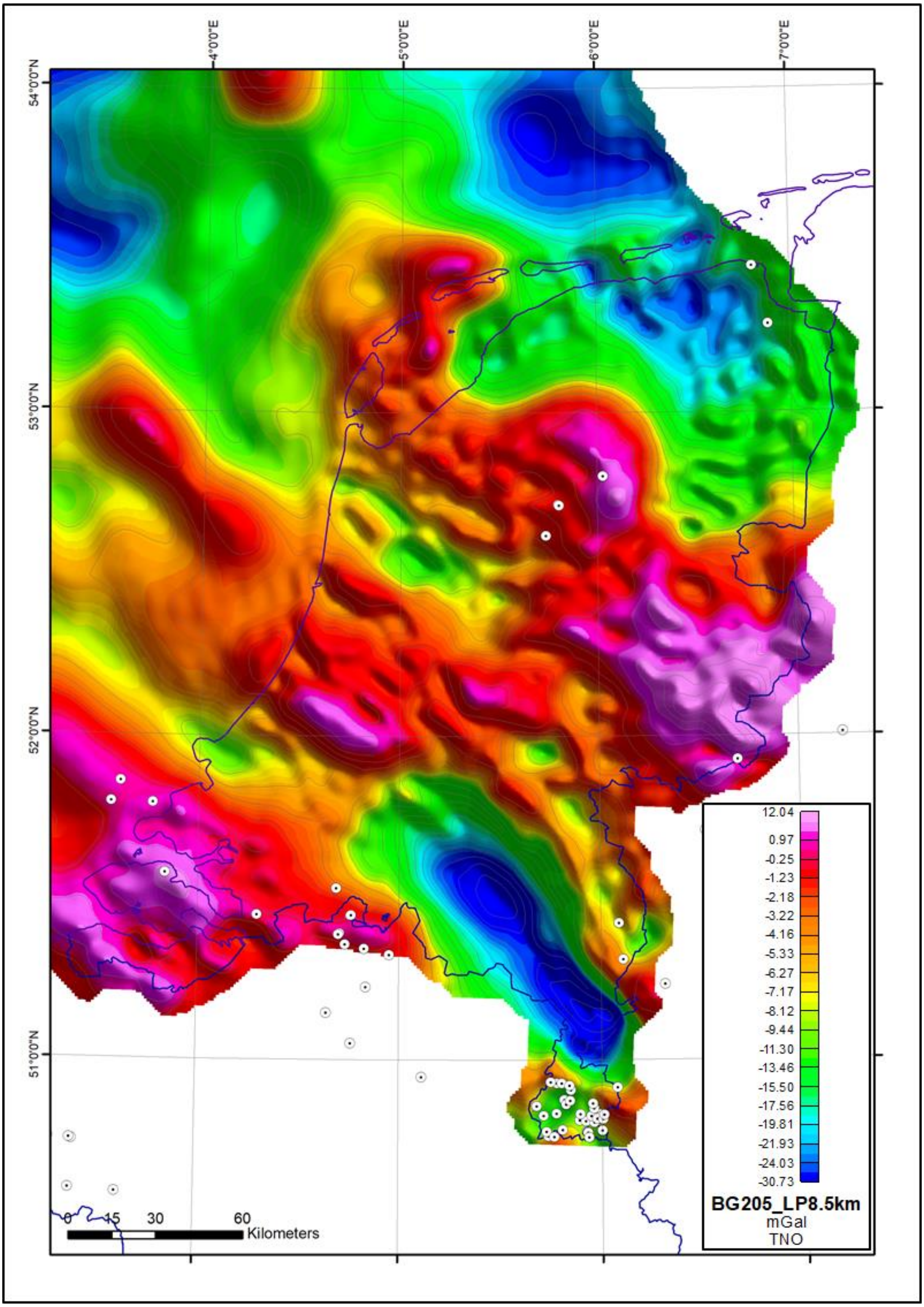

Figure 15. BG LP8.5km map. Wavelengths shorter than 8.5km have been removed.

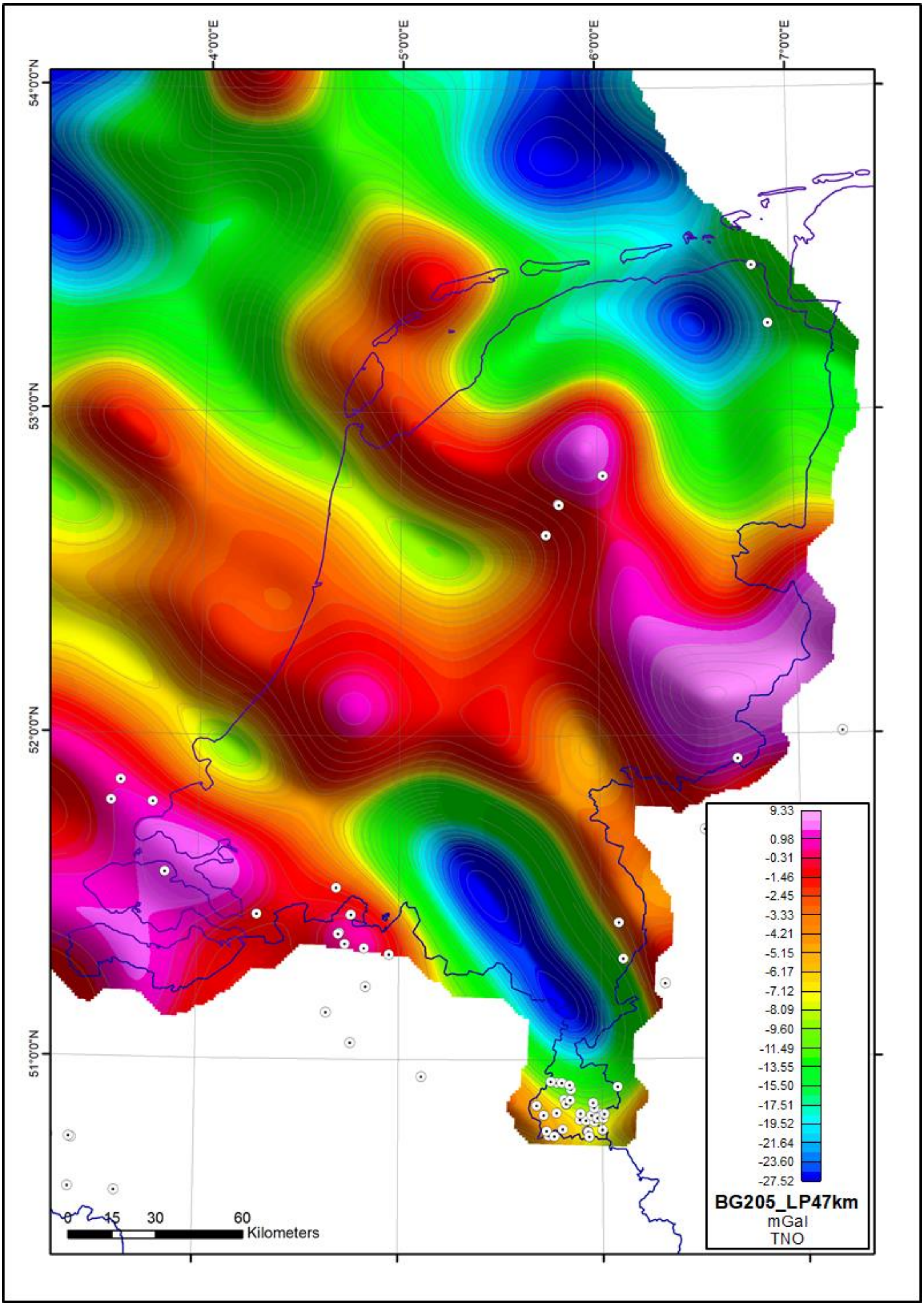

Figure 16. BG_LP47km map. Wavelengths shorter than 47km have been removed.

5.4. Filtering and Enhancements

Filtering and enhancement is undertaken to detect contacts between juxtaposed rocks of different density and/or susceptibility which allow for geological interpretation, often related to faults. The software used for the analysis and processing is Oasis Montaj-Geosoft. Interpretations were made in ArcGIS (ESRI). Of interest is not only the position of the fault plane inflexion line but also of the slope, or the depth of the contact. Slopes can be computed by the Tilt Derivative (TDR) and by the Horizontal Gradient (HG). The difference is that TDR is presented in radians and the TDR anomalies are not sensitive to depth whereas HG is presented in mGal/m or nT/km and is a gradient magnitude and sensitive to depth (Geosoft, 2019). The First Vertical Derivative (1VD) has its maximum above the centre of the causative body and is commonly applied to exaggerate the anomalies for visual inspection (Geosoft, 2019). Figure 17 demonstrates the filter responses in cross-section view to a causative body and its edges.

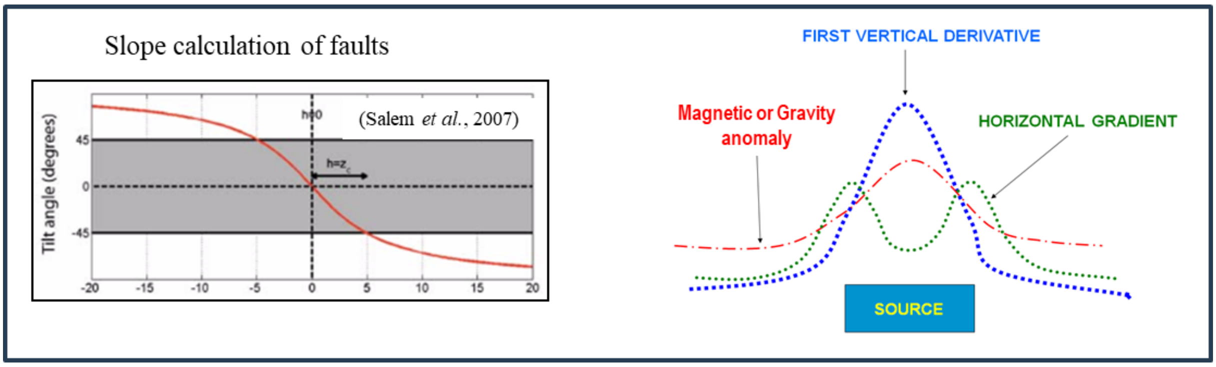

Figure 17. Explanation of the principle of Tilt (slope) Derivative (Angle), Horizontal Gradient and Vertical Derivative (modified after Salem et al., 2007).

5.5. Interpretation of igneous intrusions and lineaments

Igneous intrusions or extrusions often produce specific chaotic and/or circular HG magnetic anomaly patterns (Figure 13) whereas fault contacts tend to be more linear. With regards to the position of a fault inflexion line (Figure 17), standard practice is to follow the TDR zero-contour (yellow intervals in Figure 14). See Chapter Results for several examples.

5.6. Depth to Magnetic Source Detection

In seismic data dikes and sills are not always easy to distinguish from carbonates. Therefore, in exploration use is made of the gravity-density and magnetic-susceptibility properties of rocks to support seismic interpretation. One of the techniques available and applied in this project is the 3D Extended Euler Depth To Magnetic Source modelling. This technique is more suitable for detection of depth to a magnetic source in 3D than the Werner Deconvolution or Peter's Half slope techniques, which are more applicable to 2D and 1D analysis (Geosoft, 2019). First, the processing workflow requires input of grid derivatives of the RTP or DRTP such as first horizontal derivatives in X and Y directions, 1HDX and 1HDY respectively, and the first vertical derivative 1VD.

5.7 Structural Indices

Next, the source shape (geometry) Structural Index has to be chosen per run. This requires apriori choices on what kind of geological feature shall be detected. For the in depth description and explanation on the method, please consult the Geosoft website. Table 4 lists the Structural Indices and various geometries depending on gravity or magnetic data utilization.

Geologic model	number of infinite dimensions	Magnetic SI	Gravity SI
sphere	0	3	2
pipe	1 (z)	2	1
horizontal cylinder	1 (x-y)	2	1
dyke	2 (z and x-y)	1	0
sill	2 (x and y)	1	0
contact	3 (x, y and z)	0	NA

Table 4. Structural indices and related geometries in gravity and magnetic data (source: Geosoft, 2019).

In this project the objective is to detect dikes and magnetic basement surfaces (contacts). Therefore the Structural Indices of 0.1 and 0.5 have been chosen for the contacts, and Structural Indices of 1.0 and 2.0 for the dikes.
A SI is appropriate for a certain model or feature when the cluster of solutions produced by a run is tight and focused.

6 RESULTS

6.1. Interpretation Of Rock Types – Qualitative

In this study, the objective of the interpretation and modelling of gravity and magnetic data is to identify and map Dinantian carbonate build-ups, igneous intrusions and deep structures. This potentially supports the seismic interpretation, especially in areas where coverage of seismic data is scarce and or the seismic data has not been imaged deep enough. Igneous intrusions are of interest because igneous intrusions have the capability to trigger limestone dolomitization, a process that improves the reservoir quality of limestone (Van Hulten, 2012).

In seismic data the difference between carbonates and basalts for instance is not always evident, yielding an uncertain interpretation. Inferring lithologies from gravity and magnetic data, requires rock properties information such as magnetic susceptibility and density (Prieto, 1998; Van Heiningen *et al.*, 2018). Especially density information from density logs, corrected sidewall or core samples provides robust but local information. Alternatively, one needs to assume value ranges for these parameters based on examples of key lithologies (Table 5).

Rock type	density range (kg/m3)	avg. density (kg/m3)	susceptibility range (µcgs)	avg. susceptibility (µcgs)
limestone	2,04-3,04	2,54	0,002-0,280	0,141
dolomite	2,43-2,97	2,70	0-0,075	0,038
basalt	1,78-3,06	2,74	1,290-6,050	3,670
metamorphic basement	2,39-3,09	2,74	0-5,824	2,912
crystalline basement	2,73-2,85	2,79	2,350-2,410	2,380

Table 5. Main rock types under investigation.

It is recommended to undertake 2D gravity & magnetic modelling to arrive at a quantitative geological interpretation. Figure 18 presents a qualitative geological interpretation that assumes a relatively low density sedimentary cover on high density limestones, highly magnetic and dense basement and known presence of low density salt accumulations.

Candidate locations for low susceptible - high density limestone formations such as the Dinantian reef and platform carbonates are marked with “?” in Figure 18 and will be suject to further quantitative interpretation.
A gravity-low with magnetic-low is typical for thick salt accumulation. In Figure 18 it can be seen that in the North of The Netherlands, there is a significant effect on gravity and magnetic by the thick Zechstein salt sequence resulting in a BG low. There the thick sedimentary sequence yields a magnetic low (Figure 19) due to the deep Magnetic Basement.

A situation of a gravity-high with magnetic-high acompanied by circular to chaotic HG anomalies are indicative of an igneous intrusion. The host rock sediments for an igneous intrusion in general are less dense and almost not magnetic susceptible. When igneous rock is intruded into crystalline basement however, this relationship is reverse at the Basement-sediment interface because crystalline basement is denser than the intrusion. The sign of the magnetic anomaly depends on the composition of the basement, i.e., an intrusion can be represented as a relative magnetic high or low.

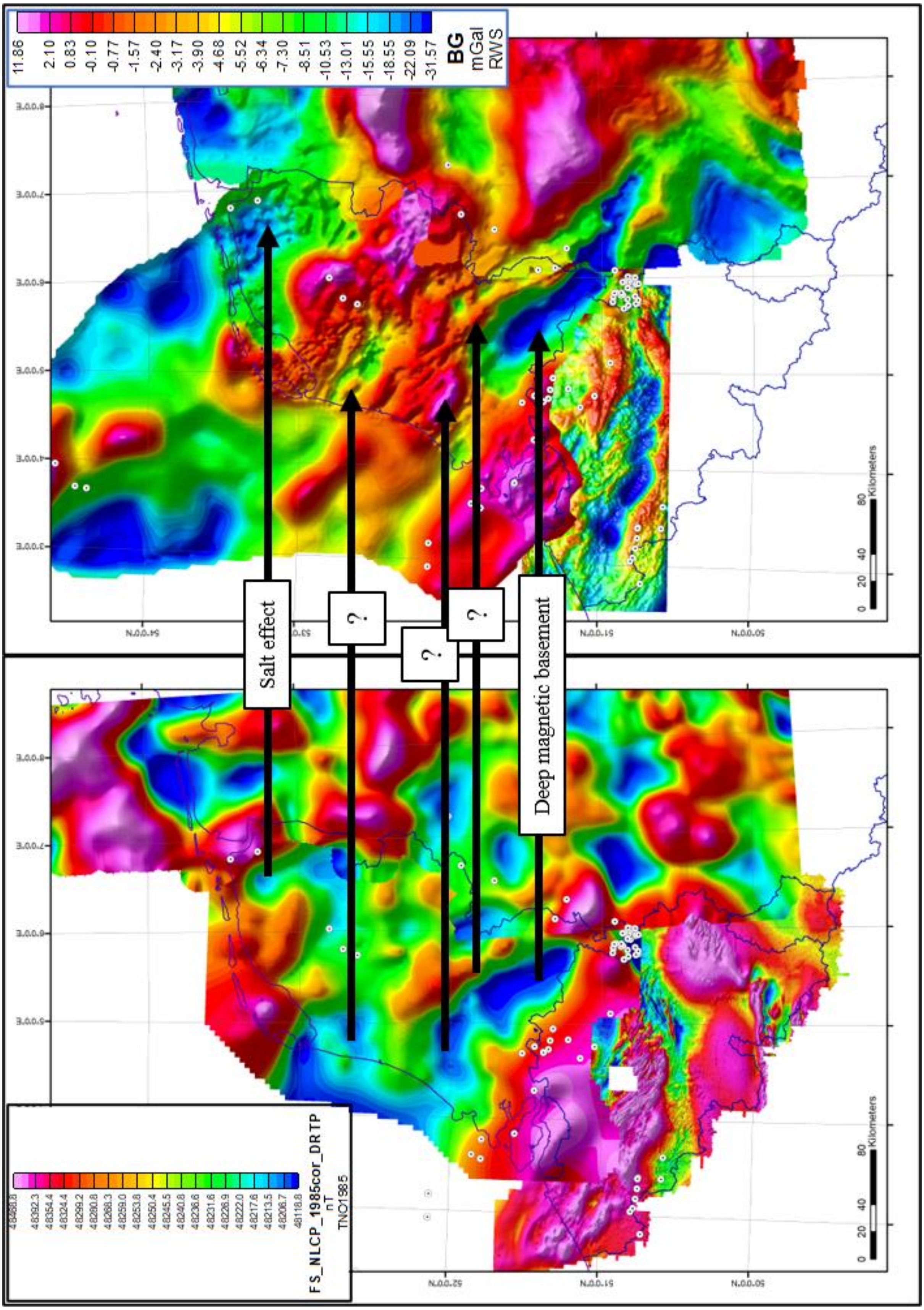

Figure 18. Interpretation rationale comparing magnetic (left) and gravity (right) anomalies.

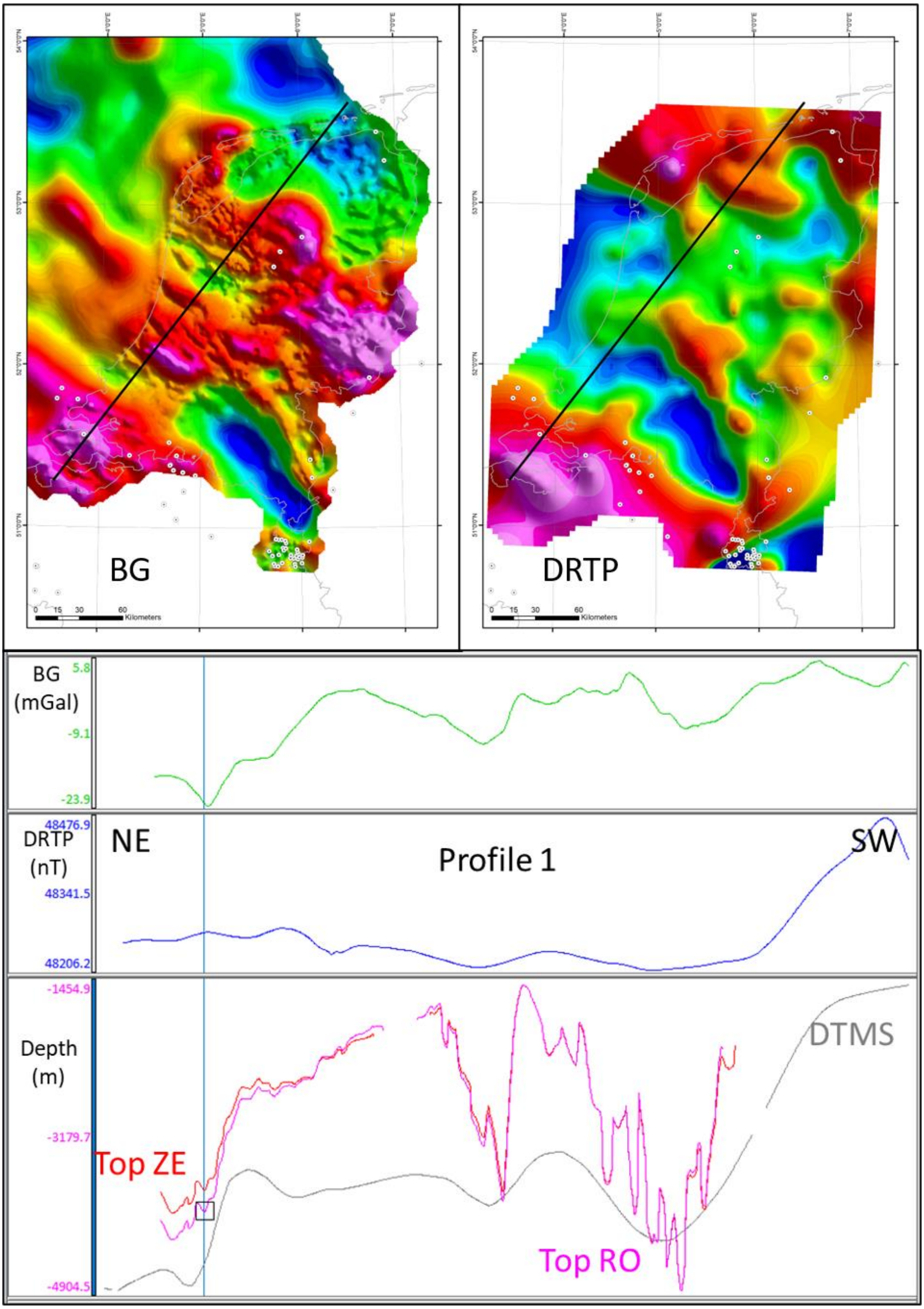

Figure 19. BG and DRTP profile demonstrating salt thickness effect on gravity.

6.2 Carbonate Build-ups

Confirmed carbonate build-ups of Dinantian age are those penetrated by wells and which were subject of petrophysical analysis (Carlson, 2019 - SCAN). In all figures from Figure 8 onwards, the Dinantian wells are indicated with white dots on the maps.
Since gravity and magnetic anomalies are the result of the sum of sub-surface mass and susceptibilty respectively (super-position effect), known carbonate build-ups do not always have the same gravity and magnetic signature. Another complicating factor for the comparison is that the gravity and magnetic surveys have a very different set up and density.

A number of scenarios are described here:

- The UHM-02 build-up resides on a magnetic-high and a gravity-medium. An explanation may be that the site is supported by a basement high, but the thick Zechstein salt succession supresses the gravity.
- At LTG-01 there is a magnetic-low and a gravity high, which confirms the carbonate presence and a deeper magnetic source.
- At WSK-01 a magnetic-medium and gravity high may be in agreement with a Dinantian carbonate structure that is expected to be present according to Mozafari et al. (2019). However, there are also igneous intrusions interpreted on seismic data and encountered in the well (Ten Veen *et al*., 2019). Although thin, these intrusions may be capable of producing a magnetic-medium. In addition, the basement is not much deeper than TD at WSK-01. Therefore the magnetic signal can also be enforced overall by the magnetic basement.
- KSL-02 is characterised by a magnetic-high and a gravity-high, located on the eastern flank of what is thought to be a LBM-basement high at the south side of the RVG. The LBM-basement is composed of lower Palezoic metamorphosed rocks with a relatively strong magnetic susceptibility compared to the LBM-sedimentary cover.
- At KTG-01, where the Dianantian carbonates developed in a platform facies, both a magnetic- and a gravity-high characterise the subsurface. Most likely the LBM basement gravity and magnetic signals overrule the signal of the relatively thin sedimentary cover.
- The candidate locations for limestone formations (areas with low susceptible - high density, marked with “?”in Figure 20) have to be further investigated when new seismic, gravity and magnetic data becomes available. An example is the pronounced WNW-ESE trending gravity-high and magnetic-low at 52.0°N-4.7°E (Reeuwijk), and a similar observation is located at 52.6°N-4.9°E (Noord-Beemster). In line with the Noord Beemster location, also the sub-surface of the Amsterdam-region and the FP have good potential to contain large Dinantian carbonates build-ups.

6.3 Igneous Intrusions

Igneous intrusions have been manually digitized on contours of DRTP HG-maxima and verified against the BG filter maps (best practice industry standard: e.g. Reeves, 2005; Gibson and Milligam, 1998). The interpreted polygons obtained from long wavelength maps are interpreted to be deep structural or deep stratigraphical contacts; those from shorter wavelengths to represent shallower contacts (Reeves, 2005).

Figures 20 and 21 present igneous intrusive complexes mapped on two different HG filter maps and compared to the corresponding filter restults on the BG anomalies. The Bergen Op Zoom (BOZ), Zuidwal (ZDW) and Kastanjelaan (KSL) igneous complexes are evident circular/ellipsoid polygonal

DRTP-HG anomalies. Hereafter, the igneous intrusions interpreted on DRTP and BG grids are referred to as "Gm Igneous intrusions".

When the GM Igneous intrusions are compared to intrusions penetrated by wells, reported and analysed by Van Bergen & Sissingh (2007), it can be deducted that intrusions penetrated by wells, if of large enough lateral dimensions and thick enough, correlate with GM Igneous intrusions (Figure 22). Examples are ZDW, GEL-03 and BHH-01. The on BG and DRTP interpreted igneous intrusions east of UHM-02 and east of KSL-02 are confirmed by Van Bergen & Sissingh (2007). Surprisingly, the large Rotliegend volcanic province in the eastern part of Drenthe, mentioned by Van Bergen & Sissingh (2007), for a large part did not yield any magnetic and gravity high. Possibly, there the volcanics are of a too low susceptibility and too low density contrast and perhaps too thin to be detected by the magnetic and gravity data used in this study.

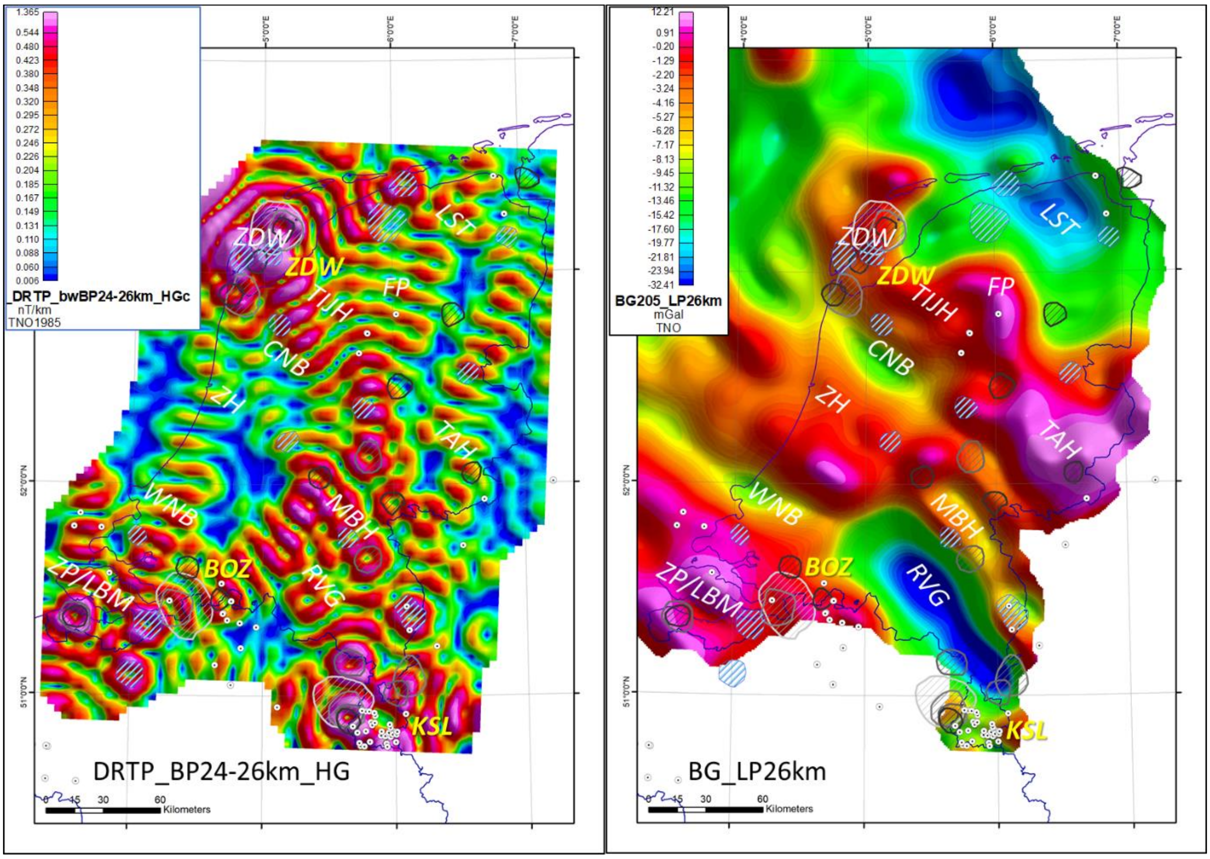

Figure 20. GM Igneous intrusions mapped on DRTP_BP24-26km_HG compared to BG_LP26km anomalies. For the legend see Figure 23.

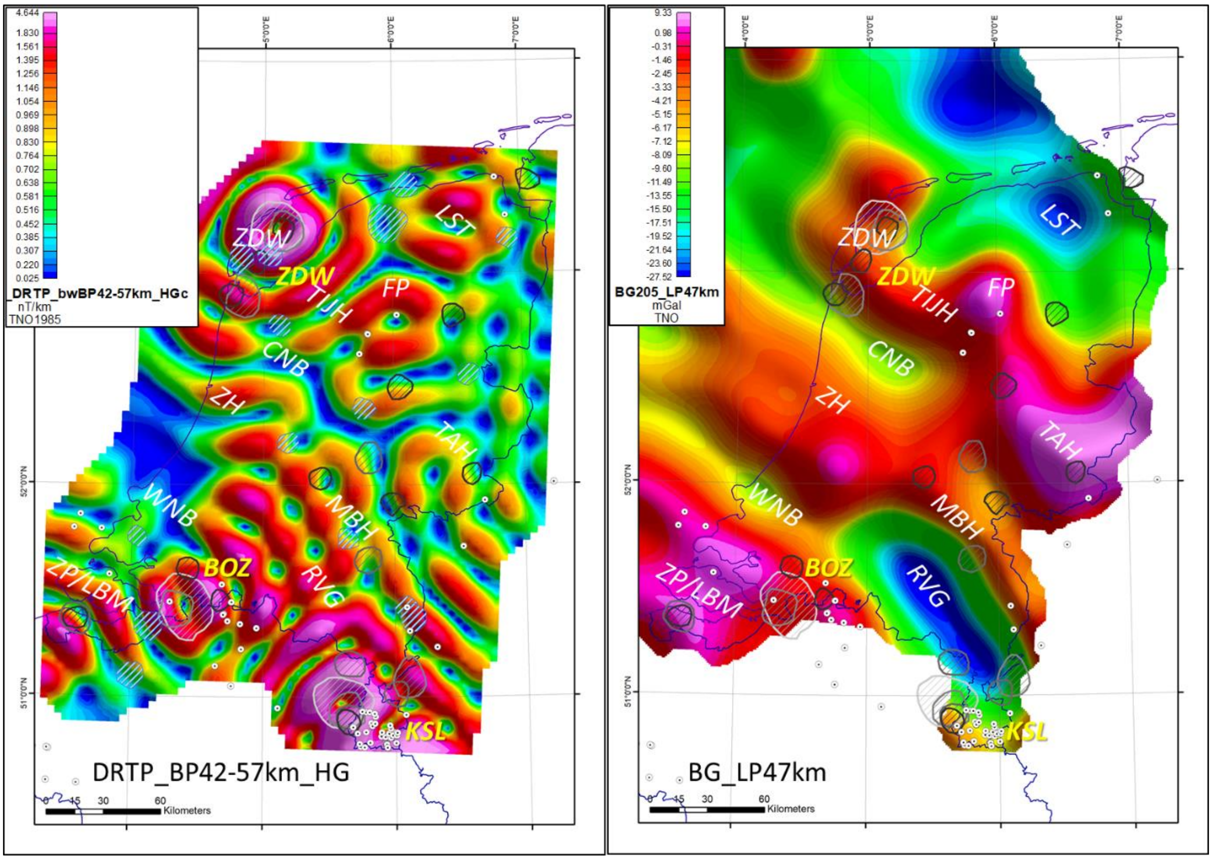

Figure 21. GM Igneous intrusions mapped on DRTP_BP42-57km_HG (left) compared to BG_LP47km anomalies (right). For the legend see Figure 23.

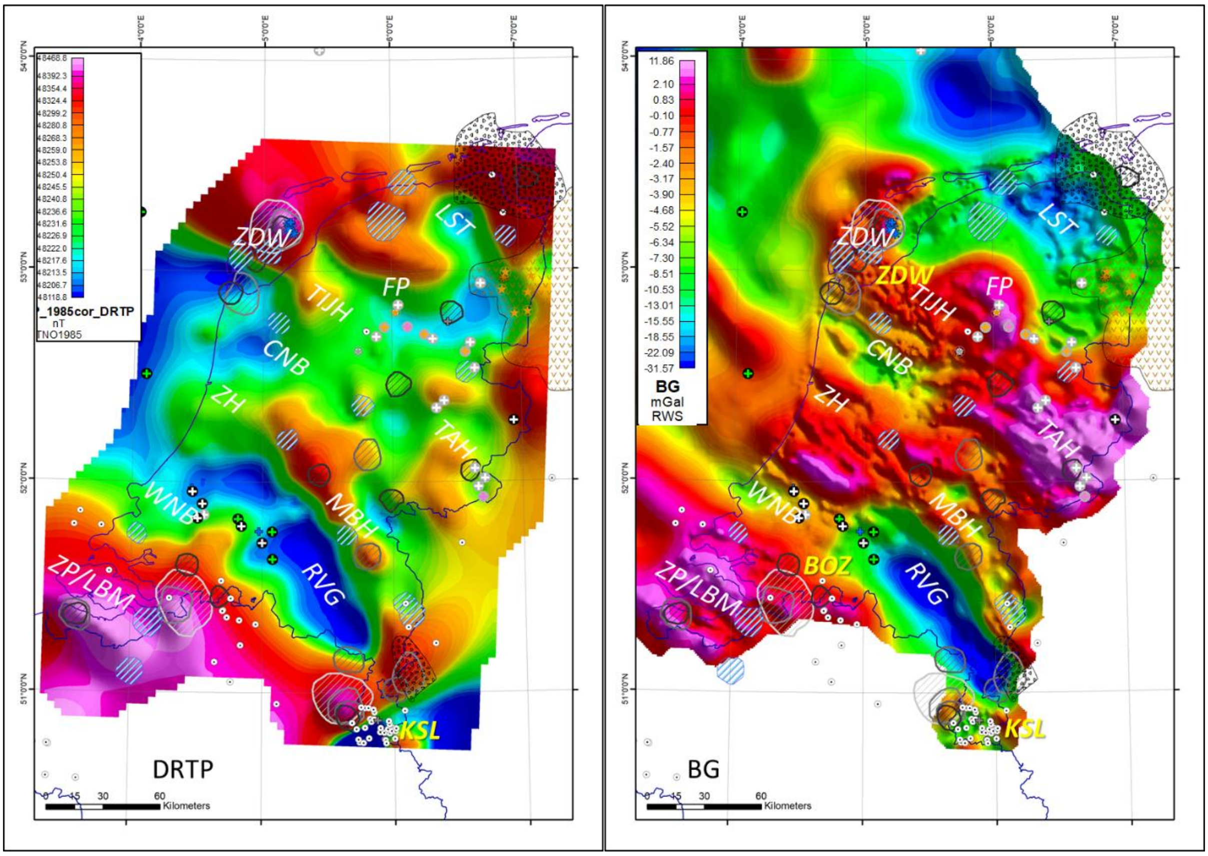

Figure 22 (previous page). GM Igneous intrusions mapped on DRTP (left) and BG (right) compared to Van Bergen & Sissingh (2007) igneous intrusions reported from wells. For the legend see Figure 23

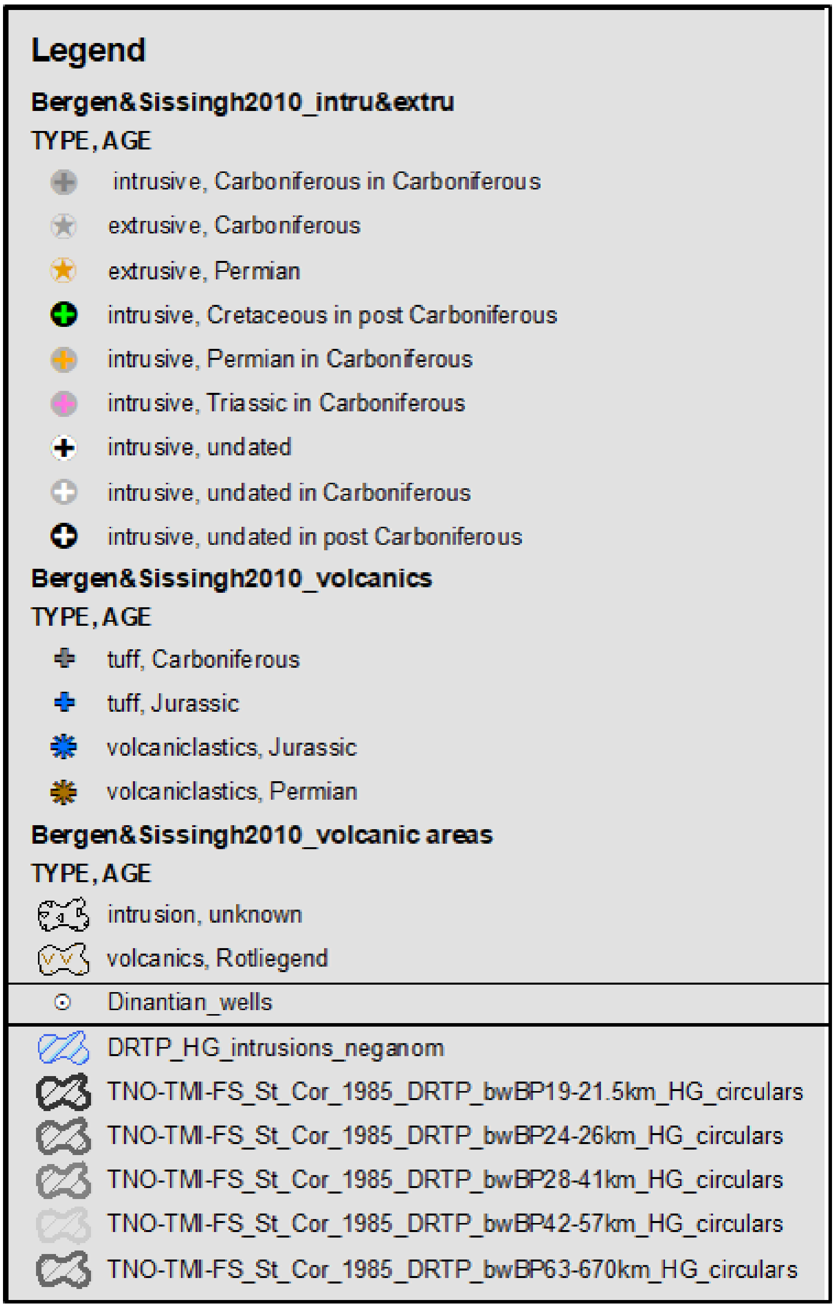

Figure 23. Legend to figures 20 to 22.Depth To Magnetic Source Modelling – Igneous Intrusions & Magnetic Basement

6.2. Depth To Magnetic Source – Igneous Intrusions

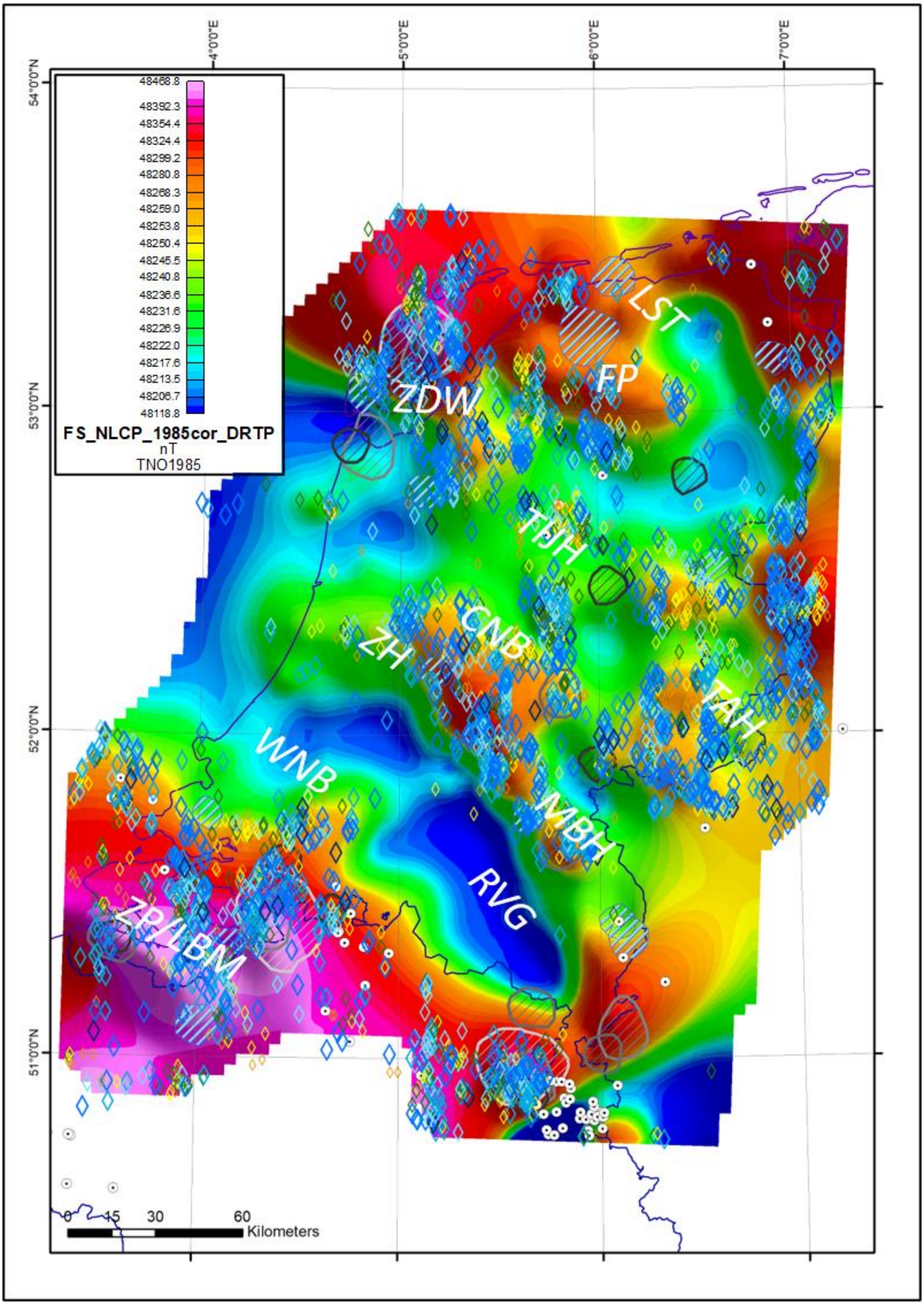

Figure 24. DTMS-dikes SI2.0 & 1.0 solutions on DRTP compared to GM igneous intrusions.

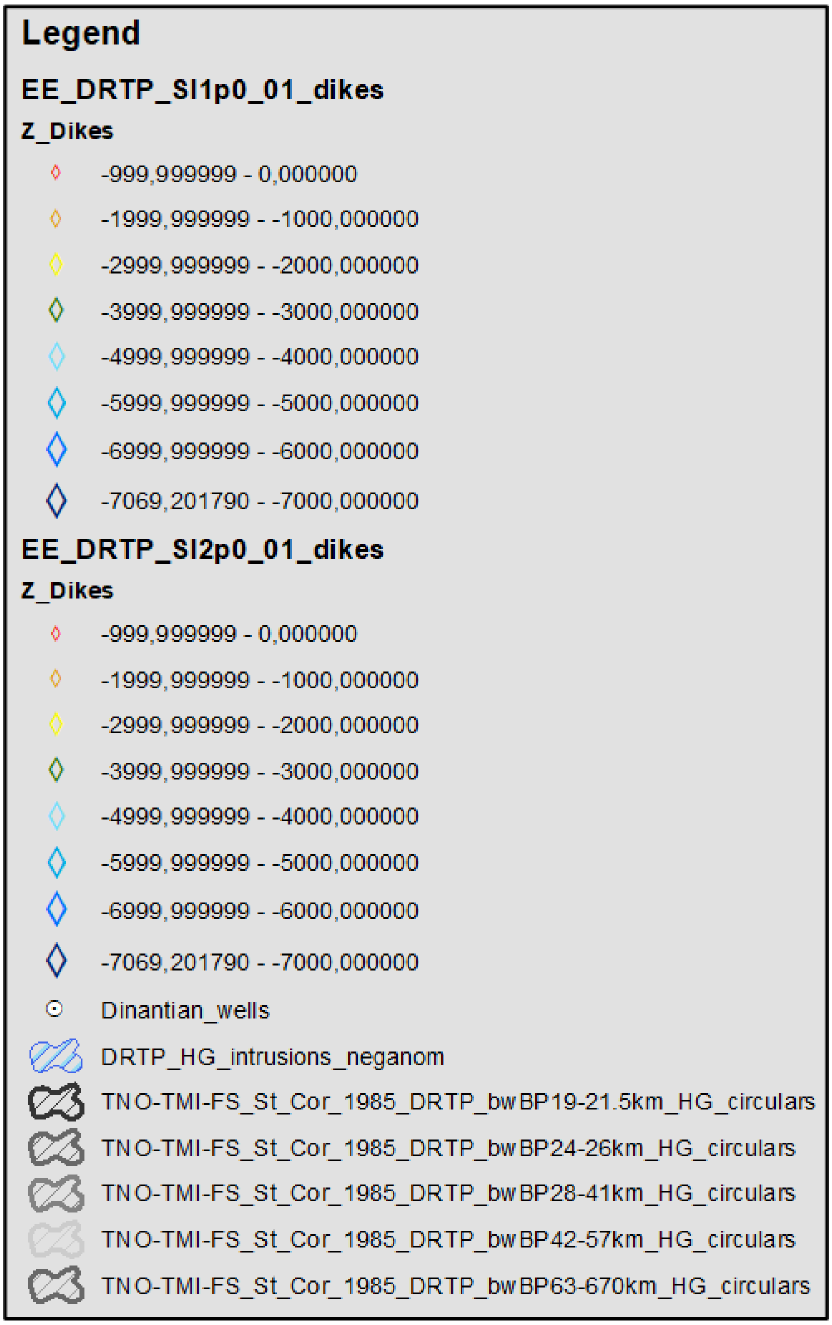

Figure 25. Legend to figure 24.

In addition to the interpretation of igneous intrusions on DRTP and BG filter maps, which resulted in the polygons, the Depth To Magnetic Source technique was applied to detect dikes and sills, using the Structural Indices 1.0 and 2.0. The result is presented in Figure 24.

It can be observed that dike solutions (diamonds) locally correspond to edges of mapped igneous complexes (polygons) and are situated on the flanks of or on top of the magnetic highs. Also, dike solutions align along structural trends such as the PBF-MBH. Few dikes have been detected in the deep part of the RVG, LST, LSB and WNB. The depth range of the dike solutions is between 8 and 1 km sub-surface.

6.3. Depth To Magnetic Source Magnetic Basement

Thus the SI 0.1 and 0.5 depth solutions for contacts and surfaces are the input for the generation of the Depth To Magnetic Basement grid. Prior to gridding the depth solutions, first the depth solutions data set had to be checked for outliers that plot within established TNO-DGM5 formations. In a non-thrusted geological setting, the Top of Magnetic Basement depth solutions shall not plot within the sedimentary section. Despite the inversion phases that have taken place in the Netherlands sub-surface over geological time, not much over-thrusting is assumed to exist which could place DTMS Magnetic Basement depth solutions within the sedimentary section in the Netherlands sub-surface. Figure 26 presents the resultant surface for the Top Magnetic Basement with the depth solutions as circles for the SI 0.1 and SI 0.5.

It can be observed that the general morphology of the Magnetic Basement corresponds to the known basement highs and basins. Though, given the low data density of the underlying magnetic data set, more detail can be obtained on the Magnetic Basement surface with a new and more dense magnetic survey that would cover the complete onshore.

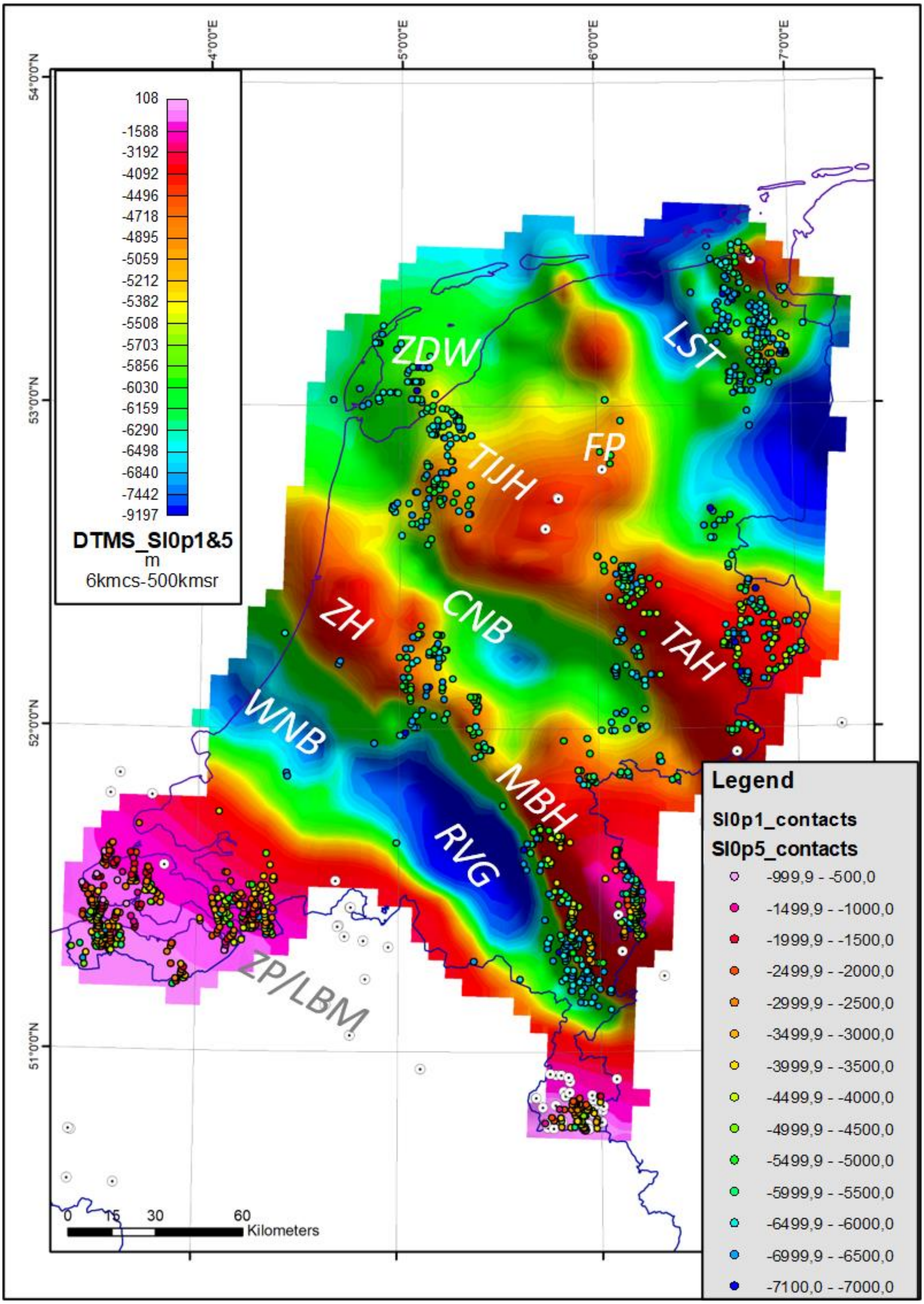

Figure 26. DTMS-contacts SI0.5 & 0.1 depth solutions on the resultant DTMS-Magnetic Basement depth grid.

6.4. Interpretation Of Graviy & Magnetic Integrated Structures

Lineaments have been manually digitized on BG-TDR zero-contours (Figures 27 and 28) and on DRTP-HG maxima (Figure 29), following standard industry best practice (e.g. Gibson and Millegan, 1998). The lineaments are to be regarded as the inflexion lines of the faults planes or stratigraphic contacts that separate juxtaposed high from low density rocks and high from low susceptible rocks (Salem *et al*., 2007 and Prieto, 1998). Lineaments obtained from long wavelength maps are inferred to be deep contacts, whereas those from shorter wavelength maps to be shallower contacts.

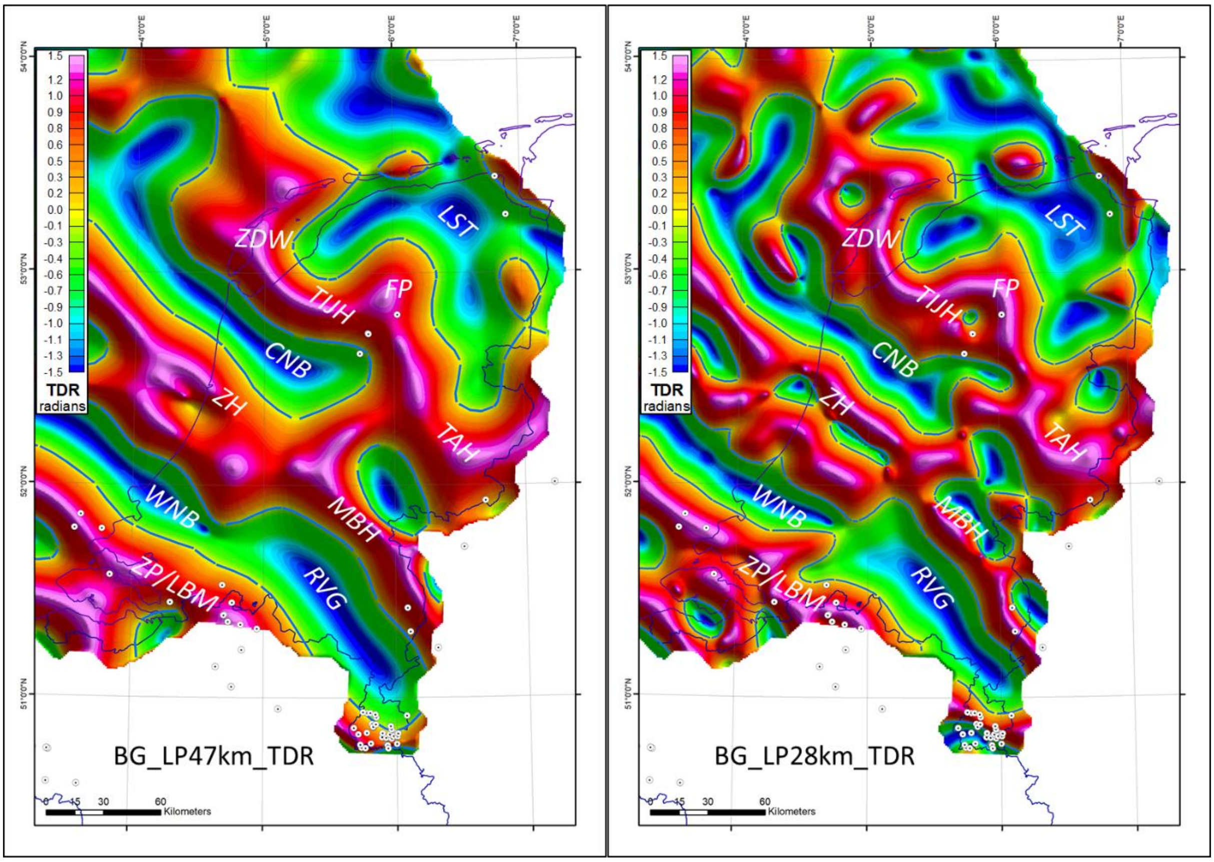

Figure 27. Lineaments interpreted on BG-LP47km_TDR and on BG-LP28km_TDR.

Well-known structural highs stand out as gravity highs and magnetic highs (Figures 27, 28 and 29): Zandvoort High (ZH), Texel-IJselmeer High (TIJH), Friesland Platform (FP), Twente-Achterhoek High (TAH), Maasbommel High (MBH) and Zeeland Platform-London Brabant Massif (ZP-LBM). The Roer Valley Graben (RVG), West Netherlands Basin (WNB), Central Netherlands Basins (CNB) and Lauwers Sea Trough (LST) appear as gravity lows due to their thick, low density sediment cover with a deep, dense basement and as magnetic lows due to deep-seated magnetic basement covered by magnetic low sediments. Igneous intrusions in the sedimentary cover may change this rule of thumb locally.

All the BG and DRTP lineaments have been combined in the "GM Integrated structures" data set. The GM Integrated structures rose diagram is presented in Figure 30. In this rose diagram it can be observed that NW-SE orientations dominate over N-S, WSW-ENE and NE-SW successively.

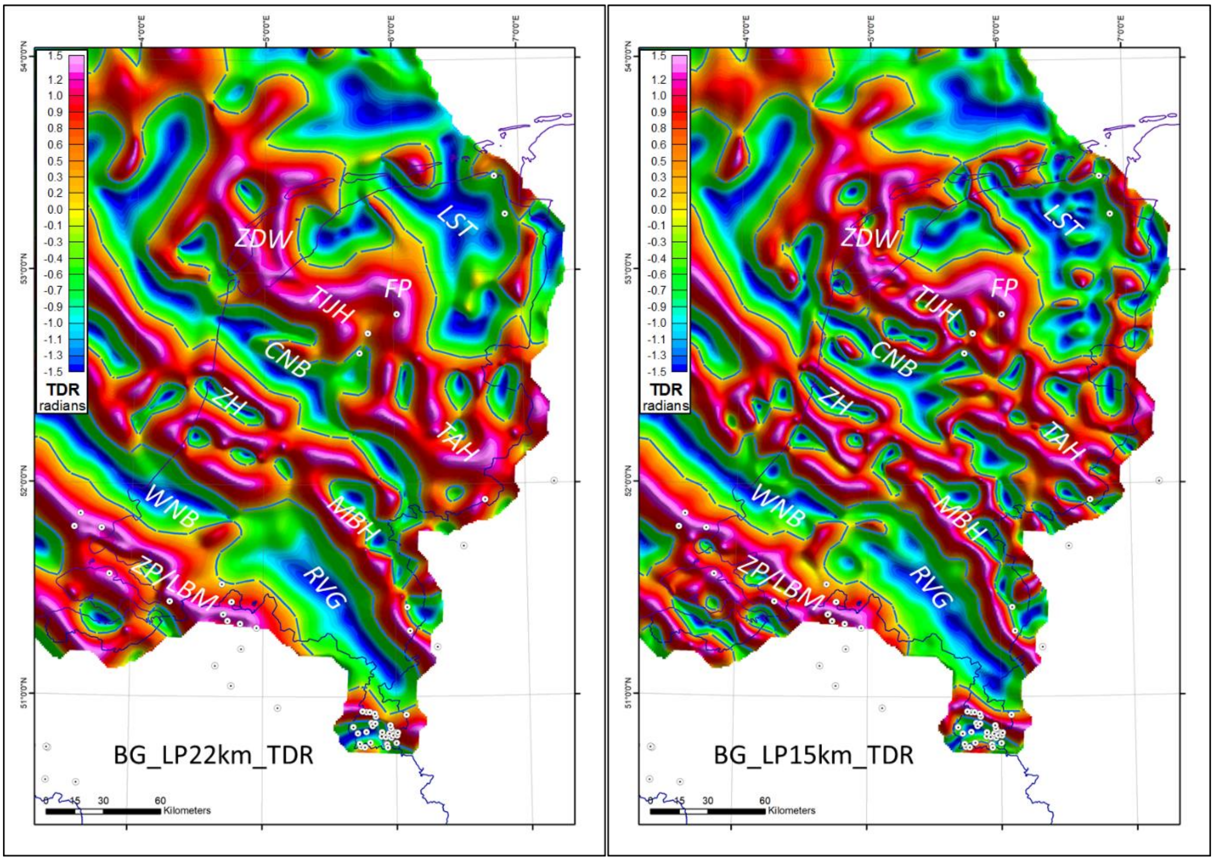

Figure 28. Lineaments interpreted on BG-LP22km_TDR and on BG-LP15km_TDR.

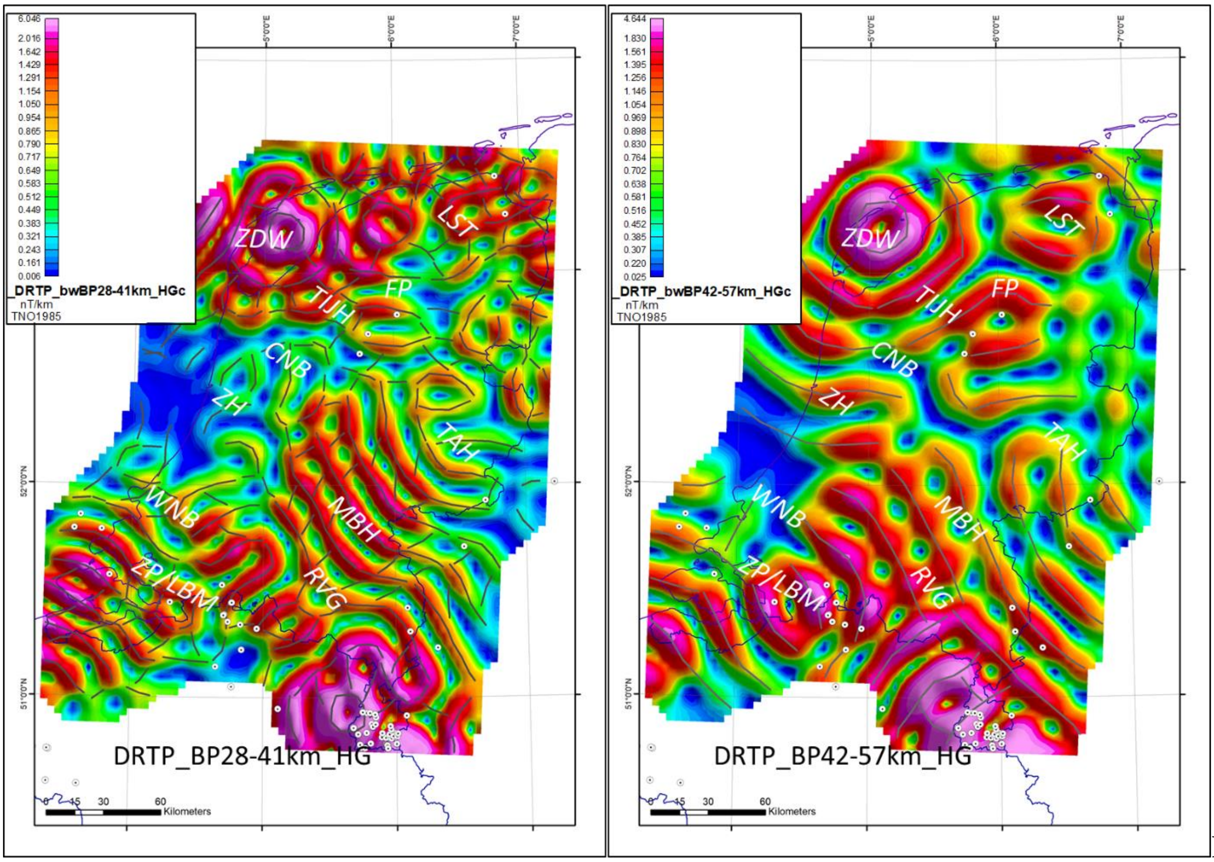

Figure 29. Lineaments interpreted on DRTP-BP28-41km_HG & DRTP-BP42-57km_HG maxima.

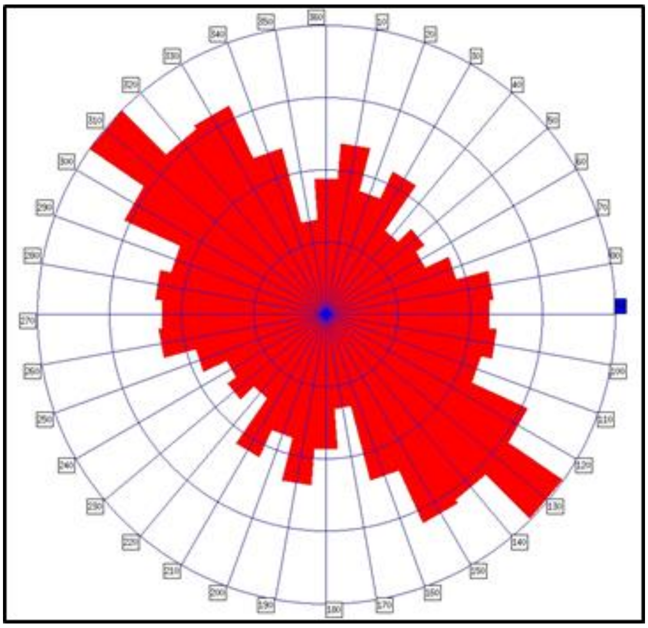

Figure 30. Rose diagram of the GM Integrated structures data set.

In map view, the following structural relationships become clear on DRTP (Figure 31), BG (Figure 32) and Magnetic Basement (Figure 33): Regional and continuous NE-SW (and NNE-SSW in the eastern RVG) structures can be observed that offset shorter and discontinuous NW-SE structures in the RVG – WNB region. This relationship is witnessed by the left-lateral displacement in the LBM flank with the RVG-WNB and in the MBH-ZH and even TAH-TIJH. The main structures of the LST are NW-SE, cross-cutting NE-SW structures.

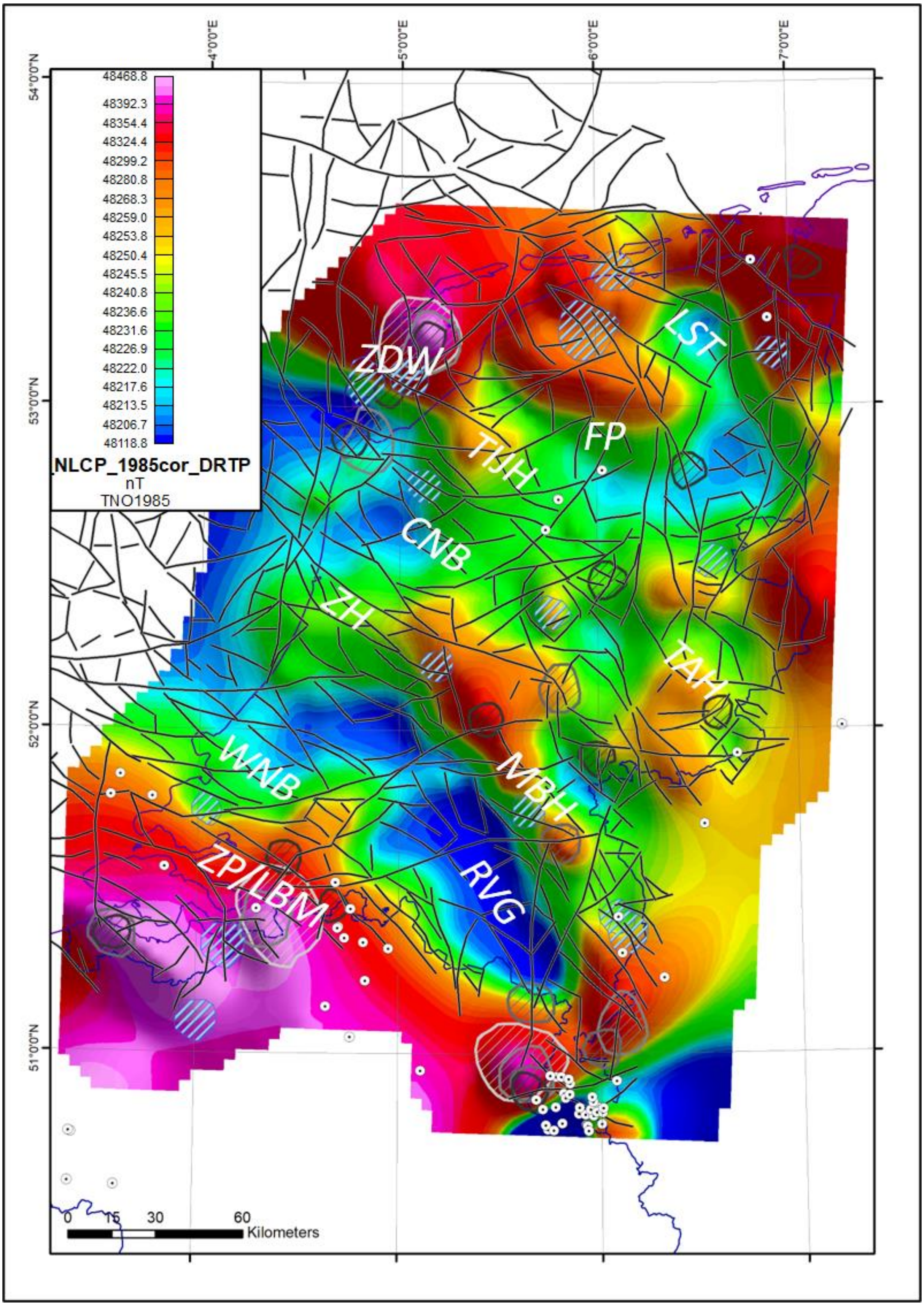

Figure 31. DRTP overlain by the GM Integrated structures and GM Igneous intrusions.

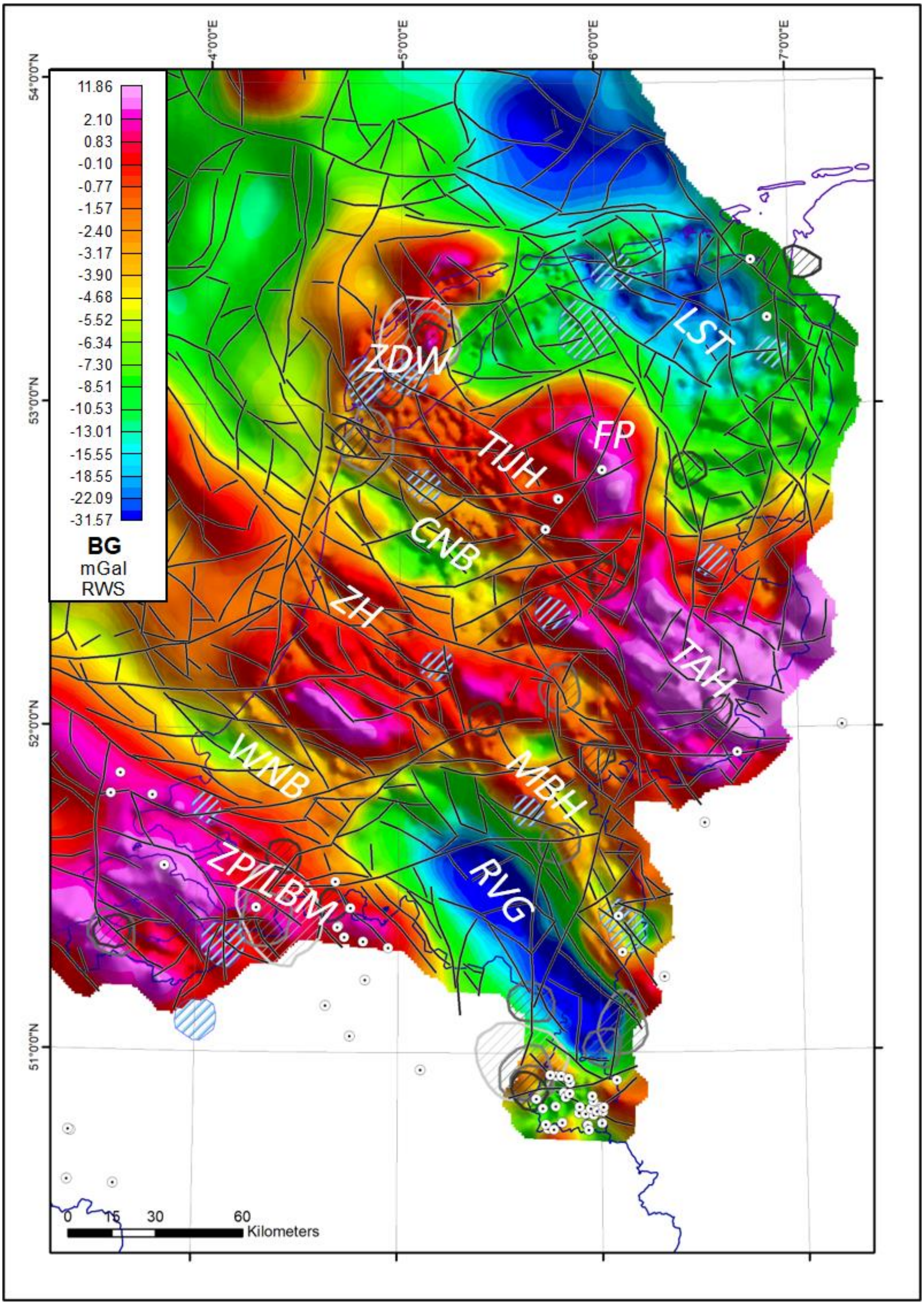

Figure 32. BG overlain by the GM Integrated structures and GM Igneous intrusions.

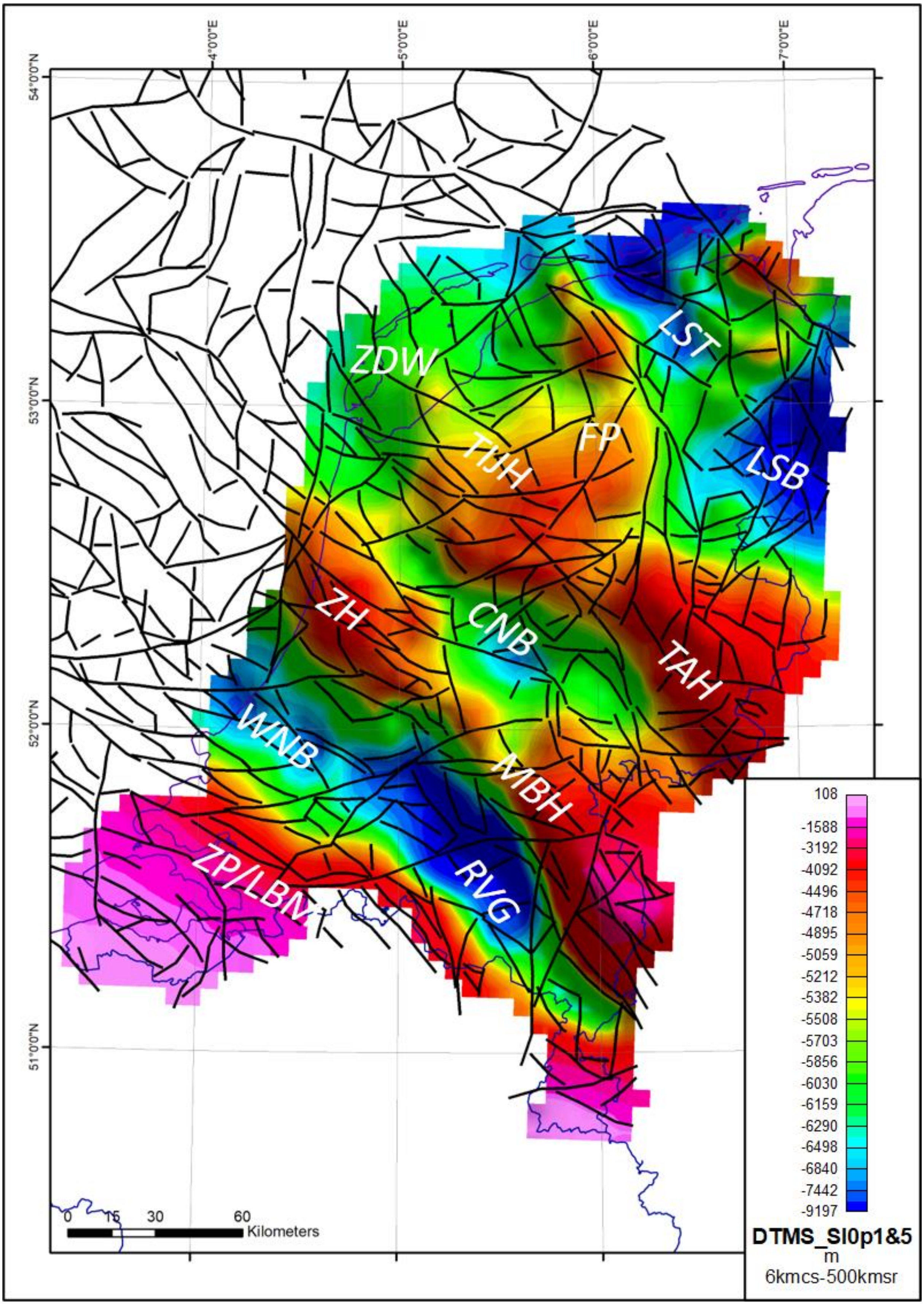

Figure 33. Depth to Top Magnetic Basement overlain with GM Integrated structures.

7 SYNTHESIS

7.1. Comparison GM igneous intrusions to seismic interpretation igneous intrusions

An attempt was made to investigate if the DTMS dikes and sills could be identified in the seismic data. In one of the cases, near the WSK-01 well, volcanics could be inferred from the DTMS-dike depth solutions in the seismic data (Figure 34). Van Bergen and Sissingh (2007) reported a Triassic intrusion in the Carboniferous section in well WSK-01. The intrusion could also be seen on the 2D seismic data lines 751069-751066 (Figure 34) where they are represented as diachronous reflections at 750ms and 2000ms that appear to be fault related. Other intrusions penetrated by wells and reported on by Van Bergen and Sissingh (2007) are present in the nearby wells COR-X, GEL-3, GEL-5.

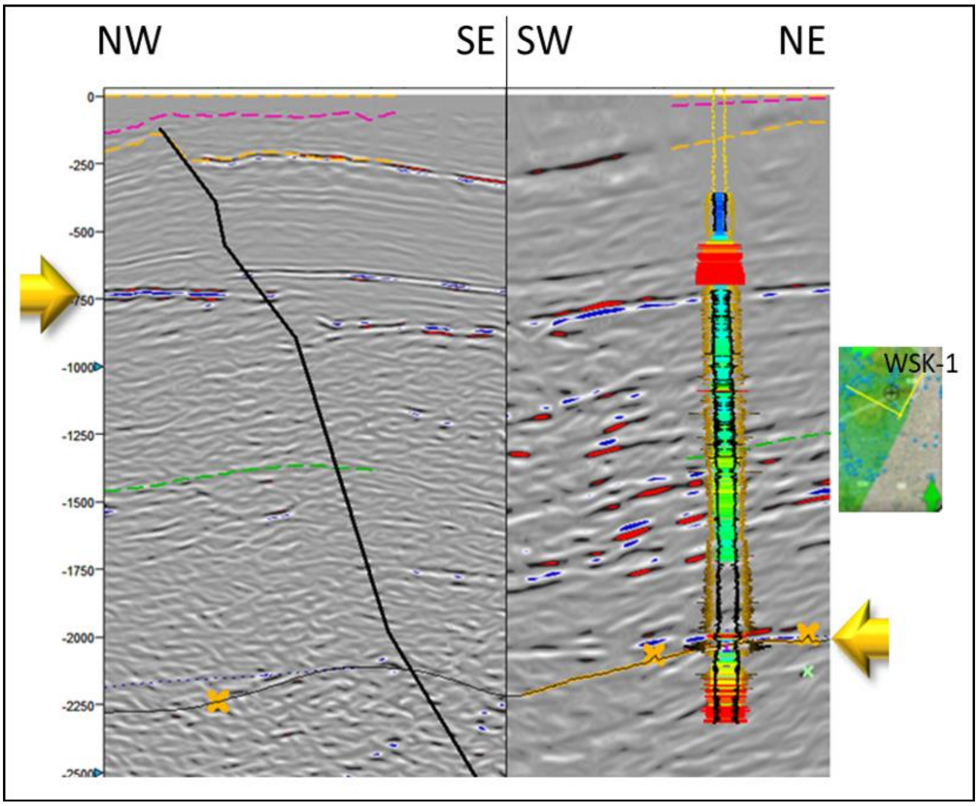

Figure 34. WSK-01 region with igneous intrusions interpreted on seismic compared with GM igneous intrusions. Modified after Ten Veen et al. (2019) – SCAN Report.

In addition to the comparison of DTMS dike depth solutions in a number of seismic sections, the DTMS dike depth solutions (SI 1.0 and SI 2.0) have also been classified according to their stratigraphic correlation based on the TNO-DGM5 depth grids. A 200m vertical error was allowed for the depth solutions in the classification with respect to the base of the stratigraphic unit.
In Figures 35 to 42 the TNO-DGM5 depth grids are presented and dike depth solutions which lie wihin above that grid but below the grid of the overlying stratigraphic unit plotted on top. It can be observed that the Rotliegend and Zechstein groups host most of the DTMS-dikes. The Altena, Rijnland and Chalk groups also contain dikes. Only few dikes have been detected by the DTMS technique in the other groups. Given the low data density of the underlying magnetic data set, probably many more dikes can be present within the sedimentary section.

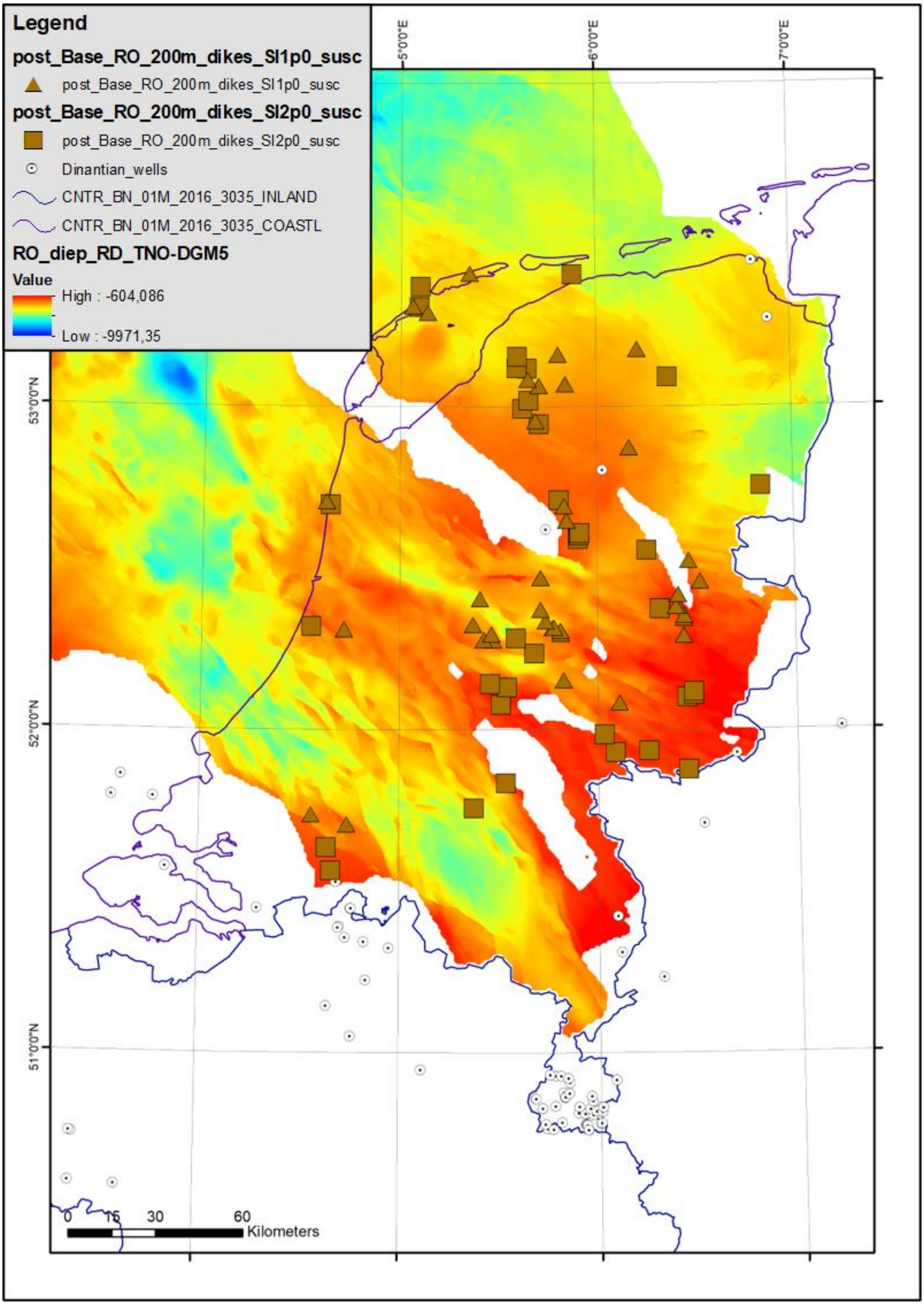

Figure 35. TNO-DGM5 depth grid of base Rotliegend Gp overlain by DTMS-dikes which reside in the Rotliegend Gp.

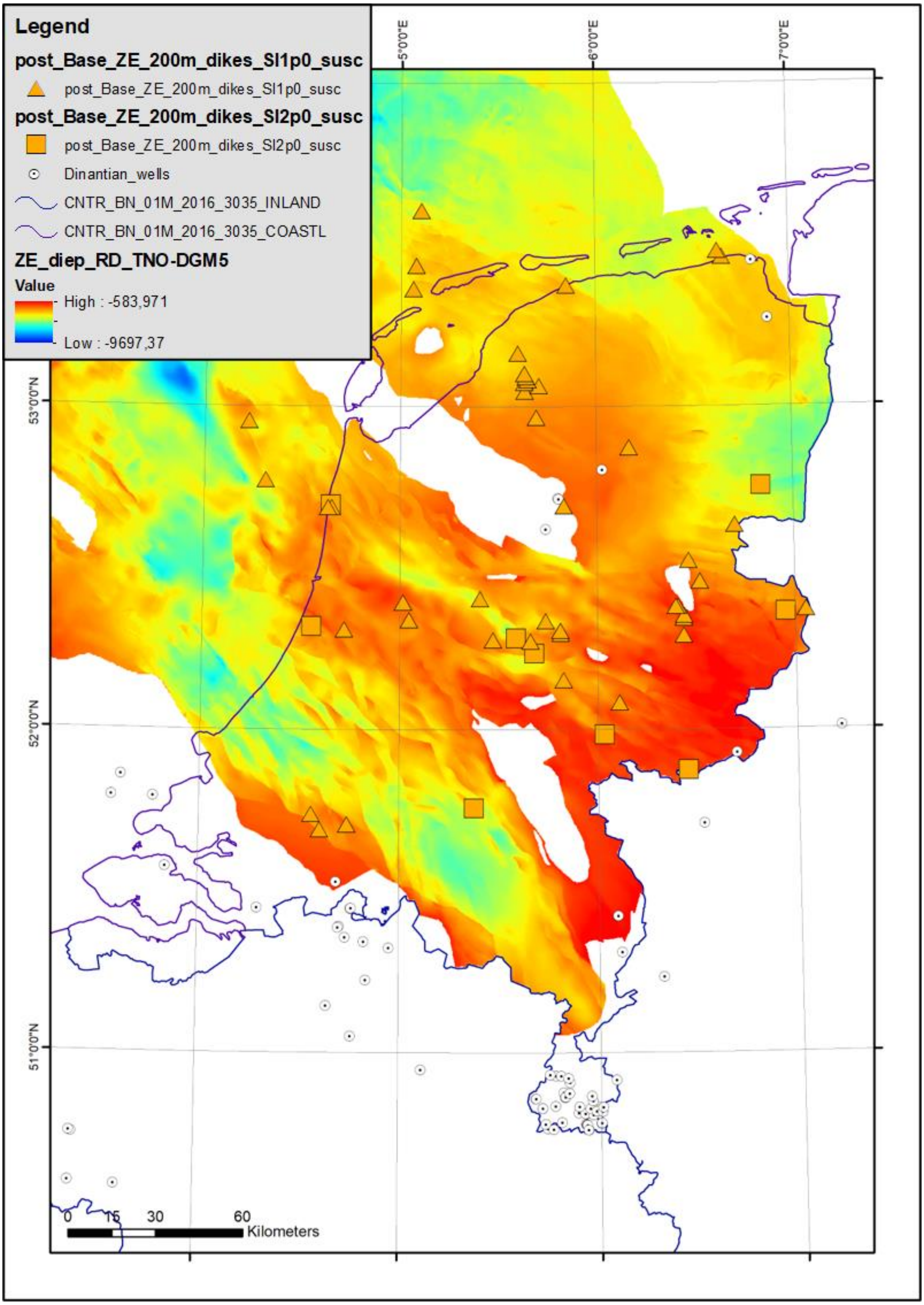

Figure 36. TNO-DGM5 depth grid of base Zechstein Gp overlain by DTMS-dikes which reside in the Zechstein Gp.

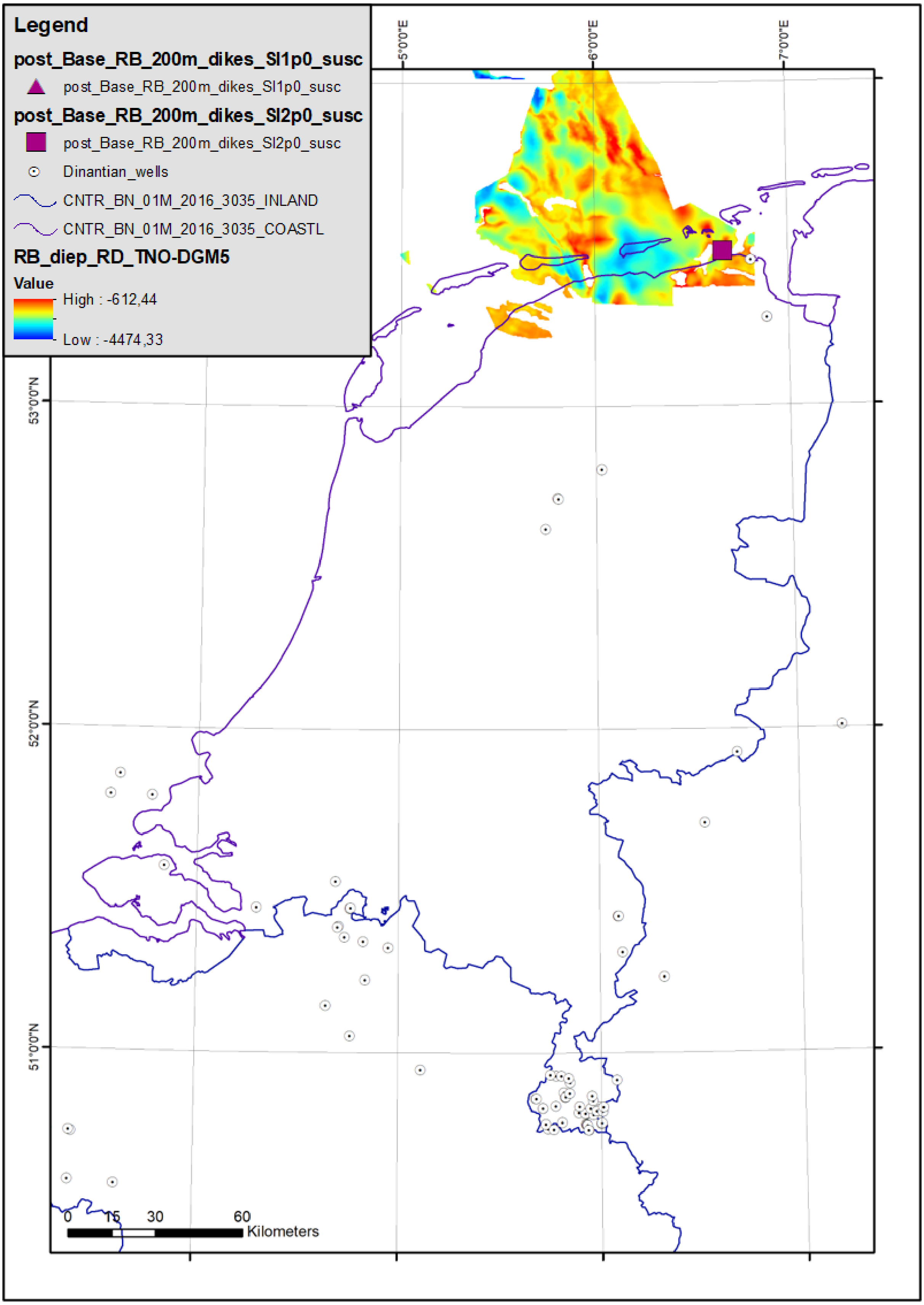

Figure 37. TNO-DGM5 depth grid of base Main Bunter Gp overlain by DTMS-dikes which reside in the Main Bunter Gp.

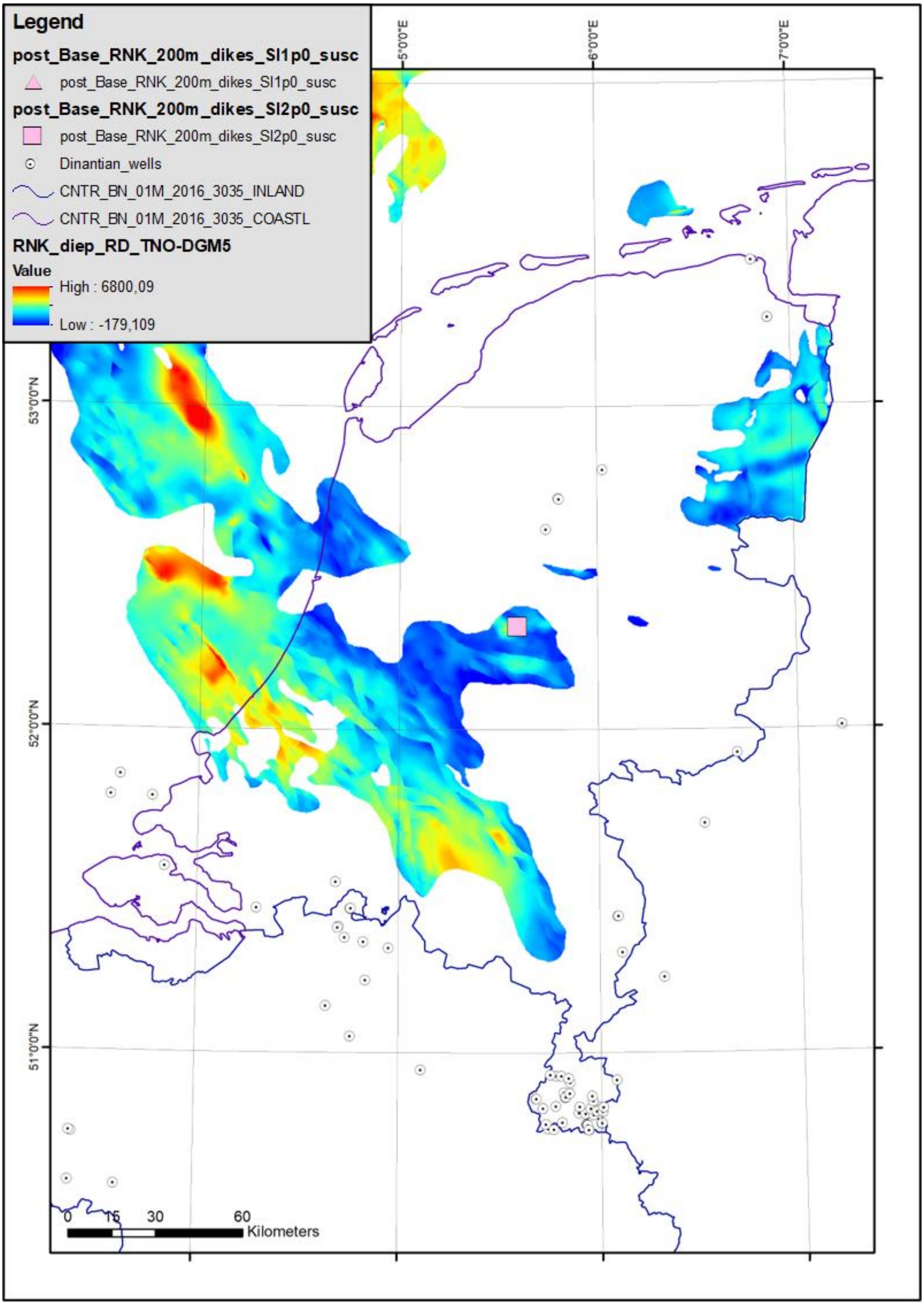

Figure 38. TNO-DGM5 depth grid of base Keuper Gp overlain by DTMS-dikes which reside in the Keuper Gp.

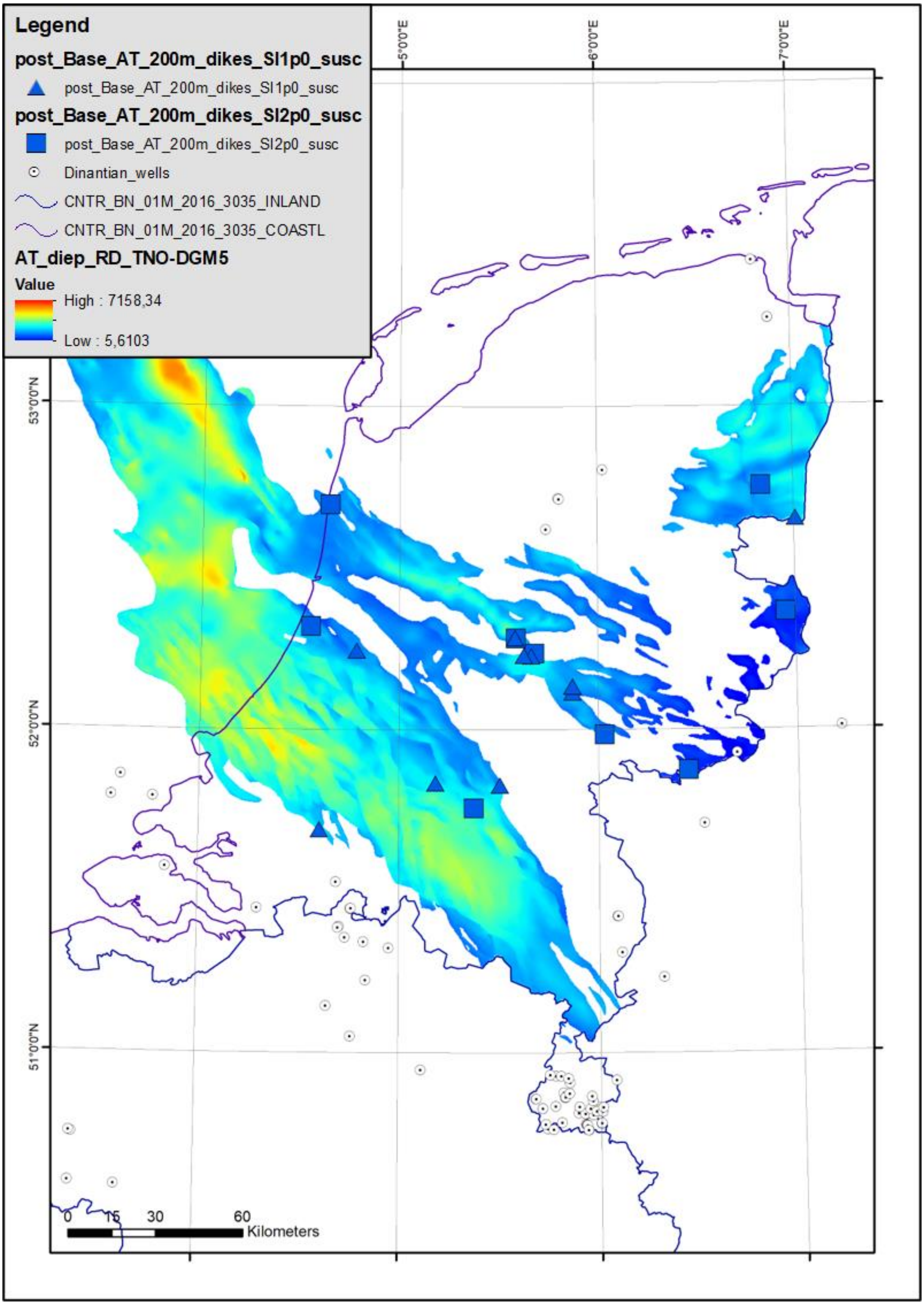

Figure 39. TNO-DGM5 depth grid of base Altena Gp overlain by DTMS-dikes which reside in the Altena Gp.

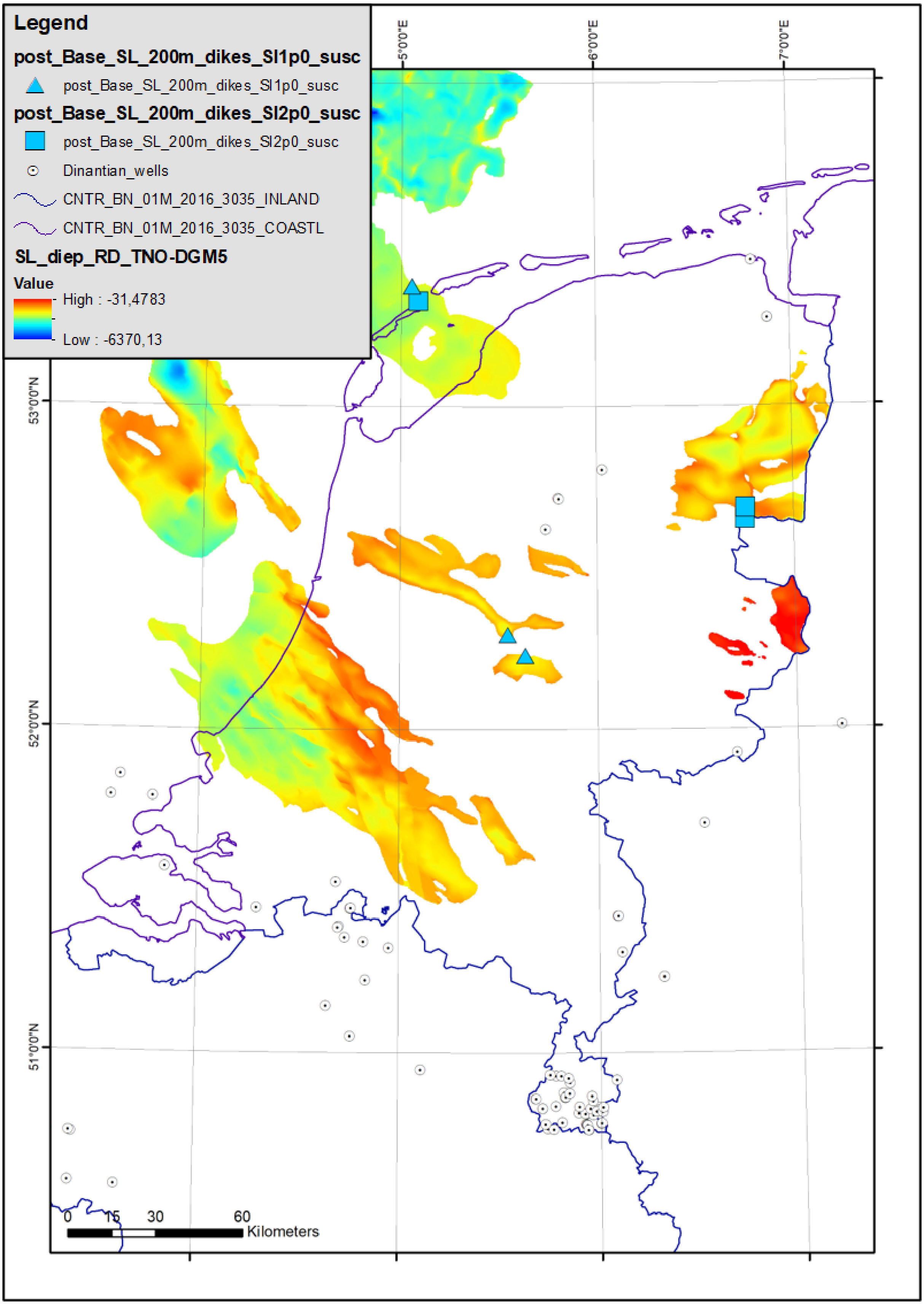

Figure 40. TNO-DGM5 depth grid of base Schieland Gp overlain by DTMS-dikes which reside in the Schieland Gp.

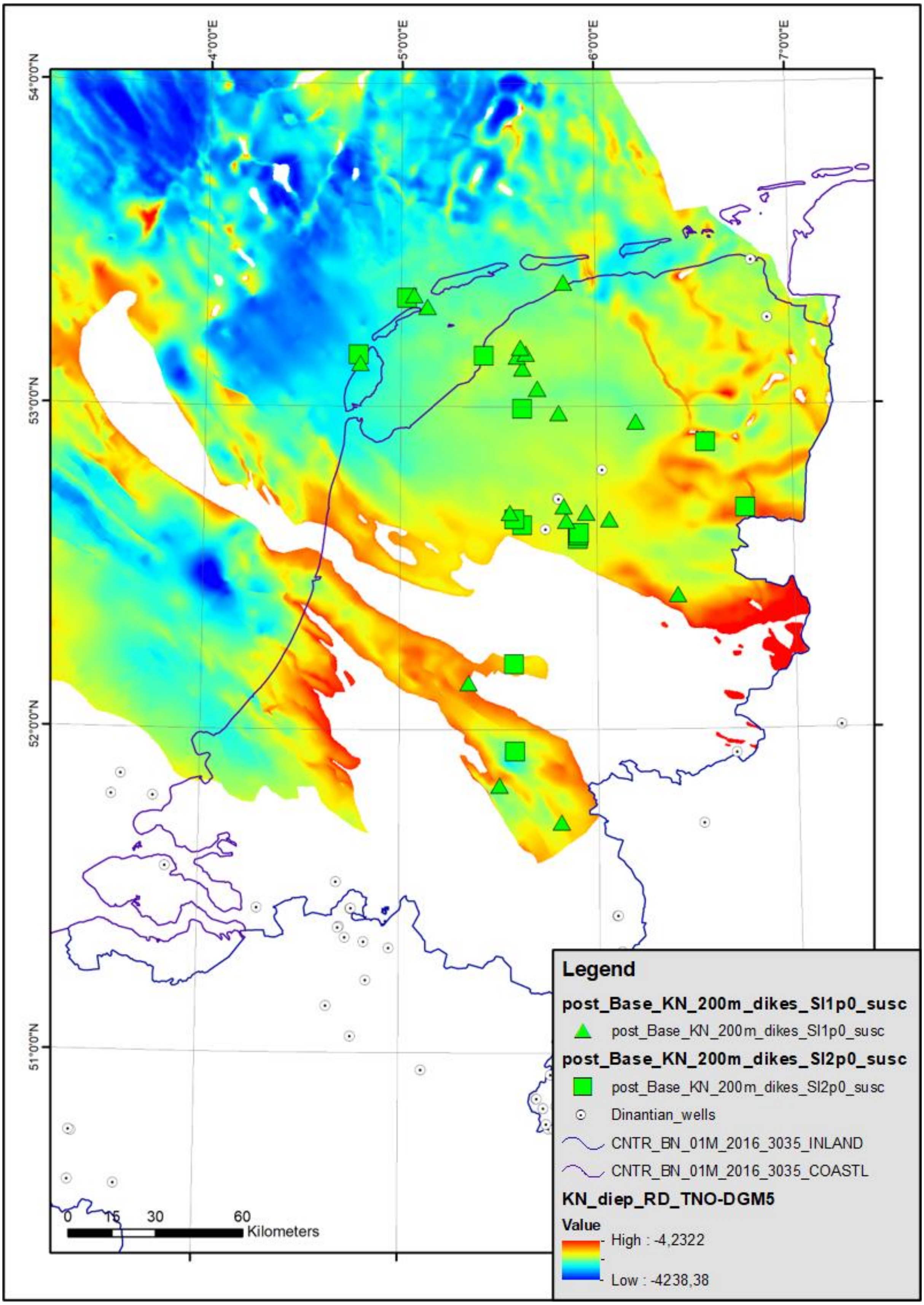

Figure 41. TNO-DGM5 depth grid of base Rijnland Gp overlain by DTMS-dikes which reside in the Rijnland Gp.

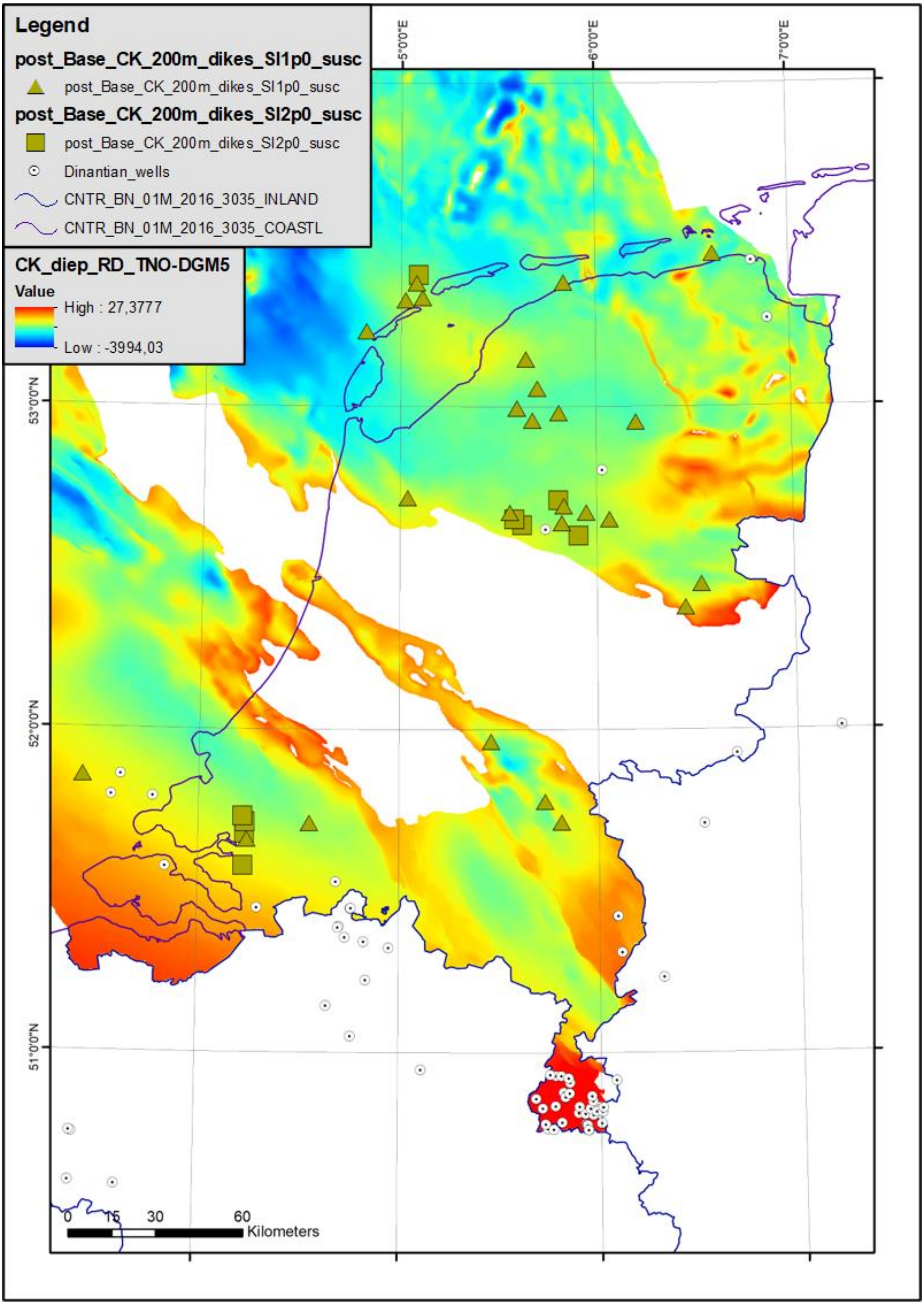

Figure 42. TNO-DGM5 depth grid of base Chalk Gp overlain by DTMS-dikes which reside in the Chalk Gp.

7.2. DGM5 faults per stratigraphic level compared to GM Integrated structures

The pre-Permian faults broadly follow the Magnetic Basement morphology and the NW-SE oriented GM Integrated structural elements (Figure 43). On the west flank of the RVG however, the pre-Permian faults developed a high angle to the main NW-SE GM Integrated structural elements trend. On the threshold between the WNB and the RVG the pre-Permian faults terminate against the regional NE-SW oriented GM Integrated structures. On the eastside of the RVG, the regional N-S GM Integrated structures seem to play a role in the deflection of the pre-Permian faults.

Similar to the pre-Permian faults, the Top Zechstein Gp faults broadly follow the Magnetic Basement morphology and the NW-SE oriented GM Integrated structural elements (Figure 44). Some of the top Zechstein Gp faults terminate against the GM Integrated structures. In general the N-S to NE-SW trending GM Integrated structures seem to play a role in the deflection of the top Zechstein Gp faults. In the LSB region, top Zechstein Gp faults appear to terminate against the N-S to NE-SW oriented GM Integrated structures.

Similar to the deeper faults, the Top Main Bunter faults broadly follow the Magnetic Basement morphology and the NW-SE oriented GM Integrated structural elements (Figure 45). Some of them seem to terminate against the N-S to NE-SW oriented GM Integrated structures.

Also the Top Keuper faults broadly follow the Magnetic Basement morphology and the NW-SE oriented GM Integrated structural elements (Figure 46). Some of them seem to terminate against or to be deflected by the N-S to NE-SW oriented GM Integrated structures.

Seeming more clearly than for the deeper faults, the top Schieland Gp faults terminate against N-S to NE-SW oriented GM Integrated structures. Nonetheless they follow the NW-SE oriented GM Integrated structures and morphology of the Magnetic Basement (Figure 47).

Similar to the top Schieland Gp faults, the top Rijnland Gp faults terminate against N-S to NE-SW oriented GM Integrated structures, especially in the LSB region. Nonetheless they follow the NW-SE oriented GM Integrated structures and morphology of the Magnetic Basement (Figure 48).

The top Chalk Gp faults, similar to the deeper faults, follow the morphology of the Magnetic Basement and NW-SE oriented GM Integrated structures. However, E-W to NE-SW to N-S GM Integrated structures appear to dictate where the top Chalk Gp faults terminate, occasionaly where top Chalk Gp faults laterally step and follow the E-W to NE-SW to N-S GM Integrated structures. This is the case for example on the southwest flank of the RVG (Figure 49).

The top North Sea Gp faults are mainly oriented NW-SE and as such follow the Magnetic Basement morphology and the GM Integrated structures along the Magnetic Basement (Figure 50). In contrast to the deeper faults, the top North Sea Gp faults do not deviate where they cross the E-W to NE-SW to N-S GM Integrated structures.

Not only onshore but also offshore the GM Integrated structures evidently coincide with steps and offsets in the SCAN-top and base Dinantian depth grids (Figures 51 and 52). Examples are the steps in the top Dinantian and base Dinantian grids: LBM front, RVG, WNB, FP, TAH and LST. As such the GM Integrated structures provide confident guidelines for the interpretation of top and base Dinantian in the white areas.

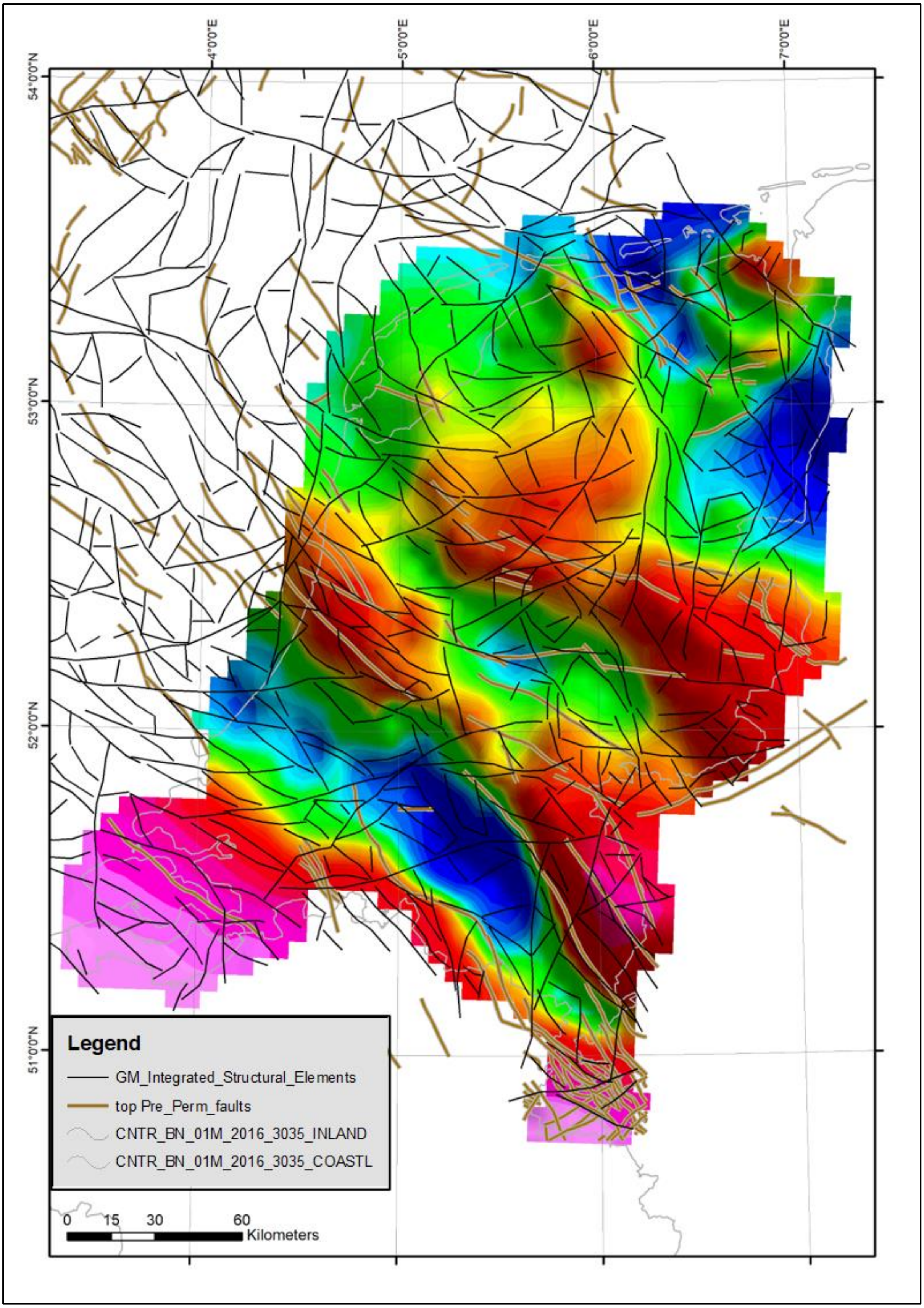

Figure 43. DTMS overlain by GM Integrated structures compared to DGM5 pre-Perm structures (TNO).

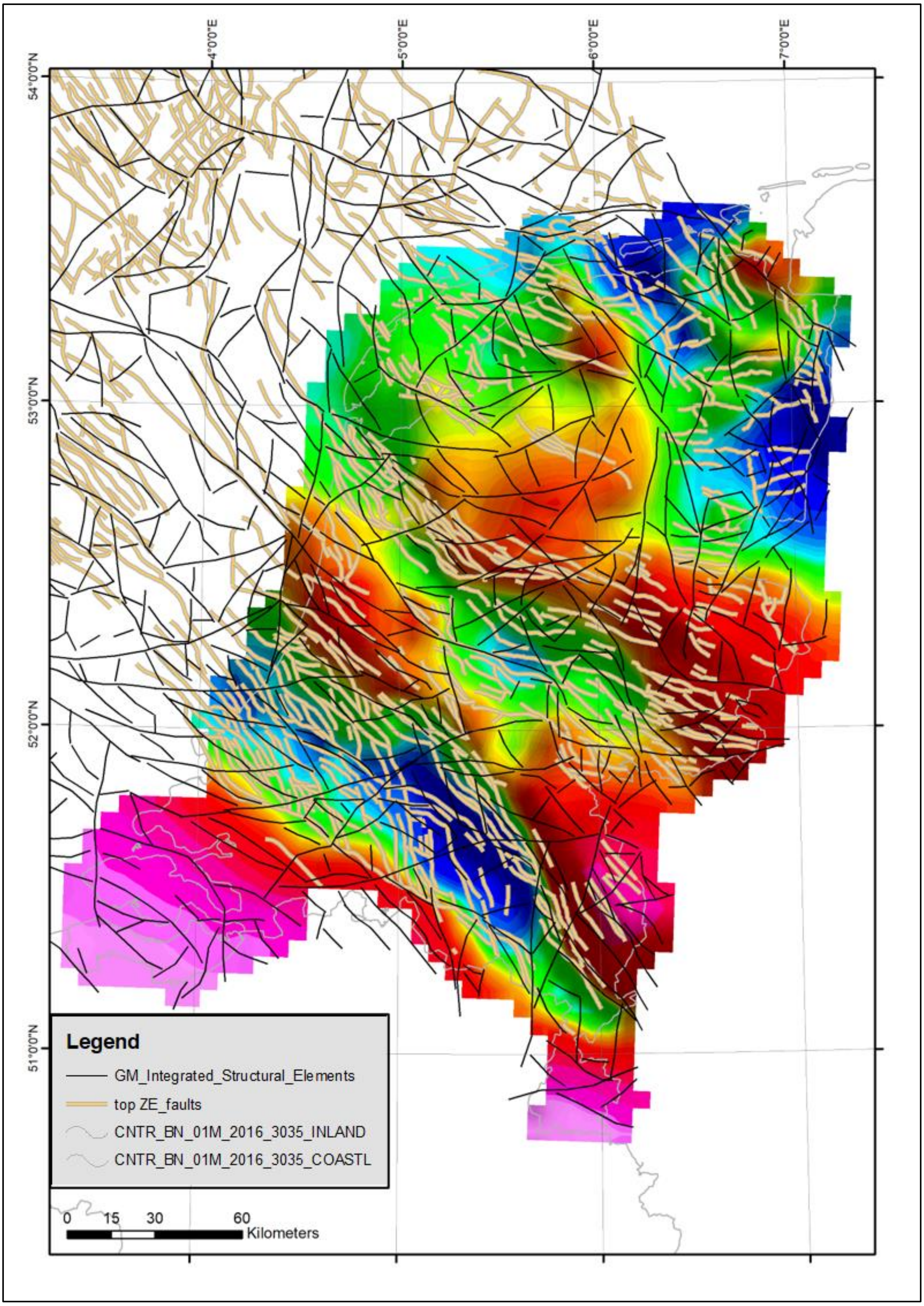

Figure 44. DTMS overlain by GM Integrated structures compared to DGM5 top Zechstein Gp structures (TNO).

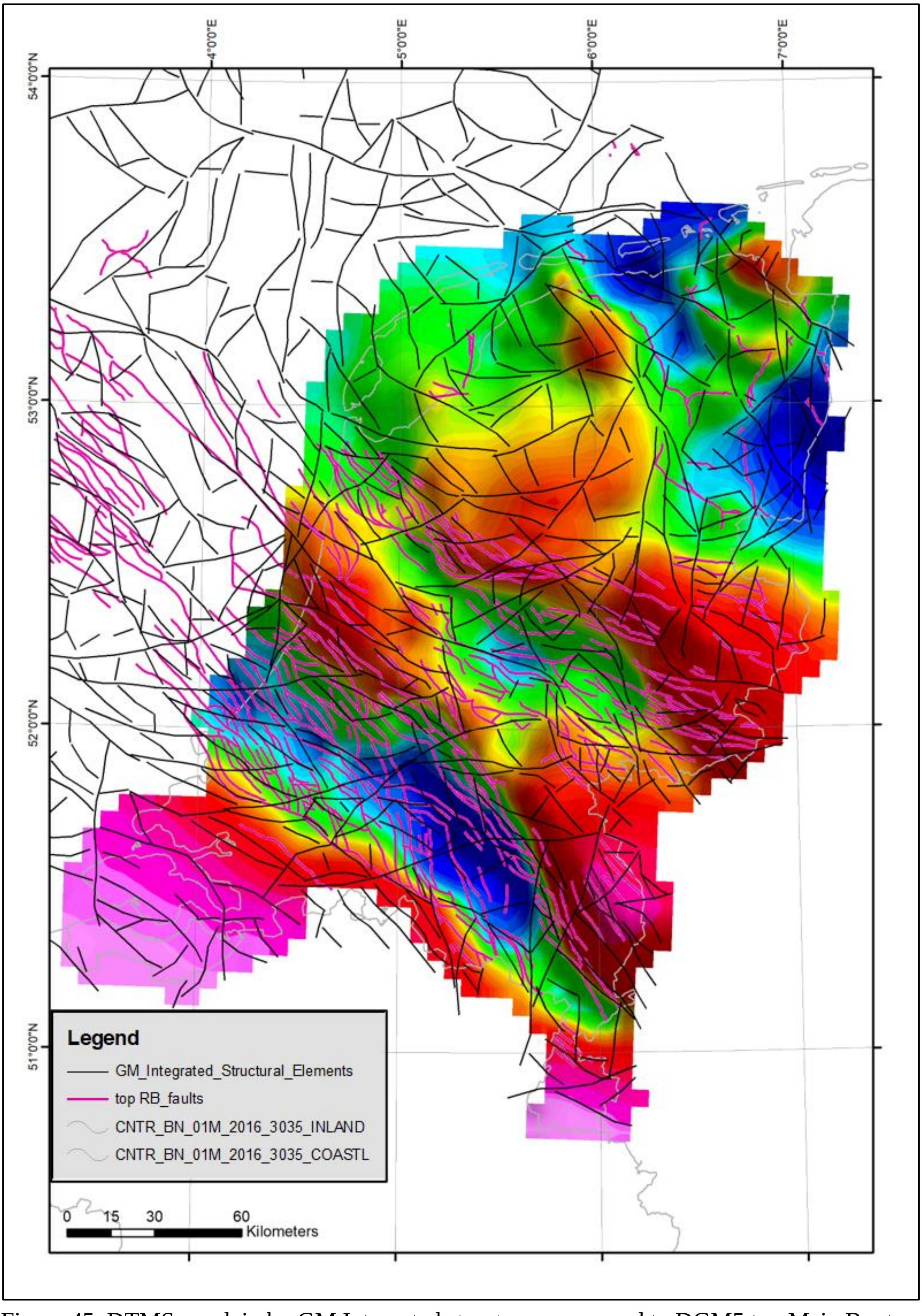

Figure 45. DTMS overlain by GM Integrated structures compared to DGM5 top Main Bunter structures (TNO).

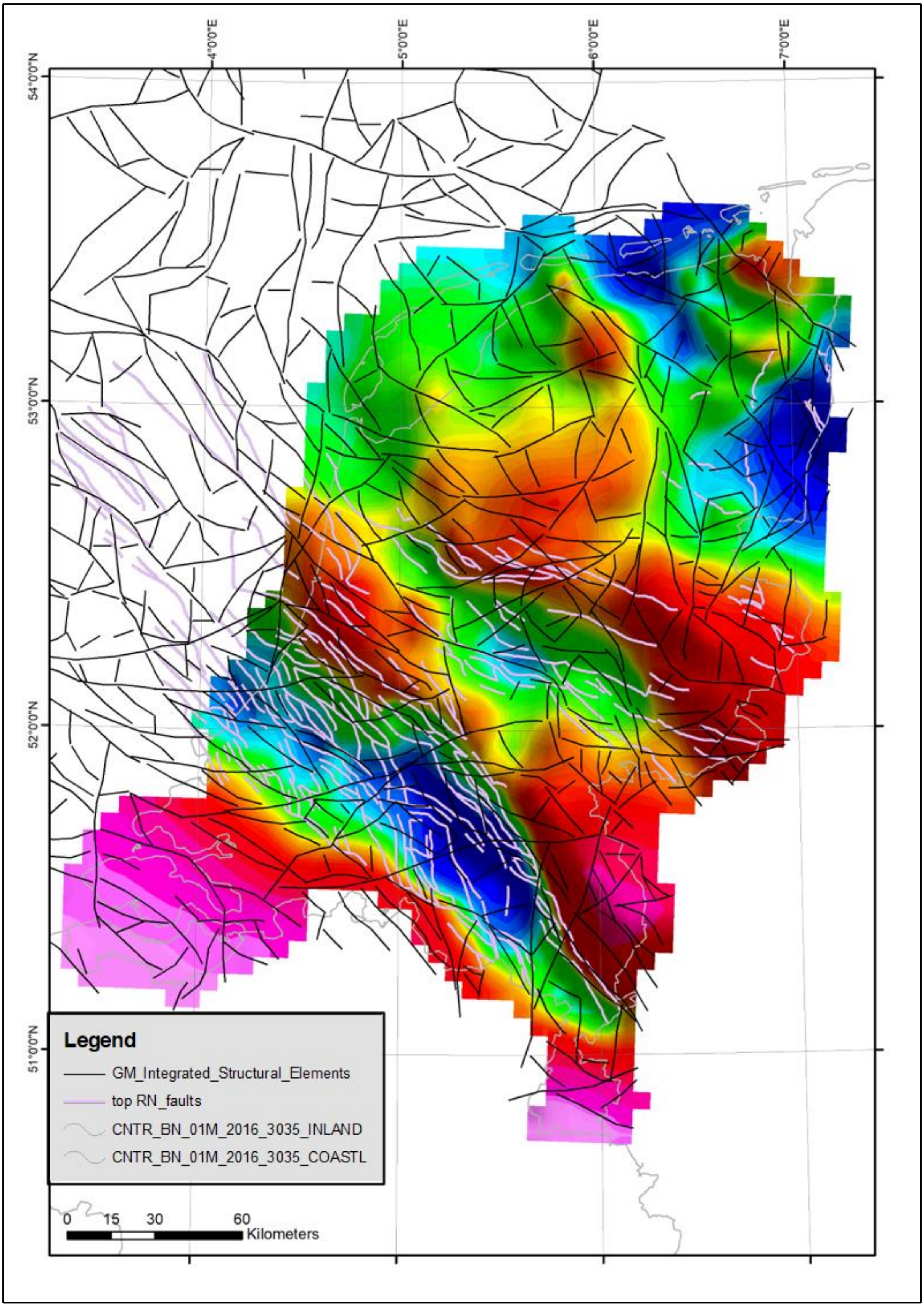

Figure 46. DTMS overlain by GM Integrated structures compared to DGM5 top Keuper structures (TNO).

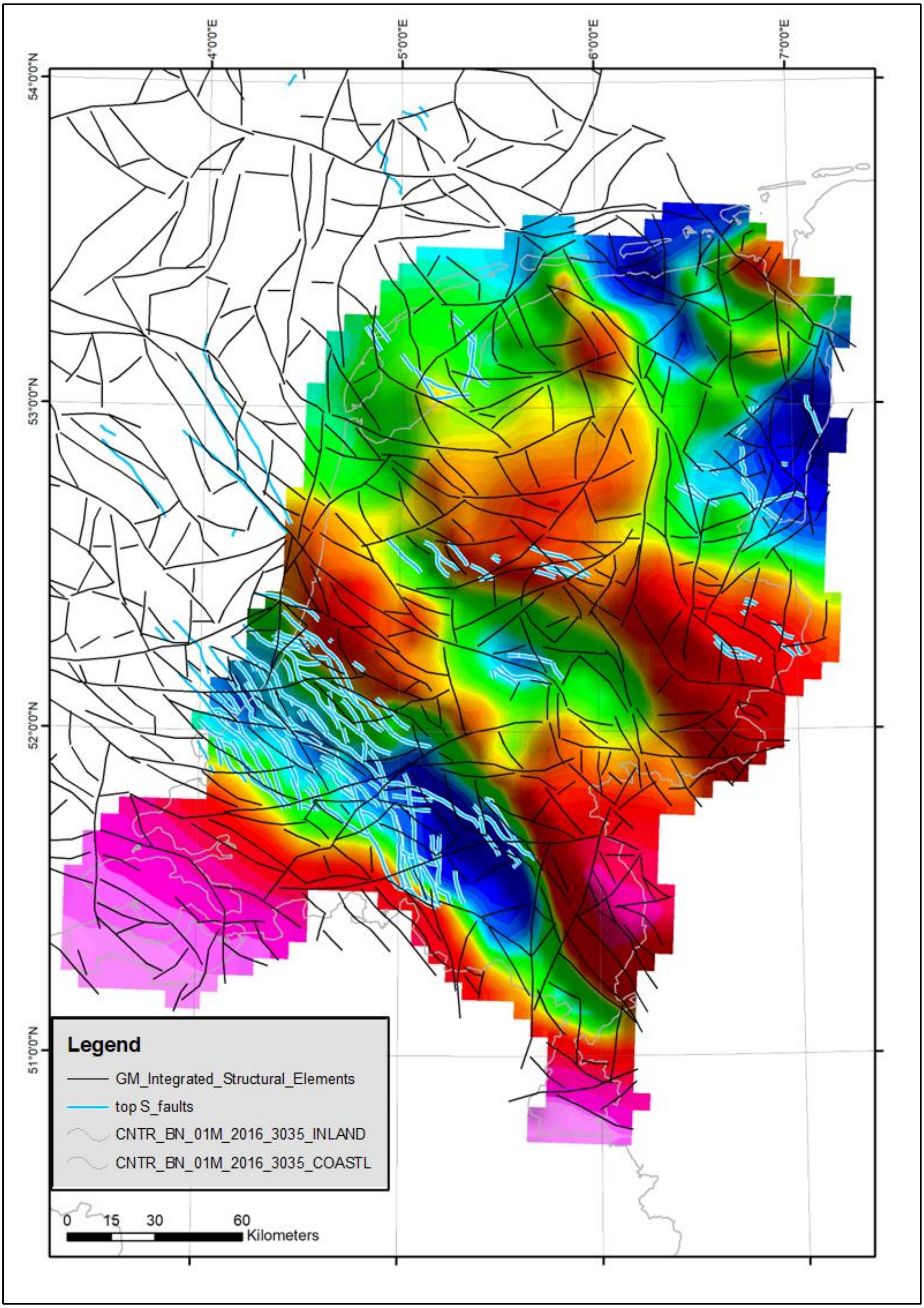

Figure 47. DTMS overlain by GM Integrated structures compared to DGM5 top Schieland Gp structures (TNO).

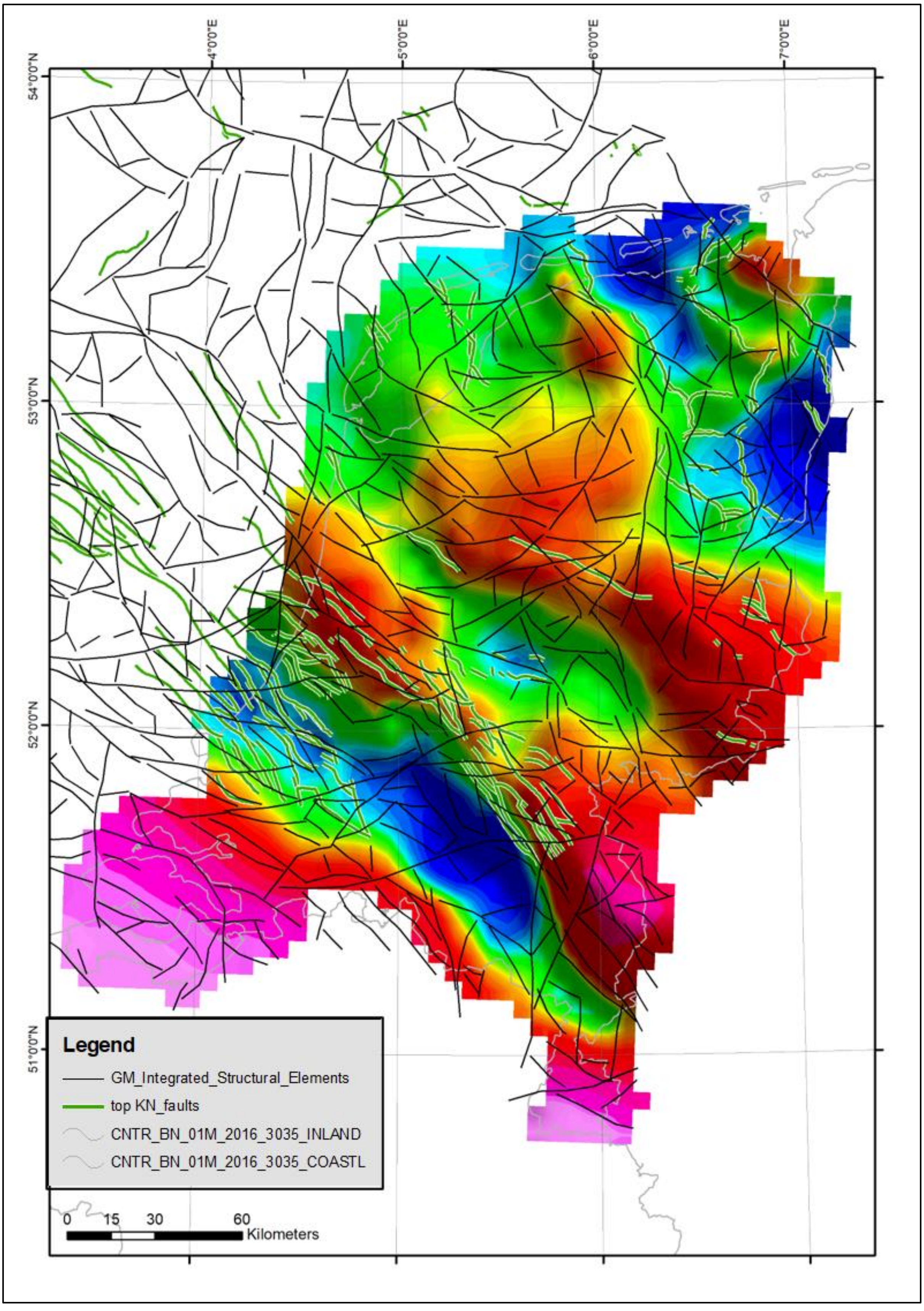

Figure 48. DTMS overlain by GM Integrated structures compared to DGM5 top Rijnland Gp structures (TNO).

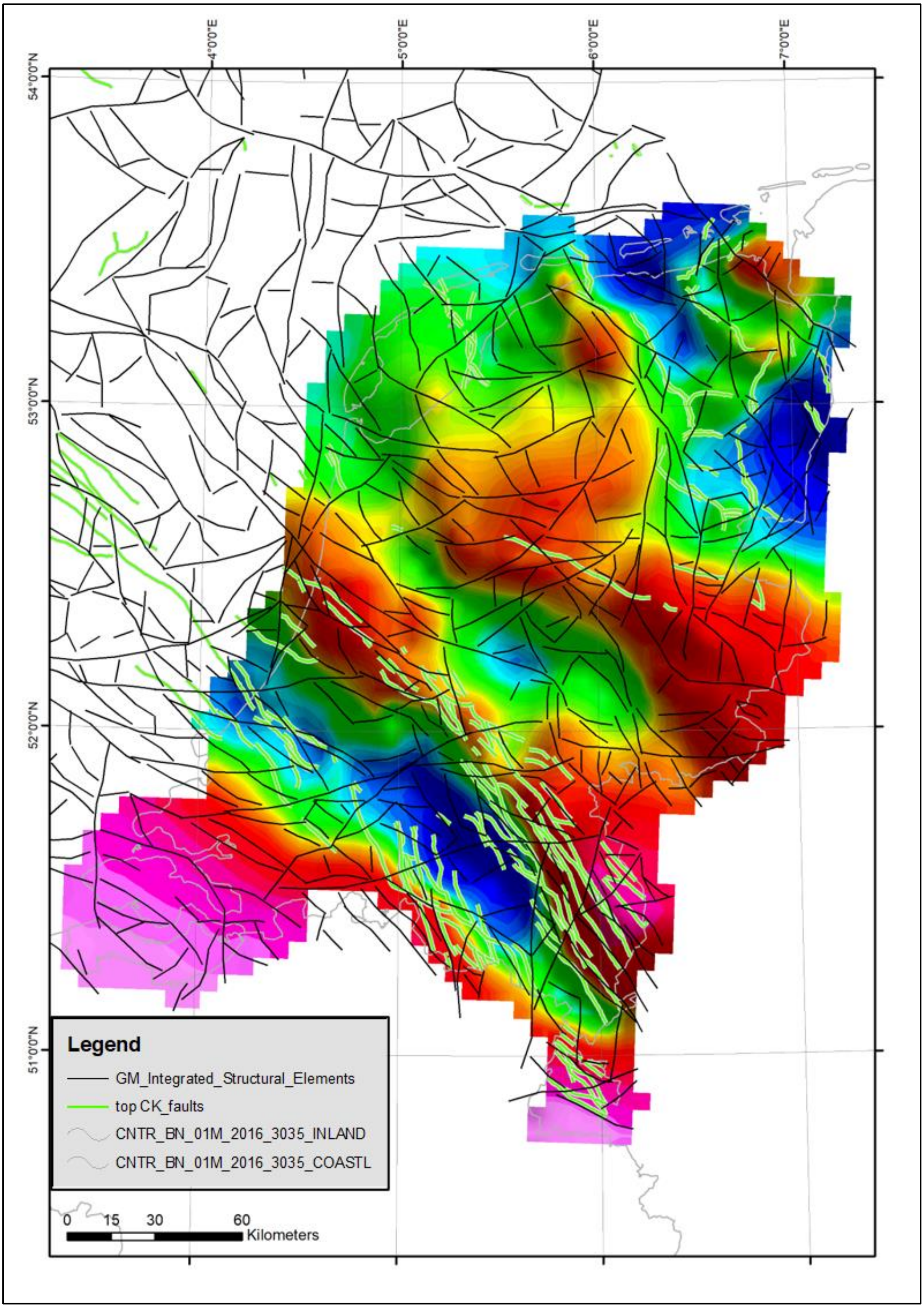

Figure 49. DTMS overlain by GM Integrated structures compared to DGM5 top Chalk Gp structures (TNO).

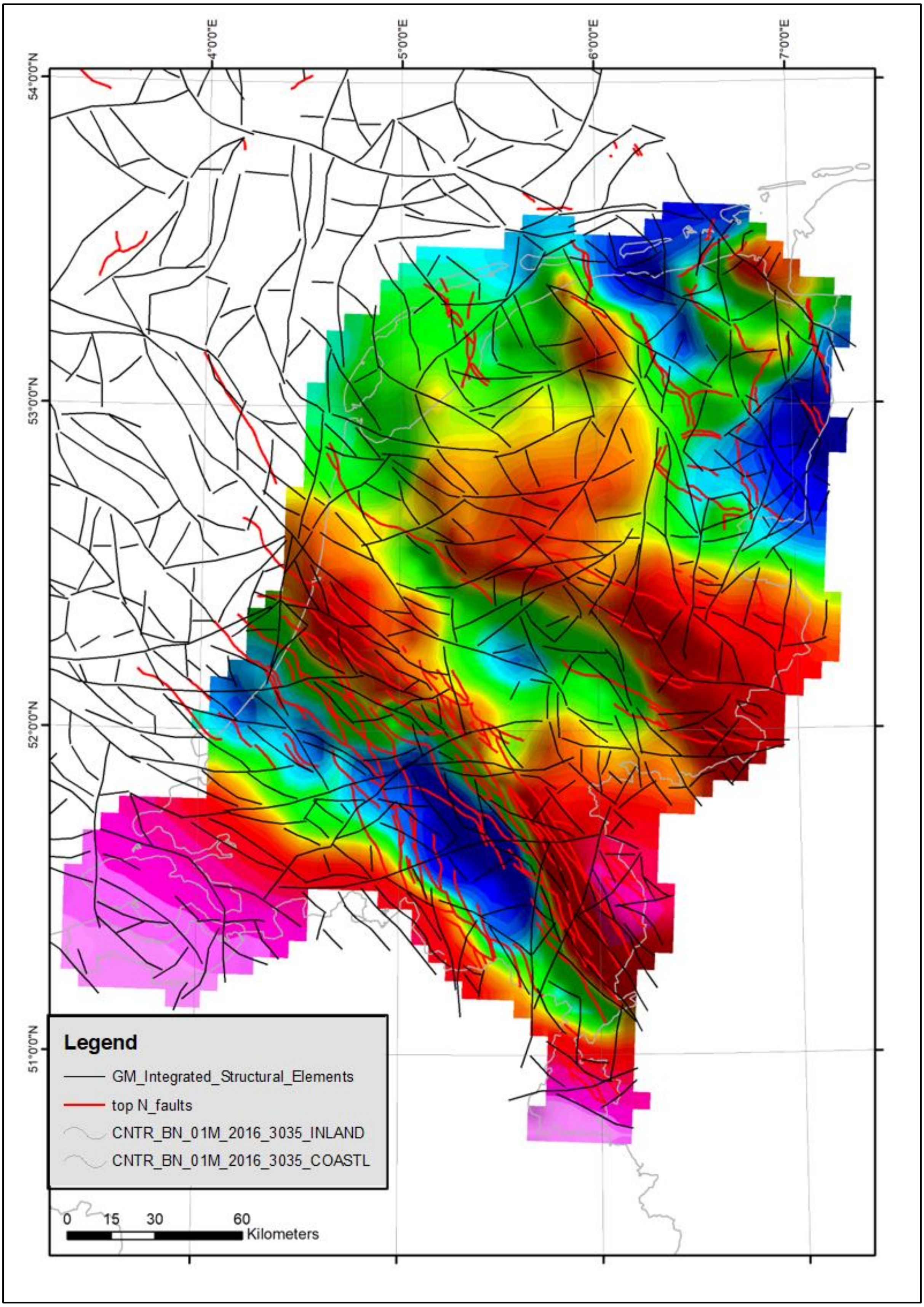

Figure 50. DTMS overlain by GM Integrated structures compared to DGM5 top North Sea Gp structures (TNO).

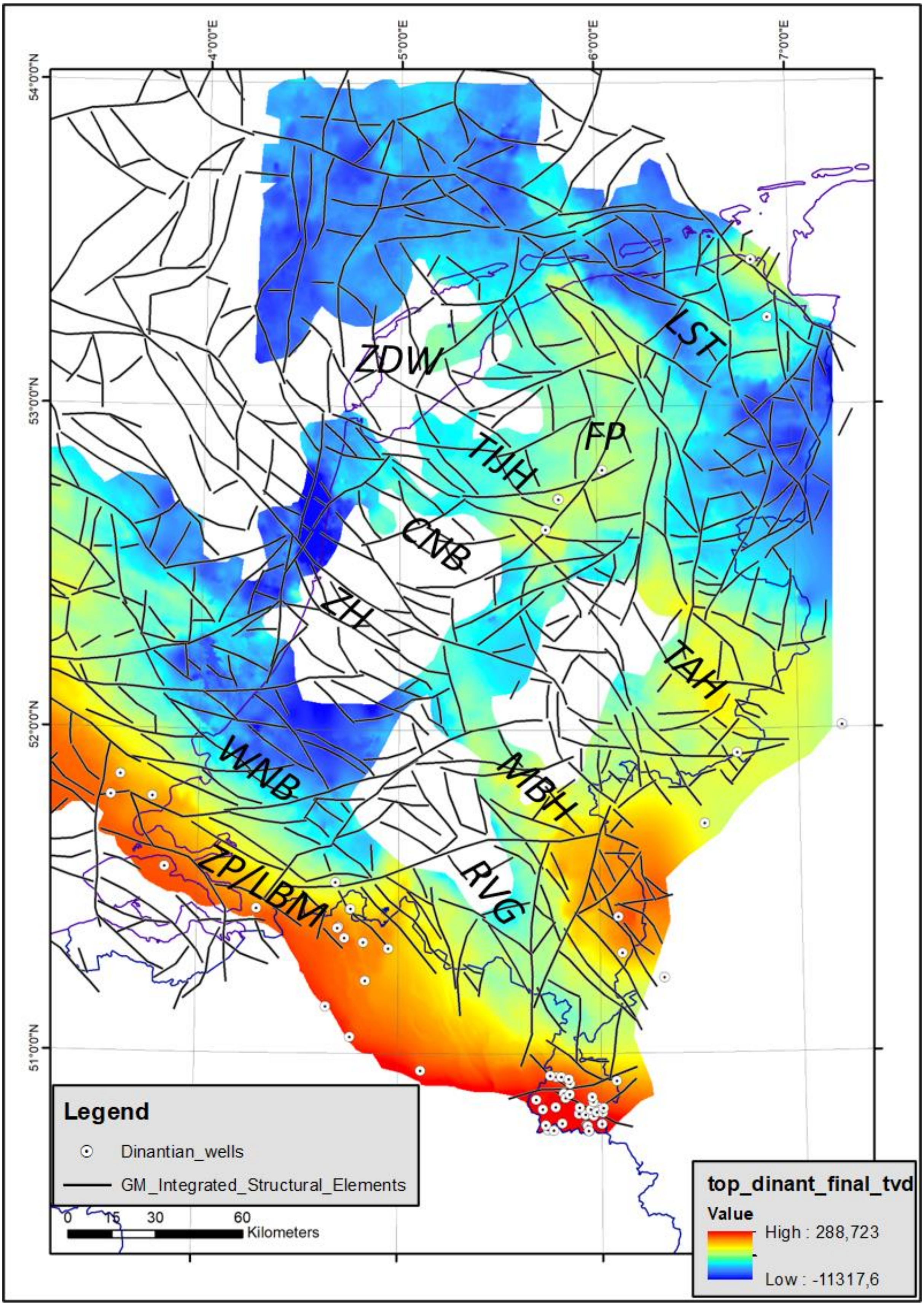

Figure 51. SCAN top Dinantian depth grid overlain by GM Integrated structures.

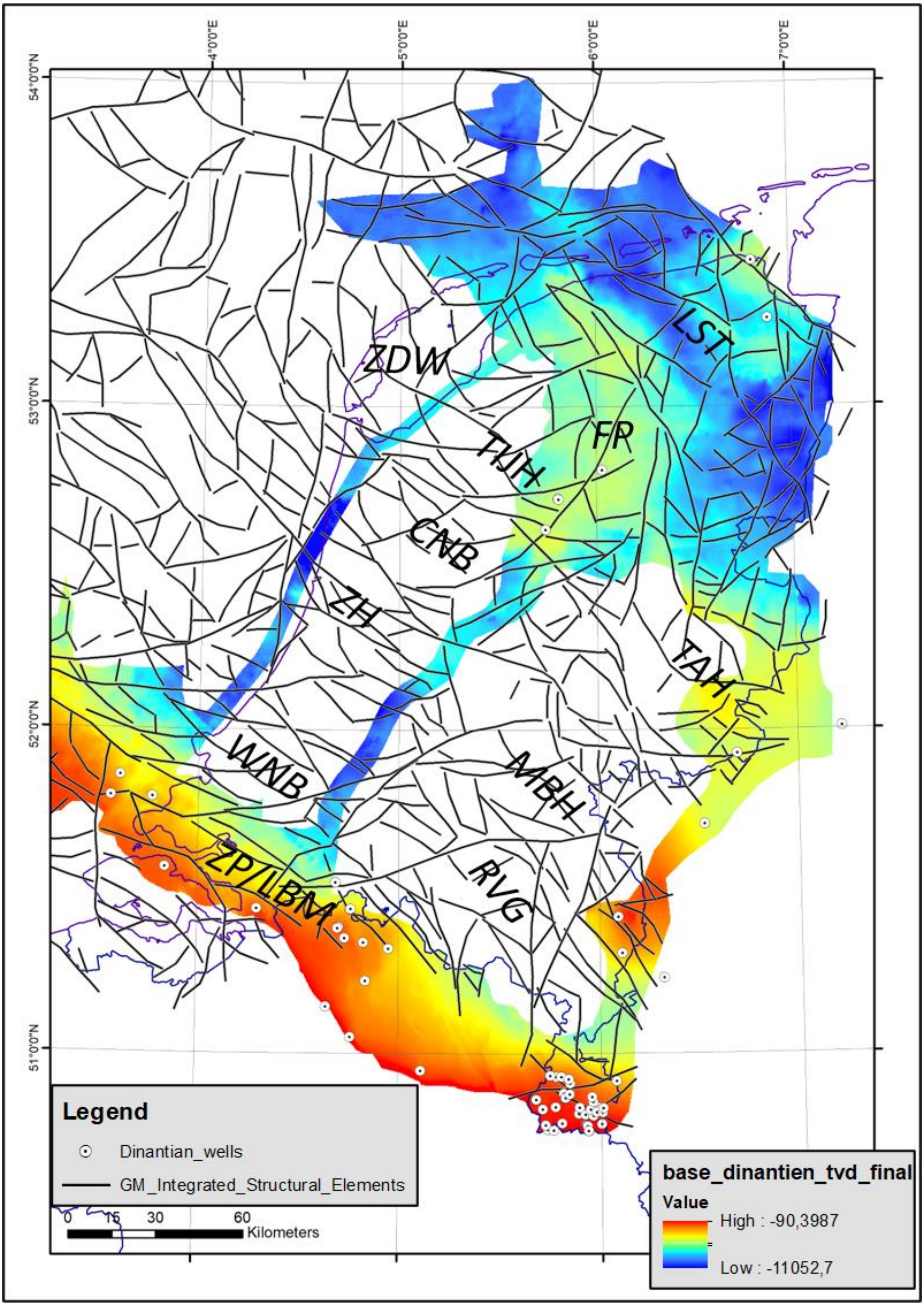

Figure 52. SCAN base Dinantian depth grid overlain by GM Integrated structures.

7.3. Comparison Top Magnetic Basement To Top and Base Dinantian

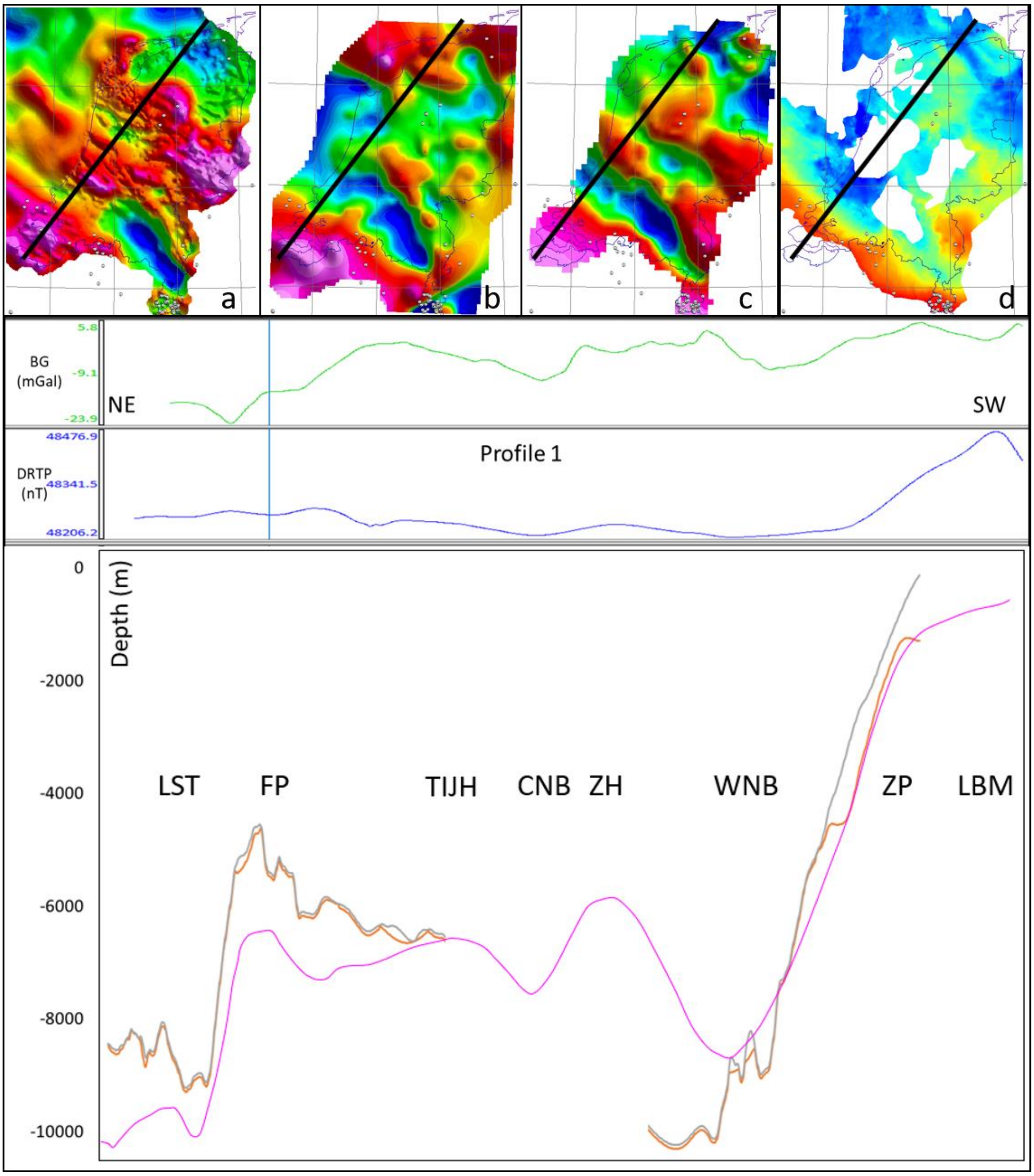

Figure 53. Comparison Top Magnetic Basement with Top Dinantian and Base Dinantian along profile 1 with basement highs and basins indicated. Grids of BG (a), DRTP (b), Top Magnetic Basement (c) and Top Dinantian Depth (d) and highlighted in bold black is the profile presented in the top panel. The central panel displays the cross-section along the profile of BG and DRTP anomalies. The bottom panel compares the Top Magnetic Basement (magenta) versus Top Dinantian (grey) and Base (orange) Dinantian depth grids. Note the good correpondence between top Magnetic Basement and Base Dinantian along the LBM and ZP, whereas from the WNB northwards this correspondence is lacking.

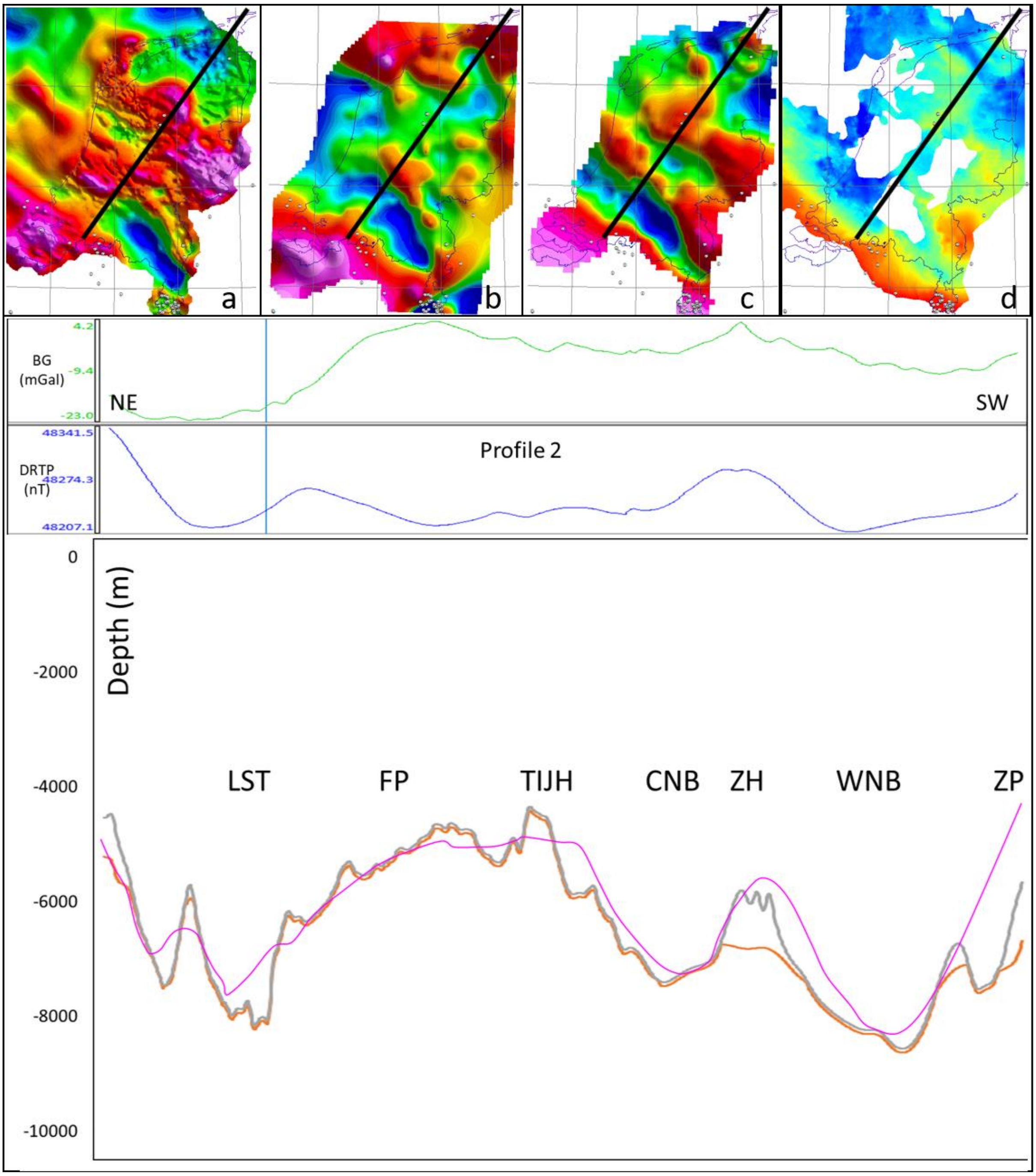

Figure 54. Comparison Top Magnetic Basement with Top Dinantian and Base Dinantian along profile 1 with basement highs and basins indicated. Grids of BG (a), DRTP (b), Top Magnetic Basement (c) and Top Dinantian Depth (d) and highlighted in bold black is the profile presented in the top panel. The central panel displays the cross-section along the profile of BG and DRTP anomalies. The bottom panel compares the Top Magnetic Basement (magenta) versus Top Dinantian (grey) and Base (orange) Dinantian depth grids and shows a general correspondence.

7.4. Value for Exploration

The result of the DTMS for the SI 0.1 and SI 0.5 combined in the Top Magnetic Basement depth grid was compared to the final Top Dinantian depth grid. Important to note is that the uncertainty in magnetic depth computation is in the order of 10% which corresponds to an uncertainty of 800m at 8km depth. In addition, there is only well control on the Top Dinantian down to the deepest well TD which means on average not beyond 5km depth for those few control points. The sparsity of good quality seismic data has led to large gaps ("white spots") in the Top Dinantian depth map. Also, the seismic velocity information for the Dutch sub-surface at larger depths, especially below the top Rotliegend Gp, is sparse and therefore the depth conversion of the Top Dinantian time grid is uncertain in those data-poor regions. As a consequence, the depth of both grids and their comparison, need to be treated with caution at larger depths.

A general observation in Figures 53 and 54 is that at many locations the Base Dinantian is residing above the Top Magnetic Basement. At KTG-01 (ZP region) for instance, the Top Magnetic Basement coincides with the Top Devonian. A possible explanation is that in the area the Top Devonian clastics contain high concentrations of magnetic minerals, similar to Top Devonian clastics reported from the the UK. In the western FP region (Figure 53), the Base Dinantian is situated ~1,000-1,500m above the Top Magnetic Basement, providing space for Devonian and perhaps older (metamorphosed) rocks on top of the Magnetic Basment. In the east on the FP, the Top Magnetic Basement is very close the Base Dinantian which may indicate that the Top Devonian clastic deposits which are envisaged there either contain high concentrations of magnetic minerals or represent a thin layer on top of the deeper-seated Magnetic Basement. Since there is a gap in the seismic interpretion along Profile 1 for the Top and Base Dinantian in the ZH and CNB region (Figure 53), the correspondence between base Dinantian and Top Magnetic Basement is not clear.

In the WNB region however, the Top Magnetic Basement is much shallower than the Top and Base Dinantian. It would be worthwhile to undertake 2D gravity & magnetic modelling along the profiles, while applying same densities and magnetic susceptibilities to the various formations and the basement, unless there is hard evidence to have different values for the same formations based on borehole information, to test the depth conversion of the seismic interpreted horizons of the Top and Base Dinantian.

In Profile 2 (Figure 54), the Top Magnetic Basement shows a general correspondence with the strucutration of both the Top and Base Dinantian, suggesting a closeby magnetic source. Given the ~10% error in the DTMS technique, a 10% downward shift of the Top Magnetic Basement surface would already provide a decent fit with the Base Dinantian in most places. Thus, along the central profile, the Magnetic Basement may very well correlate with a high-magnetic clastics in the uppermost part of the Devonian.

One important observation is that DTMS-dikes tend to cluster at the flanks of Magnetic Basement highs whereas GM Igneous intrusions appear to predominantly support the Magnetic Basement highs (Figure 55). Dikes also tend to cluster along GM Integrated structures and occur at the edges of the GM Igneous intrusions. In the LSB region though, the DTMS dikes also occur in the basin part where Van Bergen and Sissingh (2007) report the Rotliegend tuff province (Figure 22 and Figure 56).

Mozafari et al. (2019) mention the presence of karsts in the Dinantian carbonates that might be controlled by faults. Besides karsts, also dolomitisation improves reservoir quality of limestones. Van Hulten (2012) proposed that igneous intrusions potentially stimulated dolomitisation. An example of karstified Dinantian carbonates has been drilled is the CAL-GT wells. Figure 57 shows the spatial relationship for the CAL-GT Dinantian carbonates geothermal reservoir which is heavily karstified. Deep seated lineaments, a negative gravity anomaly igneous intrusion and a few dikes are present in the CAL-GT site subsurface. It is recommended to further investigate the spatial and temporal relationships of deep seated faults, igneous intrusions and the presence of karstified and dolomitised limestone.

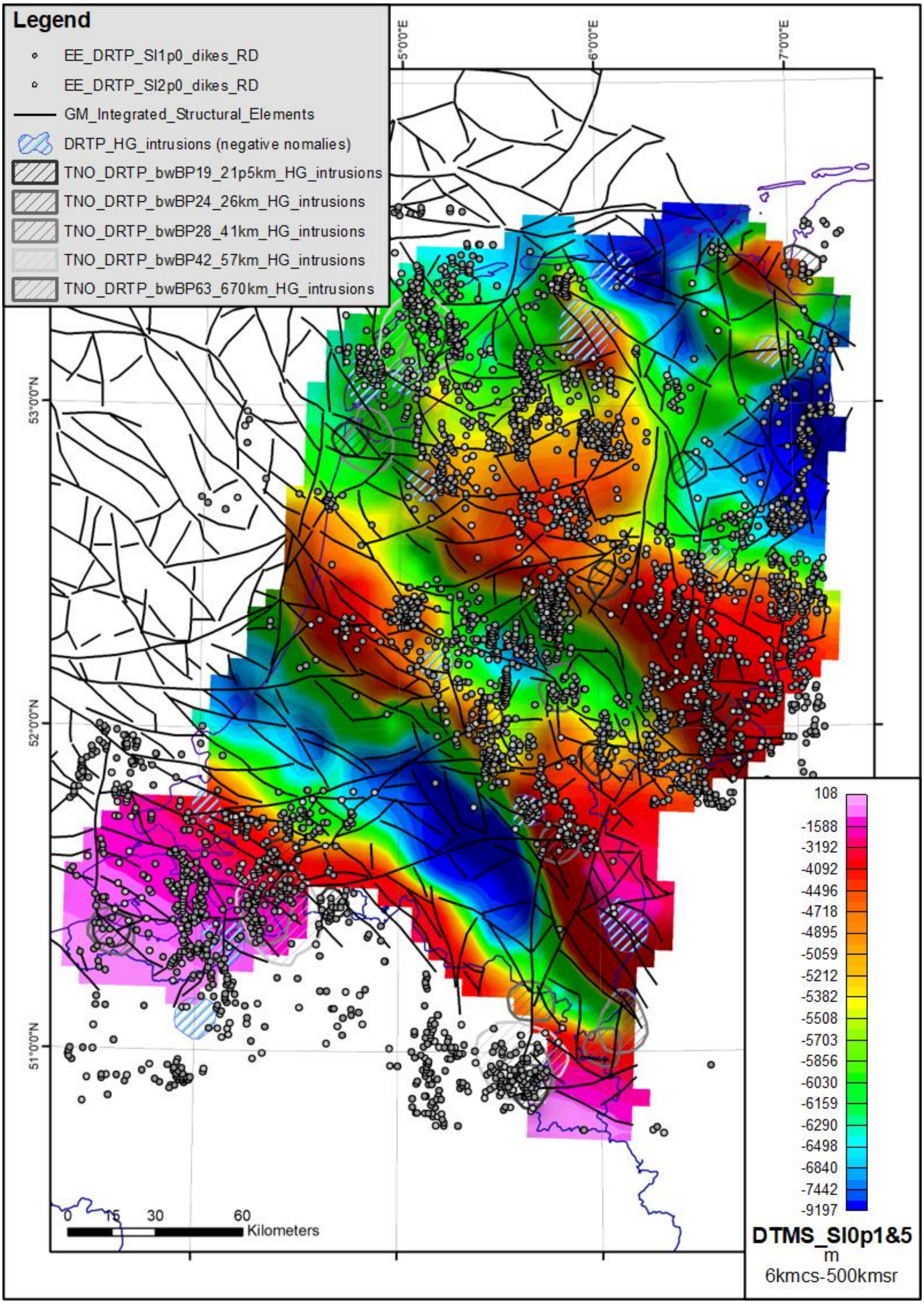

Figure 55. DTMS-dikes and GM Igneous intrusive and GM Integrated structures on the Magnetic Basement.

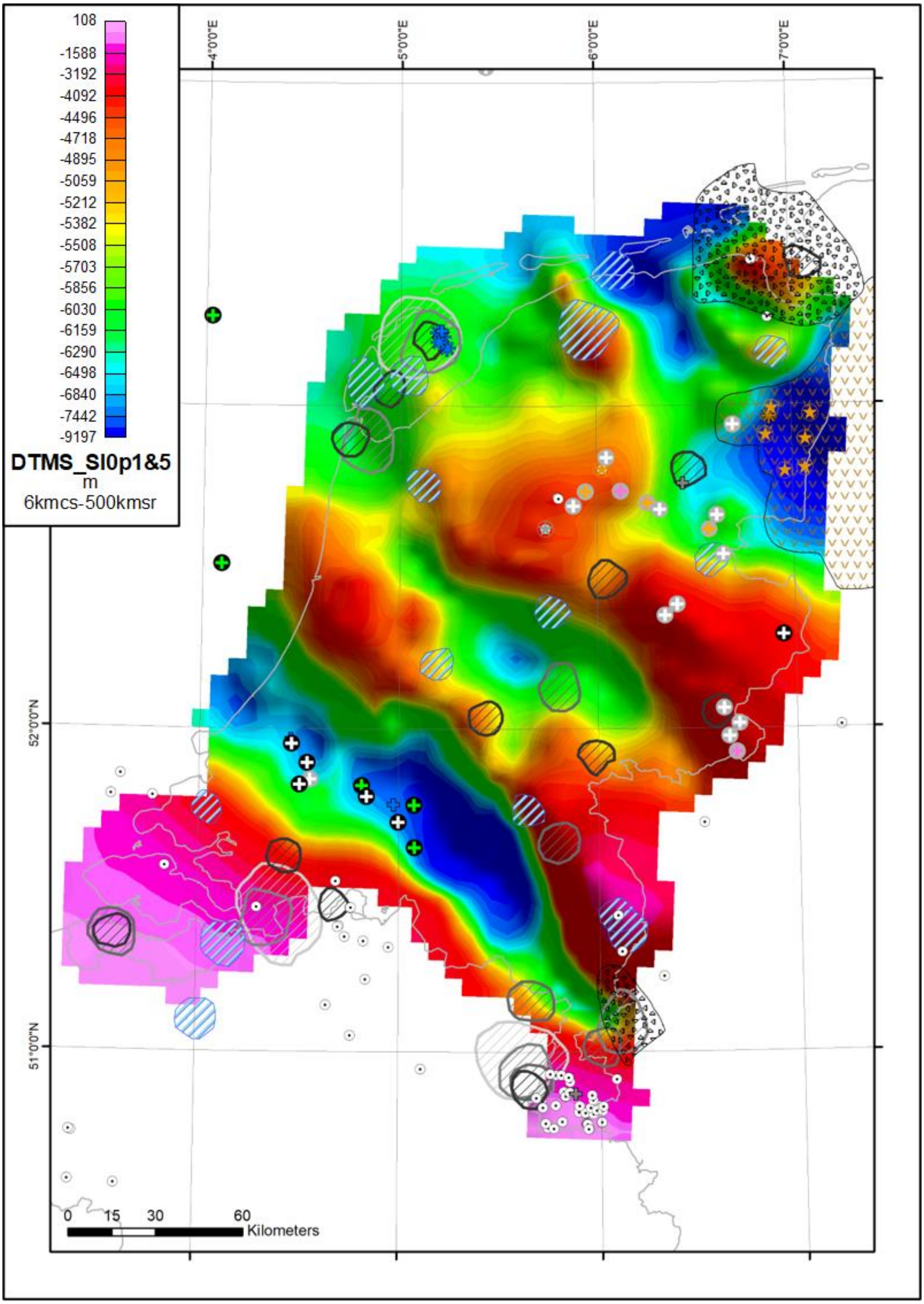

Figure 56. GM Igneous intrusions mapped on Magnetic Basement compared to Van Bergen & Sissingh (2007) igneous intrusions reported from wells. For the legend see Figure 23.

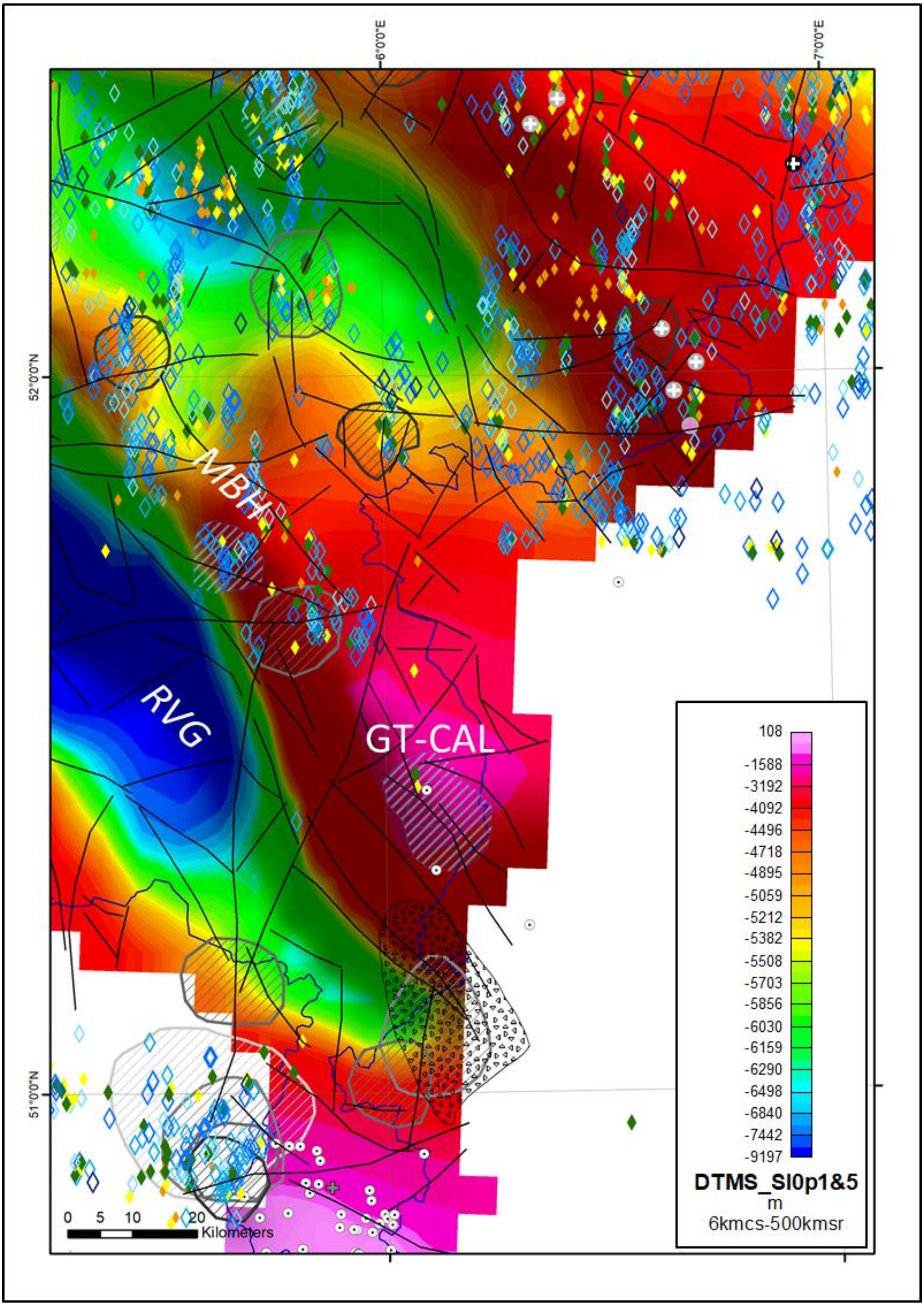

Figure 57. GT-CAL site supported by igneous intrusions and deep seated structures. For the legend, please Figures 23 and 25.

REFERENCES

- AGSO. Best practice in gravity surveying, www.agso.gov.au.
- Boxem, T.A.P., Veldkamp, J.G. and van Wees, J.D.A.M. (2016). Ultra-diepe geothermie: Overzicht, inzicht & to-do ondergrond. TNO report, R10803, 53 pp.
- Carlson, T. (2019). Petrophysical Report of the Dinantian Carbonates in the Dutch Subsurface (SCAN). Downloadable from www.nlog.nl
- Duin, E.J.T., Doornenbal J.C., Rijkers R.H.B., Verbeek J.W. and Wong Th.E. (2006) Subsurface structure of the Netherlands – results onshore and offshore mapping. Netherlands Journal of Geosciences – Geologie en Mijnbouw, 85-4, p245-276.
- Geosoft (2019) Technical papers. www.geosoft.com
- Gibson and Millegan (1998), Geologic Applications of Gravity and Magnetics: Case Histories. SEG Geophysical References Series, No. 8. AAPG Studies in Geology, #43. Society of Exploration Geophysicists and American Association of Petroleum Geologists.
- Mozafari, M., Gutteridge, P., Riva, A., Geel, C. R., Garland, J. and Dewit, J. (2019). Facies analysis and diagenetic evolution of the Dinantian carbonates in the Dutch subsurface (SCAN). Downloadable from www.nlog.nl
- Prieto (1998) Gravity/Magnetic Signatures of Various Geologic Models - An Exercise in Pattern Recognition. In Geologic Applications of Gravity and Magnetics: Case Histories. Author(s): Richard I. Gibson and Patrick S. Millegan. Society of Exploration Geophysics, Vol 8. ISBN 9781560801832.
- Reeves (2005) Aeromagnetic surveys – Principles, practice & Interpretation. Geosoft.
- Rietman (1988) Opmeting van het aardmagneetveld in Nederland, herleid naar 1985. Technische rapporten, KNMI, Ministerie van Verkeer en Waterstaat.
- Robinson, E.S. and Coruh, C. (1988). Basic Exploration Geophysics, Wiley.
- Salem, A., Williams, S., Fairhead, D., Smith, R. and Ravat, D. (2007). Tilt-depth method: A simple depth estimation method using 1st order magnetic derivatives. The Leading Edge, December 2007.
- Sejan, K., 2018. Forward and Inverse modelling of gravity anomaly for geothermal applications: Case study of Los Humeros.
- Tesauro, M. Kaban, M.K. and Cloetingh, S.A.P.L. (2008) EuCRUST-07: A new reference model for the European crust. Geophysical Research Letters, Vol. 35.
- Ten Veen, J.H., de Haan, H.B., de Bruin, G., Holleman, N. and Schöler, W. (2019). Seismic Interpretation and Depth Conversion of the Dinantian carbonates in the Dutch subsurface (SCAN). Downloadable from www.nlog.nl
- TNO (2019) DGM5 data sets. downloaded from www.nlog.nl
- Van Bergen & Sissingh (2007) Magmatism in the Netherlands: expression of the north-west European rifting history. In Geology of the Netherlands. Editors: T. Wong, D.A.J. Batjes and J. de Jager. Royal Netherlands Academy of Arts and Sciences.
- Van Heiningen, P.S., Kaymakci, N., Van Hoegaerden, V. and Moser, T.J. (2018) Identification and characterization of Dinantian as a potential geothermal reservoir in the Roer Valley Graben by integrated gravity and magnetic modeling. Extended abstract accepted for talk at EAGE Copenhagen, June 2018.
- Van Hulten (2012) Devono-carboniferous carbonate platform systems of the Netherlands. Geologica Belgica (2012) 15/4: 284-296.
- Van Wees, J.D.A.M. (2017). Image-D8.4 Combination and Integration. Downloadable from http://www.image-fp7.fr/reference-documents/deliverables/Forms/AllItems.aspx

Daalsesingel 1
3511 SV Utrecht
scan@ebn.nl
www.scanaardwarmte.nl

Onderzoek in de ondergrond voor aardwarmte